Electro - optics in industry

David Miller Ring

ELECTRO - OPTICS

IN INDUSTRY

by

DAVID MILLER RING

A thesis submitted to the University of Durham
in candidature for the degree of
Master of Science

ABSTRACT

This thesis is concerned with the application of electro optical instrumentation and techniques to solving measurement, inspection and quality control problems in an international glass manufacturing firm.

Firstly a review is carried out of equipment available to the industrial scientist. Three areas are studied: sources, media, and detectors.

A number of problems which have arisen are then discussed, and the techniques used to solve them are described. The problems include the monitoring and control of 'foreign' substances in glass cullet prior to being fed into the furnaces; measuring the flatness of large areas of thin glass without using mechanical contact; the construction of a small stable infra red interferometer based on the Smartt point diffraction interferometer; rapid measurement of the curvature of ophthalmic lens surfaces; monitoring the position of wire mesh in wired glass; and measurement of very small amounts of haze on glass surfaces.

CONTENTS

LIST OF FIGURES

LIST OF TABLES

LIST OF PLATES

CHAPTER 1 INTRODUCTION

This thesis gives an account of the applications of geometrical and physical optics within an international glass manufacturing firm. The applications have arisen out of attempts to solve some of the problems that have occurred in the production of glass and in its subsequent processing into various products. Most of the problems are concerned with quality control.

It is important to point out that in an industrial environment problems need to be solved quickly (timescales of a few months are normal) and when solved the solutions are usually judged in terms of their effect on efficiency of production and whether they are profitable to apply, rather than on their elegance or academic content. Consequently, financially cheaper solutions are usually preferred, and some solutions, though demonstrably correct, are never even utilised.

The thesis begins with a review of current electro optical instrumentation. This is a study of the range of equipment available to the industrial scientist. The review is in three parts; sources, media and detectors. The emphasis is on the suitability of various components to problem solving with geometrical and physical optics, and on the improvements that can be expected in various fields in the near future. More equipment has been included in the review than is used in the practical work. This is done in order to maintain a more balanced and complete view of available instrumentation than would otherwise have been possible.

In the practical work, the first problem to be discussed

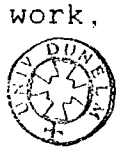

is the monitoring and control of 'foreign' substances in glass cullet prior to being fed into the furnaces. This is quite a serious problem in terms of quality and in terms of fouling the production line conveyor belt system. A solution is required that will work on a conveyor belt delivery and is essentially automatic. This problem is discussed in chapter 3.

In chapter 4 the problem of measuring the flatness of large areas of glass (such as car windscreens before they are bent to shape) is discussed, where the solution has to avoid mechanical contact with the glass. A Schlieren method was devised and is described.

Interferometry is used as a measurement and inspection tool in the production of lenses, prisms and other optical components. Usually two beam interferometry is used, but this is adversely affected by vibrations, and refractive index variations in air, because the two beams are separated. Recently there has been interest in the use of 'common path' interferometers which would be free of these problems. In chapter 5 a description is given of how the point diffraction interferometer, designed by Smartt for use in the visible region, has been redesigned and adapted for use in the infra red region, in an attempt to modify a two beam interferometer built for use with infra red light. A critique is given of its relative suitability.

In chapter 6 a number of smaller applications, typical of problems arising in the glass industry, are described. These include rapid measurement of the curvature of ophthalmic lens surfaces, monitoring the position of the wire mesh in wired glass, and the measurement of very small amounts of haze on glass surfaces.

Finally it should once again be stressed that all the practical work described is constrained by the needs of the company, and not carried out for academic interest.

CHAPTER 2 REVIEW OF ELECTRO - OPTICAL INSTRUMENTATION

2.1 Introduction

The purpose of this chapter is to outline the electro - optical equipment available for instrumentation today. The physical properties and purposes of a range of equipment and materials is reported, and the advantages, drawbacks and costs of the various alternatives are discussed. The review is divided into three main areas of interest: commercially available sources, optical materials, and detectors.

2.2 Light Sources

2.2.1 Introduction

In this part of the review, coherent and incoherent light sources are discussed. Here, lasers are regarded as coherent, and all other light sources relatively incoherent.

2.2.2 Coherent Light Sources

2.2.2.a Helium Neon Lasers

This is perhaps the most commonly used gas laser. It has a very favourable combination of price, size, performance and ease of operation.

Helium neon lasers produce a range of discrete wavelengths simultaneously. This has serious implications for instrumentation. The coherence length for conventional monochromatic light sources is a few millimeters, whereas for a multimode helium neon laser it is typically 20 - 30cm. Coherence

length becomes important in fields such as holography and interferometry, which rely on the phase information within light beams.

Helium neon lasers are made which produce only one longitudinal mode in their output beam. One such laser works as follows.

The resonating cavity of the laser has a heating coil wrapped round it. As this heats up, the mirror separation increases. Thus, although the position of the gain curve will remain constant, the comb of cavity modes will drift to lower frequencies. As each mode passes through the gain curve its intensity will increase, pass through a maximum at the centre of the curve, decrease, and finally disappear. Meanwhile another mode will begin to lase at the high frequency side of the curve. Figure 2.2.1. shows a particular mirror spacing where only two modes are lasing, with similar powers. Once the operating temperature has been reached, the heating is controlled to ensure that the lasing intensity of mode 1 remains within set limits. It does this using mode 2 as a reference value; this ensures that control of the intensity of mode 1 is independent of the overall intensity of the laser.

This type of laser has a coherence length of 20 - 30m; an improvement of around two orders of magnitude over conventional multimode helium neon lasers.

Helium neon lasers can be supplied with either a linearly polarised output, or a randomly polarised output. Linear polarisation is achieved by placing a window in the plasma tube which is inclined at the Brewster angle. Only polarisation components which align with the polarisation direction of the

FIGURE 2.2.1

LASER AT OPERATING TEMPERATURE

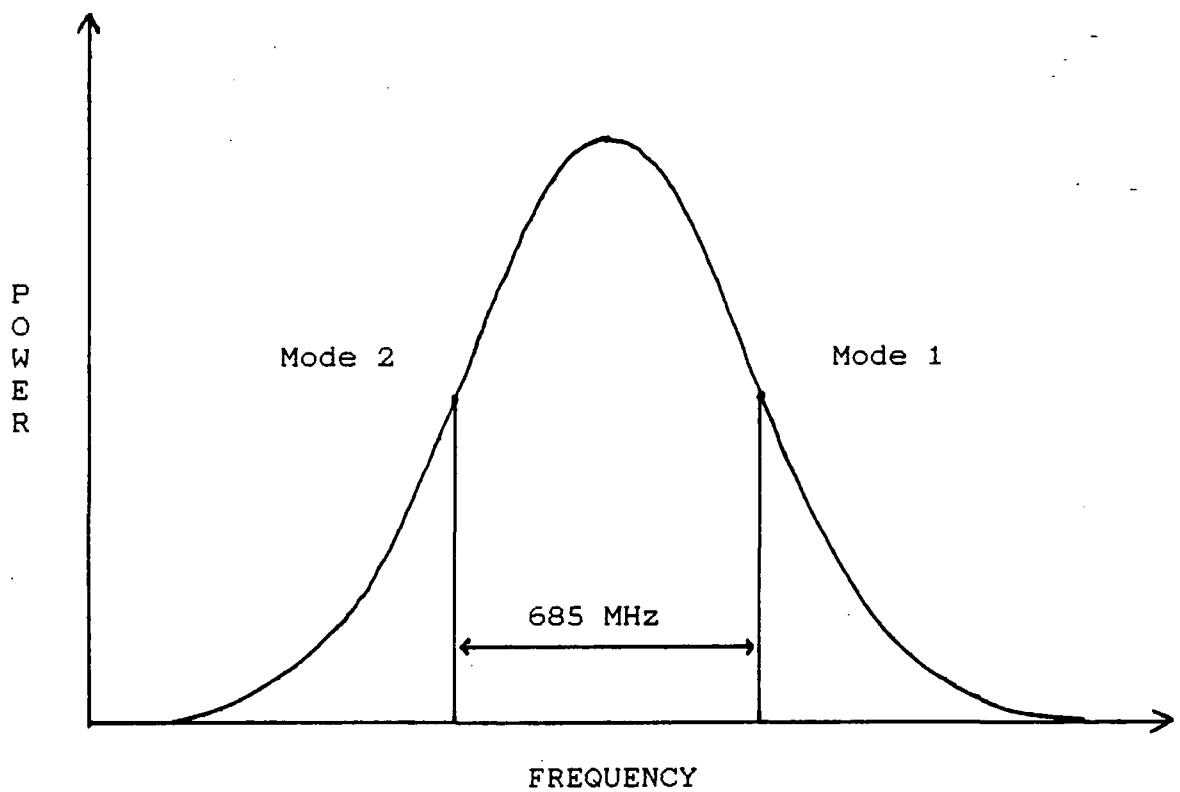

window can escape from the cavity.

Although famous for their operation at 632.8nm, helium neon lasers are becoming more versatile. For many years now versions have been available which produce 1152nm, or 3391nm radiation. More recently, 1523nm radiation lasers have been produced; and a green line of 543.5nm has appeared in what one company calls a "GreNe". Also available is a multi line tunable laser, with a wide range of output frequencies at various powers. The range of frequencies and powers is shown in figure 2.2.2.

Another aspect of helium neon laser production is size; a product is now available which is less than 100mm long and produces a 1mW output. This is excellent for uses in instrumentation.

In summary, helium neon lasers are the "bread and butter" of most laser companies. With prices starting at well under £200, the properties of laser light are available to almost anybody, and the units are truly portable. However, power outputs are limited to 100 - 200mW, and until recently only one visible wavelength was available.

2.2.2.b Helium Cadmium Lasers

Helium cadmium lasers are similar to helium neons, producing 1mW - 50mW cw radiation, but at the higher frequencies of 325nm and 442nm. The lifetime is long (5000hrs) and is limited by depletion of the cadmium. The cost of these lasers ranges from £4K to £12K.

FIGURE 2.2.2

SPINDLER AND HOYER TUNABLE HENE LASER

OPERATING WAVELENGTH (nm)	TYPICAL POWER OUTPUT (mW)
611.8	1.5
629.3	1.1
632.8	8.0
635.1	0.2
640.1	1.5
1084.4	0.1
1152.3	1.0
1152.5	0.7
1161.4	0.25
1176.7	0.15
1198.5	0.1
1206.6	0.1
1523.1	1.0

2.2.2.c Ion Lasers

Ion lasers use a noble gas; the most common versions are either Krypton or Argon. The gas is contained within the plasma tube, a version of which is illustrated in figure 2.2.3. If an argon ion laser is considered, the plasma tube, and an additional ballast (spare) tube will contain only argon at a pressure of approximately 1mm Hg. There are windows at either end of the tube to maintain the vacuum. These are mounted at the Brewster angle to polarise the output beam.

The ten visible wavelengths of light that argon will emit are shown in figure 2.2.4, as are the seven krypton lines. In order to separate these out, a simple glass prism is placed between the rear mirror and the plasma tube. This will disperse the wavelengths through a range of angles. Tilting the rear mirror will then redirect the chosen wavelength of light back to the front mirror, allowing it to lase.

The Doppler broadened spectral width of each of the laser lines in an ion laser is quite broad. Typically, the bandwidth is around 5GHz, and a 1m cavity length will support longitudinal modes 150MHz apart. This results in around thirty discrete frequencies lasing simultaneously. The coherence of a multimode ion laser is therefore quite short: around 60mm. To overcome this, an etalon is placed within the laser cavity. In a similar fashion to the entire cavity, an etalon will only transmit wavelengths which constructively interfere. However, since an etalon is very much smaller than a laser cavity, the mode spacing is proportionately greater. A properly designed intra cavity etalon will therefore reject all of the longitudinal modes except one, and cause laser power to be concentrated in

FIGURE 2.2.3

ION LASER PLASMA TUBE

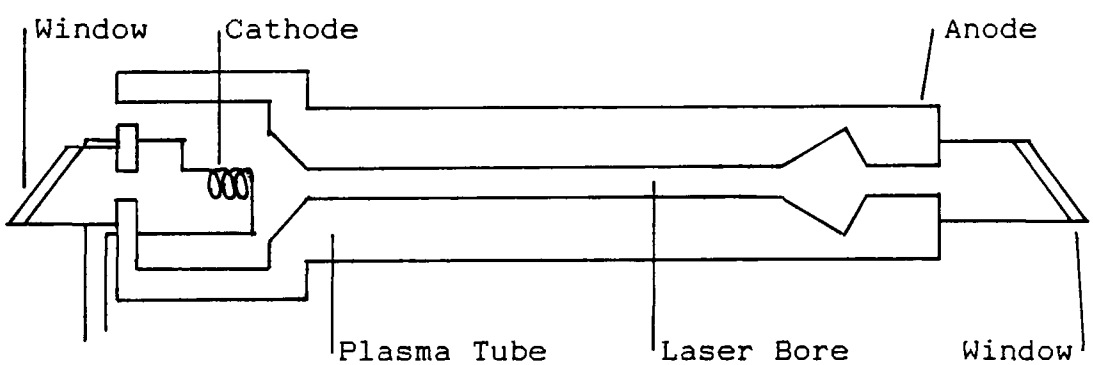

FIGURE 2.2.4

ION LASER OUTPUT WAVELENGTHS

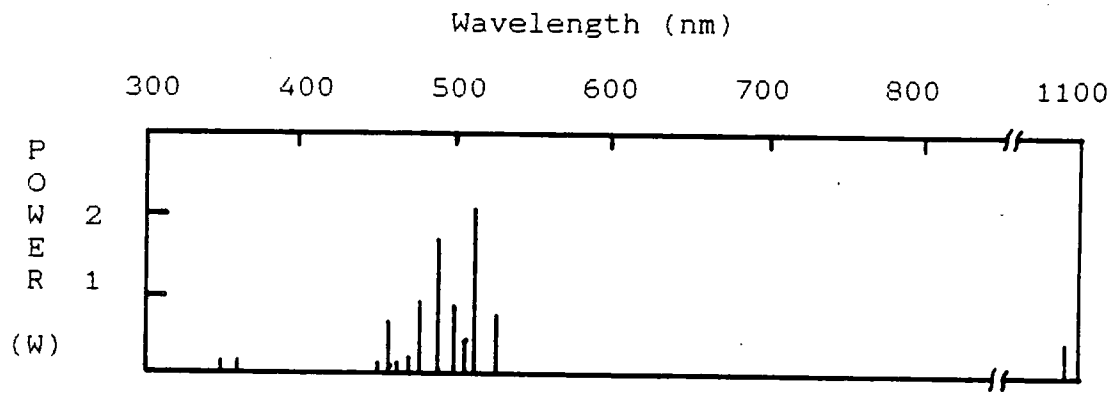

4 Watt Argon Ion Laser

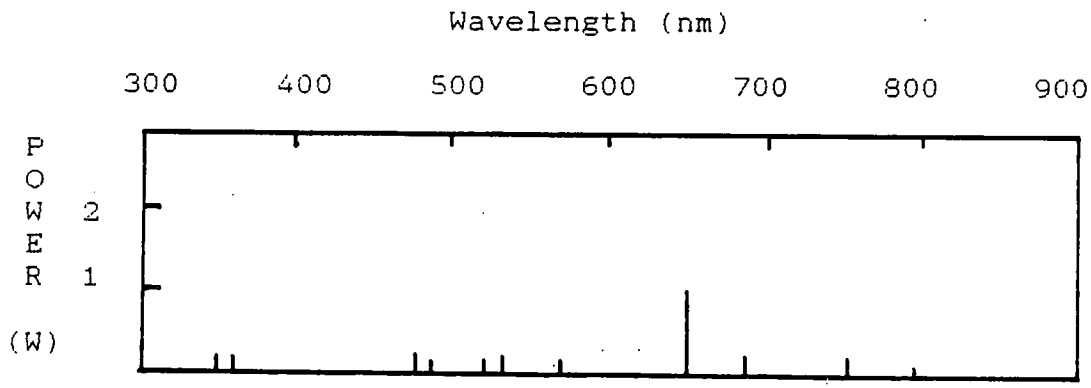

500 mW Krypton Ion Laser

this single mode. This results in a coherence length of around 100m. Consequently, practically any kind of interferometry and holography can be carried out.

Ion lasers are complex pieces of equipment, and need to be well engineered if they are to lase reliably and with a constant output power for any length of time. The power supply for a large ion laser is another complex component. A typical laser producing 4W of light in total will need a three phase power supply capable of delivering 60A on each phase. This illustrates the inefficiency of these lasers. All this electrical power is dissipated as heat, and forced air or water cooling is necessary for the laser to operate. More engineering effort is required to keep associated vibrations to a minimum, and to eliminate the possibility of water cooling leaks. Ion lasers provide very intense laser beams at a range of visible wavelengths. However, they are expensive: £5K - £25K, and high powered versions require water cooling and three phase power.

2.2.2.d Carbon Dioxide Lasers

The plasma tube of a carbon dioxide laser cavity contains a mixture of carbon dioxide, nitrogen, helium and other gases. Two types of laser cavity are used. The conventional method employs a flow of gas down a bore of typically 1cm in diameter. A more recent development is the waveguide laser. This is a hollow cylinder with a dielectric wall. It behaves very much like an optical fibre to contain the plasma within the lasing volume.

Flowing gas systems are relatively simple in principle. Once the gas has passed through the laser, it is exhausted.

Mirror alignment is as critical as for other types of laser. Many high powered units (10's of watts upwards) use this system. Waveguide systems have several advantages. The mirror alignment is less critical. Efficiency is greatly improved because the plasma is contained by the waveguide. Thus a power of 8W and more is possible in a package 40cm long. Independence from input and output gases makes the unit more portable. One disadvantage is that in a sealed off laser, the interaction between the electrical discharge and the gases causes some decomposition, resulting in harmful by - products which interfere with the lasing efficiency. As a result the plasma tube and its gas reservoir has to be emptied, purged and refilled with a fresh supply of the gas mixture.

Carbon dioxide lasers are the most commonly used gas infra - red lasers; their output at 10.6μm is generally high powered, from watts to kilowatts, and it is only recently that truly portable versions requiring only mains power have become available. Prices range from £5K to £500K.

2.2.2.e Dye Lasers

One of the properties of lasers which is of great value is their monochromaticity - however for some applications this can become a restriction; lasers such as those described above can only oscillate at discrete lines, and therefore cannot be continuously tuned. The dye laser alone allows continuous tuning across the spectrum from 400nm to 1μm.

Figure 2.2.5 shows a typical configuration of a dye laser. One of the most distinguishing features is that another laser is required as the excitation source. This is typically an

FIGURE 2.2.5

DYE LASER CONFIGURATION

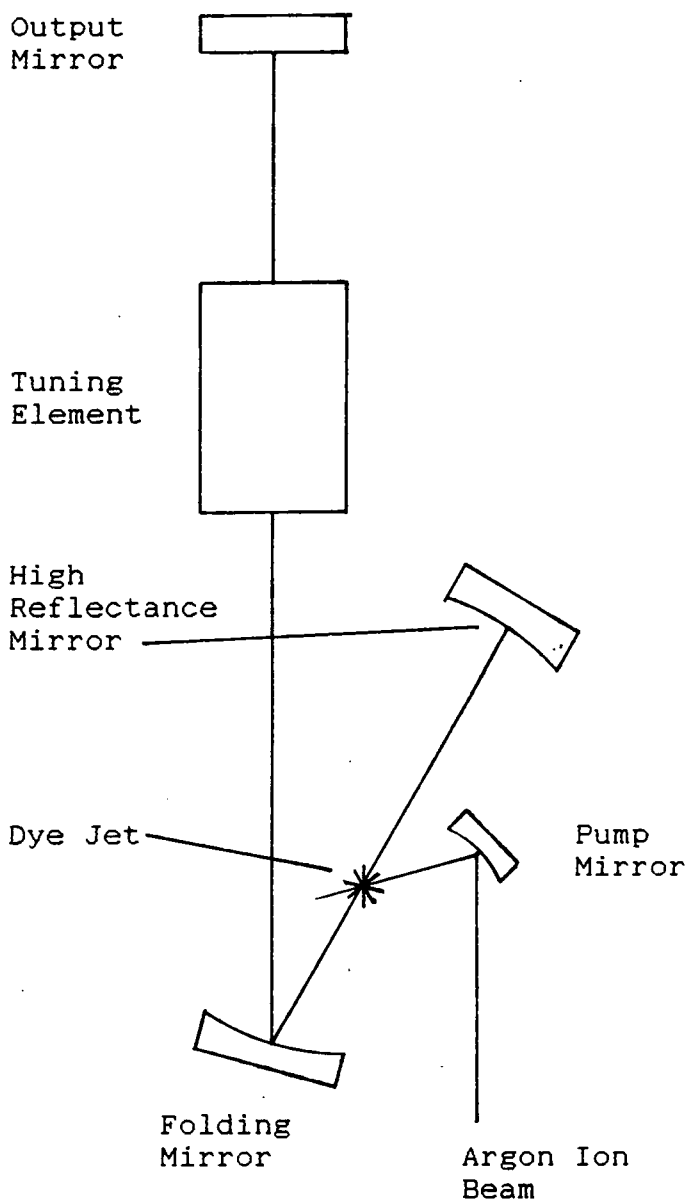

ion laser, and as is shown, this is focussed onto the dye stream, causing an extremely high level of fluorescence. The folding mirror in the diagram serves the dual purpose of focussing the light on the dye jet, and collimating the output beam.

A filter is placed within the laser cavity to restrict the range of output wavelengths; incorporated within the filter is a means by which the central wavelength can be tuned. Complex designs involving active feedback loops can maintain a linewidth of 500kHz, with a total frequency drift of less than 50 MHz per hour.

While the tunable nature of dye lasers is obviously an attractive feature, they have as yet found limited use. This is caused in the main by two things. Firstly the requirement of a pumping source can make the system cumbersome and expensive; and secondly efficient designs have in the past suffered from problems of instability and difficulty of alignment.

For this reason ordinary gas lasers are still widely used.

In table 2.2.1 the properties of gas lasers are summarised for comparison.

2.2.2.f Semi Conductor Lasers.

Semiconductor diode lasers possess a number of features not generally exhibited by other types of lasers, including extremely small size, operating simplicity, ease of modulation at high speeds, wide spectral tunability during operation, and coverage of a broad spectral range from the visible into the far infra - red region. These and other features form the basis for a

TABLE 2.2.1

SUMMARY OF LASER CHARACTERISTICS

TYPE	WAVELENGTH (μm)	POWER	LIFETIME (hours)	COMMENTS
ARGON ION	Weak UV .454; .488; .514; .523	5mW - 25W	~5000	Lifetime limited by Cathode failure. Cost £6K - £50K Efficiency 0.03% Special power and cooling required.
CARBON DIOXIDE	9.6 - 11.6 50 lines Strongest 10.6	1W - 10kW	1000 - 10000	Lifetime limited by gas mix. Large lasers use gas flow. Efficiency ‹10% Cost £4K - £200K
HELIUM CADMIUM	.325; .442	1mW - 50mW	~5000	Lifetime limited by Cadmium depletion. Efficiency 0.1% Cost £4K - £12K
HELIUM NEON	0.5 - 3.4 15 lines Strongest 0.633	0.5mW - 50mW	›2000	Lifetime probably limited by breakage. Efficiency 0.1% Cost ‹£100 - £15K
KRYPTON ION	Weak UV .406; .415; .468; .476; .568; .647; .676; .742; .799	1W - 10W	~5000	Lifetime limited by cathode failure. Cost £6K - £50K Efficiency ‹0.03% Special power and cooling required.

variety of applications in instrumentation. While these potentials have been recognised since the first development of diode lasers, realisation has, until lately, been severely hindered by low operating temperatures, poor lifetime, and other problems. Recent technological advances have led to major improvements in these areas, and to a corresponding increase in the interest in, and utilisation of, diode lasers.

Although diode lasers can be made using lead salts (PbTe, PbSe, PbS) which can produce laser radiation from 2.7μm to over 30μm, these devices operate at cryogenic temperatures (77K). The most highly engineered and tested devices are devised from the ternary alloy system $Al_xGa_{1-x}As$. These lasers, in commercially available form, can produce up to 30mW cw at 27C with threshold currents as low as 100mA.

By controlling the composition of the active region during manufacture, laser emission wavelength at any preselected value from less than 0.6μm to beyond 30μm is in principle attainable by this method. Diode lasers can also be tuned during operation by varying one of a number of parameters which affect the bandgap and refractive index. Temperature is the most used in practice, plus bias current variation, which provides a small but significant I^2R heating effect. Pressure and magnetic field can also be used. Individual lasers have been tuned from 9 - 12μm using temperature variation.

Once lasing is achieved, very small increases in supply current produce huge increases in laser power. Diode laser power circuits are therefore heavily smoothed, since it is common for the reflecting facets to be permanently damaged by the optical power densities generated within the cavity.

Research and development is highly intensive, driven by such markets as optical data storage and compact discs, in properties such as:

higher output powers,

shorter (visible) wavelengths,

specific longer infra - red wavelengths,

stable single line narrow spectral bandwidths,

very high modulation frequencies,

regular beam patterns.

Early diode lasers offered a few mW output powers in the 0.8 - 0.9μm region using GaAs and GaAlAs. More recently, devices offering up to 30mW cw at room temperature with greater than 10000hrs. lifetime have become available. These higher powers are achieved in a number of ways, for example increasing the diode output window (facet) area, and using anti - reflection coated and non - light absorbing facets.

To achieve even higher powers, multiple emitter laser arrays have become available. Optical interaction between individual emitters across a laser chip enables phase matching to occur, so that all the lasers act as a single source. Phased array GaAlAs diodes are available with powers of up to 200mW cw for around £1K - £2K, a price which is likely to fall with increasing application and production volume. With output powers likely to increase, these units compare very favourably with conventional helium neon (1 - 50mW) and air cooled (5 - 100mW) and water cooled (up to 20W) ion lasers; especially since efficiencies of diode lasers are from 1% to 20% compared with 0.01 - 1% for gas lasers.

The development of visible wavelength laser diodes is

actively pursued. The NEC Research Laboratories have announced a room temperature AlGaInP/GaAs device giving 1mW at 661.7nm. At the Sony Research Centre an AlGaInP laser produced 2mW of 671nm radiation. In principle the bandgaps available from III - V compounds would enable laser devices to be constructed with wavelengths as short as 500nm or below. To achieve this, newer materials are required such as InGaP and InAlP to create heterostructure devices. Commercial visible diode lasers are now available; Spindler and Hoyer market a 5mW 750nm version, and a 1mW 660nm unit. More are sure to follow.

2.2.3 Incoherent Light Sources.

The sources of light discussed in this section rely on spontaneous emission from a physically extended surface or volume.

2.2.3.a Incandescent Lamps

The incandescent lamp, specifically the tungsten filament lamp, is by far the most popular light source for general applications, because of its simplicity and relatively high luminance.

Although materials and fabrication technology contribute to the relative high cost of tungsten - halogen lamps over traditional incandescent versions, the "Watts per pound" scale is heavily in its favour when compared with other sources used in electro - optical instrumentation today. Also in its favour is the widespread distrust of the laser; white light is something everyone understands and is unafraid of.

2.2.3.b Gaseous Discharge Lamps

While developed primarily for their use in the field of illumination, discharge lamps also have their applications in optical instrumentation. In comparison with incandescent lamps, these sources tend to be long lived and highly efficient but require more complicated circuitry for operation and have higher initial costs. Discharge lamps exhibit "negative resistance". This means that the voltage across the arc drops as the current increases; the lamp will literally self - destruct unless an external ballast is employed to limit the current.

Low pressure arc discharge lamps are more commonly known as fluorescent lamps. In these sources a low pressure mercury arc transforms electrical energy into 253.7nm ultra - violet radiation. The walls of the lamp are coated with phosphor, which fluoresces when the ultra - violet radiation is incident upon it. The spectral output of fluorescent lamps is characterised by a broad emission band from the phosphor in conjunction with the characteristic narrow spectral lines of the low pressure mercury arc. Between the wavelength limits of 300nm and 850nm a wide variety of distributions is possible.

Medium pressure lamps operate at between 1 and 10 atm. Mercury, metal halide and sodium versions are the most common. The clear mercury lamp has a spectrum consisting mainly of strong lines at 365.0, 404.7, 435.8, 546.1 and 578.0 nm. This makes it useful for the determination of refractive indices and dispersion of materials. For illumination however the lamp is normally enclosed within a nitrogen filled outer glass envelope. This absorbs the hazardous ultra - violet radiation, and has the added

benefits of regulating the temperature of the tube and protecting it from atmospheric corrosion.

Metal additive, or metal halide lamps are produced to overcome the limited spectral distribution of the mercury lamp. By varying the choice and proportions of the additives which are incorporated, the lamps can be varied in their spectral output almost at will.

Medium pressure sodium lamps produce a broadened sodium doublet output, and are available in a range of sizes and output powers.

High pressure arc lamps produce the highest luminance available from a practical light source.

The open carbon arc produces a very intense broadband source of light. The arc is formed between two carbon rods which are consumed in the process and are fed continuously to maintain the spacing. These sources are essentially gray body radiators at about 6000K colour temperature.

The high pressure mercury arc source is operated above 10atm pressure. The lamp produces radiated energy which is distributed about evenly between the line and the continuous spectrum.

In a high pressure gas arc lamp, the arc is produced in one of the inert gases. The spectrum of the high pressure xenon arc lamp is continuous in nature in the visible region, and its close match to the output of the sun (as shown by the dotted line in figure 2.2.6) means that this lamp is often used in instrumentation as a "solar simulator".

The enclosed concentrated zirconium arc lamp uses an argon atmosphere and oxide coated cathode from which metallic

FIGURE 2.2.6

SPECTRUM OF HIGH PRESSURE XENON ARC LAMP

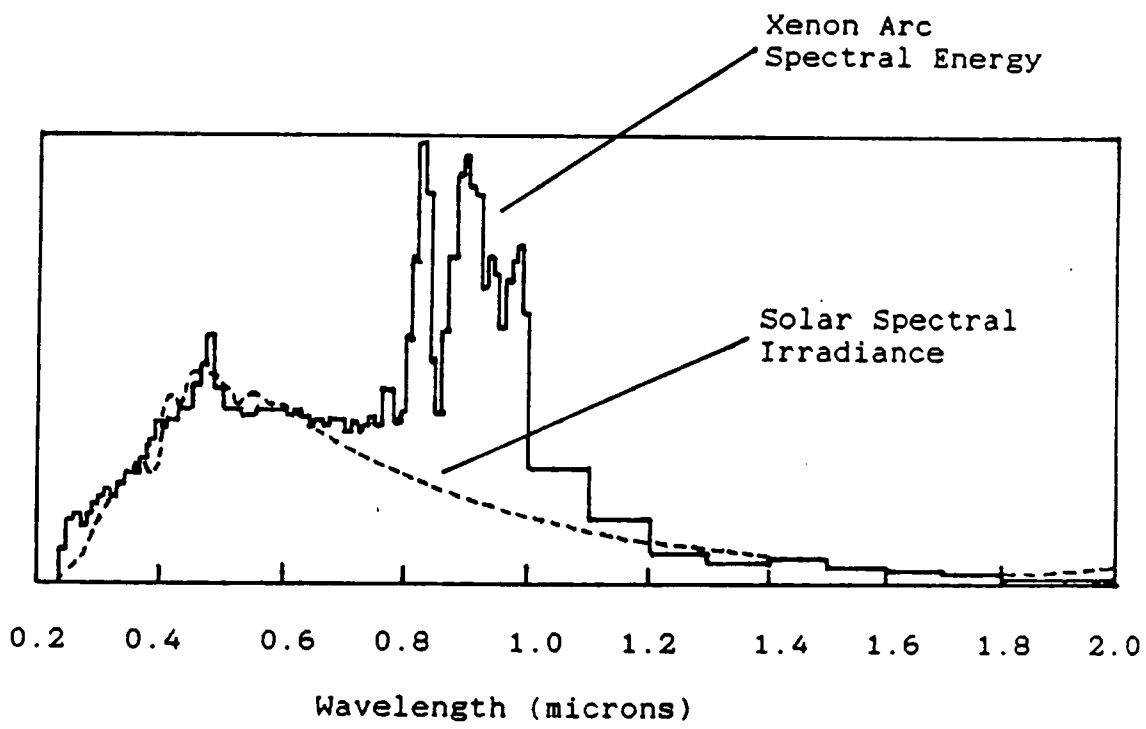

zirconium is evaporated because of the high cathode temperatures developed during operation. The emission spectrum is almost free of lines in the visible portion of the spectrum. Their small source diameters (0.13 to 2.75 mm) make them useful as high efficiency "point sources".

2.2.3.c Light Emitting Diodes

The common commercially available LED's are formed of a ternary compound of gallium arsenide and gallium phosphide $GaAs_{1-x}P_x$. The x has values between zero and one. Pure gallium phosphide (x = 1) produces 560nm radiation; pure gallium arsenide (x = 0) produces 900nm radiation. Compounds with intermediate values of x produce corresponding wavelengths within the two extremes.

An LED produces a Lambertian light distribution. This is usually modified to produce a degree of collimation, thereby increasing the apparent brightness of the unit. Normally the diode and its mount are sealed in plastic or an epoxy whose surface forms the lens. Increasing the refractive index of the material in contact with the semiconductor in this way reduces Fresnel losses, and losses due to total internal reflection.

Operating parameters for commercially available solid state lamps can only be taken as guidelines. Firstly, significant changes occur with variations in ambient temperature. From room temperature to the maximum operating temperature of around 80C, power output drops several times over (as it also does with the age of the unit) and output wavelength can increase by up to 10nm. Secondly, inherent variation between individual lamps can be as high as five to one for maximum intensity; +/- 20nm for

peak wavelength, and +/-10 degrees for the optical and mechanical axis. These tolerances can vary considerably, so care must be taken to refer to the manufacturer's specifications.

Current development of LED's concentrates on reducing the output wavelength, and increasing the output power. Recently a blue, 480nm, silicon carbide LED has become available, but the output powers are low, and the units are tens of pounds each (compared with a few pence for standard versions ordered in quantity). There exists a blue edge emitting zinc sulphide LED, with up to 100 times the output power of silicon carbide LED's, but this is at the development stage.

The search for more powerful LED's is being led at the moment by the Xerox Palo Alto Research Centre, which has a "quantum well" surface emitting LED which can produce 200mW of cw optical power at 715nm.

2.3 Optical Materials

2.3.1. Introduction

In this part of the review, the role played by optical materials in instrumentation is discussed. The study is split into three wavelength regions. This is because across the spectral region of interest the absorption peaks of oxygen, carbon dioxide and water in the atmosphere result in three spectral 'windows' at which radiation is transmitted. The mid infra - red window is generally accepted as being 3 - 5 μm; the far infra - red window 7.5 - 14 μm, and for the purposes of this discussion the other window will be described as the visible and near infra - red (0.4 - 2.4 μm). The materials available for each window will be examined with respect to their transmission, refractive index (and its variation i.e. dispersion), homogeneity, and relevant physical properties.

2.3.2. Visible and Near Infra - Red

2.3.2.a Glass

Optical glasses have been produced for hundreds of years, and there are now a great number of different types available for use in the visible and near infra - red region of the spectrum.

In glasses produced for optical systems the dependence of transmission on wavelength is kept to a minimum. The silicate optical glasses, available from major suppliers in Europe, USA and Japan, range in principal refractive index (n_d) approximately from 1.40 to 2.05 and in reciprocal dispersive power or Abbe value (V_d - the dependence of the refractive index on wavelength)

approximately from 15 to 100 where $V_d=(n_d-1)/(n_f-n_c)$. A plot of n_d against V_d for a range of available glasses is shown in figure 2.3.1. In general, glasses with $n_d > 1.6$ and $V_d > 50$, and those with $n_d < 1.6$ and $V_d > 55$ are known as crown glasses, the remainder as flint glasses. The refractive index for SiO_2 glass is 1.4528. This can be decreased by the substitution of fluorine for oxygen, or of B_2O_3. Substitution of alkali and alkaline earth oxides increases the refractive index. The need for so many different glasses results from the need for very high resolution imaging systems. The different glasses are used for correcting the various lens aberrations to minimal values. For instance in achromatic systems chromatic aberration is corrected at two wavelengths, one in the red and another in the blue part of the visible spectrum, but the spectrum between is uncorrected. However in apochromatic systems this secondary spectrum is also corrected perhaps at as many as ten wavelengths to ensure minimum chromatic aberration.

The homogeneity of optical glasses is an important consideration. In recent years optical glasses with higher homogeneity have become indispensable to the fabrication of most precise optical systems such as large telescopes, aerial reconnaissance cameras, and microlithographic cameras (used for large scale integrated circuits). Companies have their own methods of producing as homogeneous a base product as possible, but the glass must be "fine annealed" to relieve stresses in it. It is then examined for striation, normally with some shadowgraph technique, and the index variation itself is found using interferometry; commonly using the glass blank, by grinding the

FIGURE 2.3.1

N_d - V_d Diagram

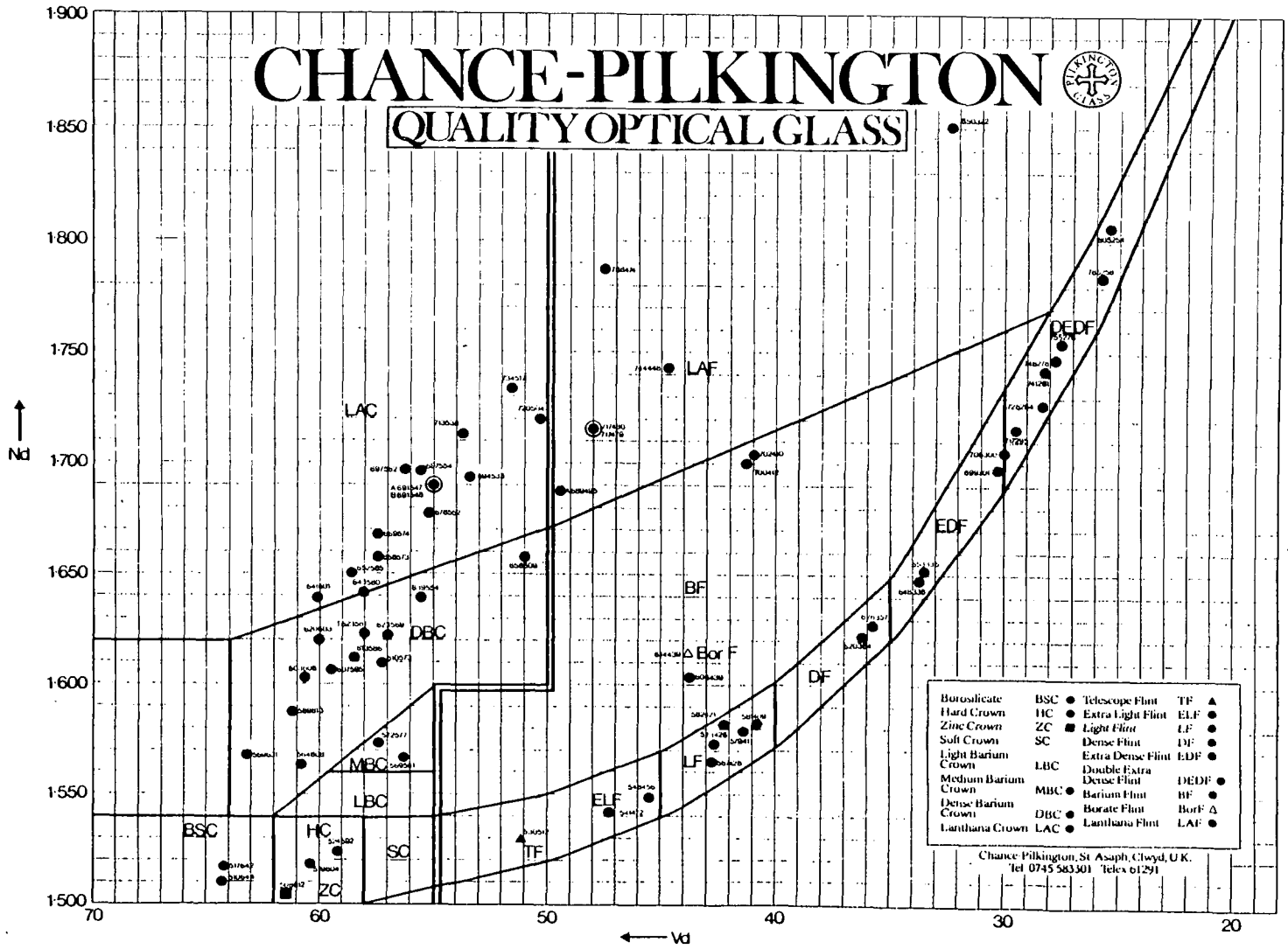

surfaces and matching them with oil to high quality polished optical flats. Normal high homogeneity specifications range in variation of refractive index from 10^{-5} to 10^{-6}.

Recent glass developments include reducing the weight of some of the dense flint glasses, to allow their aberration correction properties to be used in zoom lenses and space observation systems; producing covers for solar cells which have the appropriate spectral transmission yet with the same expansion coefficient as silicon; and producing glass for photocopying applications with restricted transmission at the low and high wavelength ends of the visible spectrum, to limit chromatic aberration.

2.3.2.b Plastics

Several plastics exist which possess optical properties, and as such represent an alternative to glass as a material. A great deal of effort was made to develop plastics for optical systems during the Second World War, and a few systems incorporating plastics were produced, but for many years since that time it was not taken as a serious competitor for glass. In some respects this is still true. However in recent years production techniques in the three main manufacturing methods for plastic optics - casting, moulding and machining - have improved vastly. As a result, plastic is a real competitor to glass in some fields. Production volume is an important factor for determining the practicality of plastic optics: if the quantities required are from one to two thousand upward, moulded plastic optics can be supplied when the quality, weight and / or other factors warrant their consideration.

In the ophthalmics industry there are a handful of manufacturers supplying spectacle lenses practically by the million. They are made of allyl diglycol carbonate - CR39. The optical properties of this material (along with the other major types) are outlined in table 2.3.1. The lenses are cast in glass moulds. The curing cycle must be carried out in carefully controlled temperature conditions to avoid the introduction of strains and distortion. Shrinkage for CR39 is high (up to 14%) as is the change in refractive index with temperature ($dn/dt = -14 \times 10^{-5}$). However in ophthalmic optics these variations do not cause problems. Plastic components can also be moulded. Compression moulding (developed to a fine art by the record industry) is used to produce fresnel lenses and lenticular lens arrays. However the majority of high quality plastic optics made in volume are made by injection moulding. The tooling mould design is highly specialised, consisting normally of a steel base and chromium stainless steel inserts. The inserts are either optically polished, or single point diamond machined.

The transmission of four of the major optical plastics is shown in figure 2.3.2. They are all similar, with good transmission across the visible range. Comparing table 2.3.1 with figure 2.3.1 will show where each of the plastics are on the n_d - V_d diagram. Acrylic is the 'crown' of plastics, polystyrene the 'flint'. Homogeneity is normally an order of magnitude down on glass; tests with acrylic lenses reveal variations of 1.7×10^{-4}, whereas glasses are specified in the 10^{-5} to 10^{-6} range. The variation in refractive index with temperature is similarly proportionately large; for acrylic $dn/dt = -8.5 \times 10^{-5}$, and BK7 glass the value is 0.3×10^{-5}. However if the application is not

TABLE 2.3.1

OPTICAL PROPERTIES OF PLASTICS

	ACRYLIC Polymethyl Methacrylate	STYRENE Polystyrene	POLYCARBONATE	CR39 ADC Allyl Diglycol Carbonate	GLASS BK7	UNITS
REFRACTIVE INDEX						
n_d (589.3 nm)	1.491	1.590	1.586	1.504	1.517	
n_c (656.3 nm)	1.488	1.585	1.581	1.501	1.514	
n_f (486.1 nm)	1.496	1.604	1.598	1.510	1.522	
ABBE VALUE V_d	61.4	31.1	34.5	56	64.6	
RATE OF CHANGE OF INDEX WITH TEMPERATURE: dn/dt	- 8.5	- 12.0	-11.8 to -14.3	-14.3	+0.3	dn/dt x 10^{-6}/°C
COEFFICIENT OF LINEAR EXPANSION	6.74	6.0 - 8.0	6.6 - 7.0	11.4	0.7	cm/cm x 10^{-6}/°C
LUMINOUS TRANSMITTANCE	92	88	89	93	99.9	%, 3.175mm thickness

FIGURE 2.3.2

TRANSMISSION OF SOME MAJOR OPTICAL PLASTICS

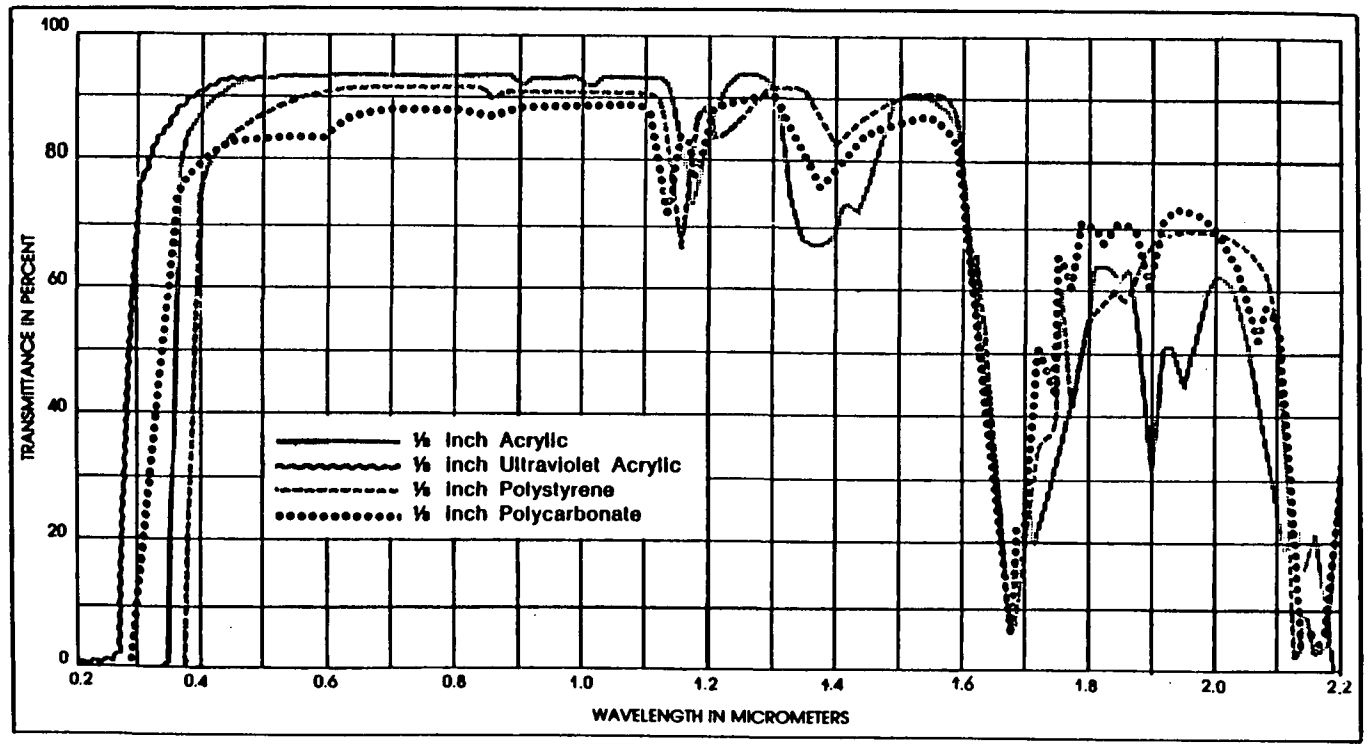

too stringent this will not present a problem: a 25mm diameter acrylic lens will change by 76μm when heated from 27C to 65C; its focal length will increase by 0.2mm. Plastics are not as abrasion resistant as glasses, and suffer the same losses from reflection, but it is difficult to put down strongly adhering coatings onto them. Thus glass will always be preferable from this point of view until the appropriate coating technology is developed.

2.3.3. Mid Infra - Red

2.3.3.a Glasses

The glasses described above for the visible and near infra - red region are versions of silicate glasses. For transmission up to 5 or 6 μm other basic types of glass are required. Calcium aluminate glasses ($CaO-Al_2O_3-MgO$) were worked on as early as 1916, and transmit up to 5μm (see figure 2.3.3). Poor weathering resistance can be overcome by anti - reflection coatings of MgF_2 or SiO. Germanium dioxide is a glass former and demonstrates a good transmission out to about 6 μm but it is expensive and has poorer mechanical properties. Corning developed a useful germanate glass composition, Corning code 9754, which is in fact a calcium alumino germinate glass. This overcame some of the problems of calcium aluminate glasses whilst retaining sufficiently robust mechanical properties and adequate infra - red transmittance (see figure 2.3.3) at only a little extra cost.

FIGURE 2.3.3

NEAR IR TRANSMITTANCE OF GLASSES

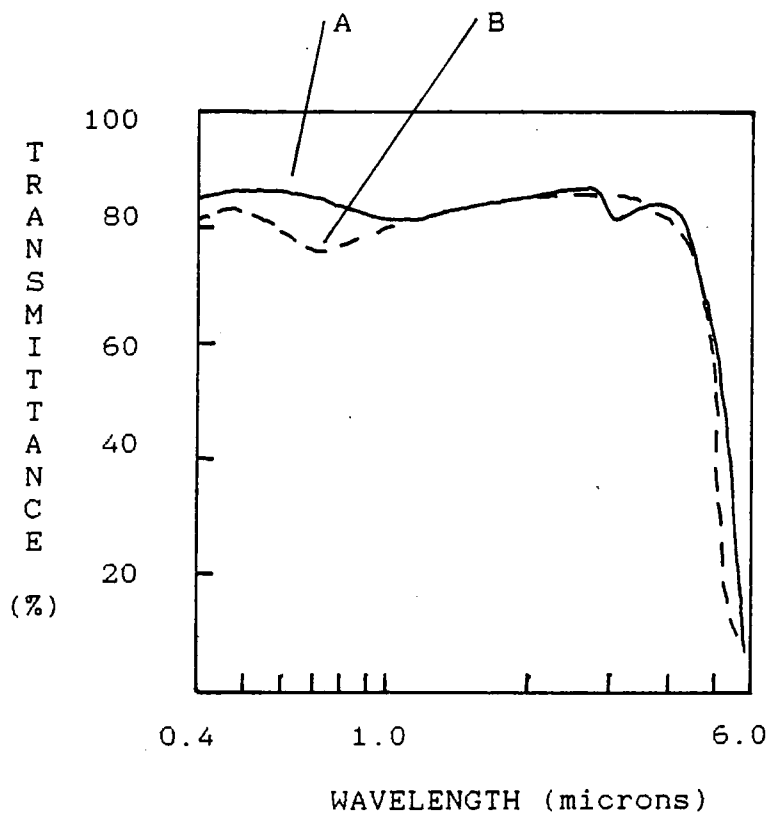

A: CORNING 9754

B: BS 37A Calcium Aluminate Glass

2.3.3.b Ceramics

During the late 1950's and early 1960's the need for airborne infra - red windows stimulated work on hot pressed ceramics, resulting in a range of hot pressed polycrystalline solids being manufactured by Eastman Kodak. MgF_2 (Irtran 1) has found extensive use as an airborne infra - red window material as it has excellent thermal and mechanical properties. Its transmission is shown in figure 2.3.4. Although it tends to scatter (8% at 2μm), the optical properties are good enough for all but high resolution imaging applications. CaF_3 (Irtran 3) was the best visually transmitting material but it scattered slightly more than Irtran 1. Its transmisson is shown in figure 2.3.4. Irtran 5 is MgO. The transmission characteristics of this are also shown in figure 2.3.4. The scatter of this material can be greatly reduced by the addition of a little LiF.

2.3.3.c Sapphire

The combination of excellent mechanical and optical properties exhibited by sapphire makes it an excellent choice for a variety of demanding optical applications. It has a wide range of transmission (figure 2.3.5). It is one of the hardest of the oxide crystals and maintains a good strength at high temperatures. It possesses good thermal properties and excellent chemical durability. However its high strength and hardness make it difficult to shape, and its hexagonal crystal structure results in anisotropic properties.

FIGURE 2.3.4

NEAR IR TRANSMITTANCE OF CERAMICS

A: IRTRAN 1 MgF_2

B: IRTRAN 3 CaF_2

C: IRTRAN 5 MgO

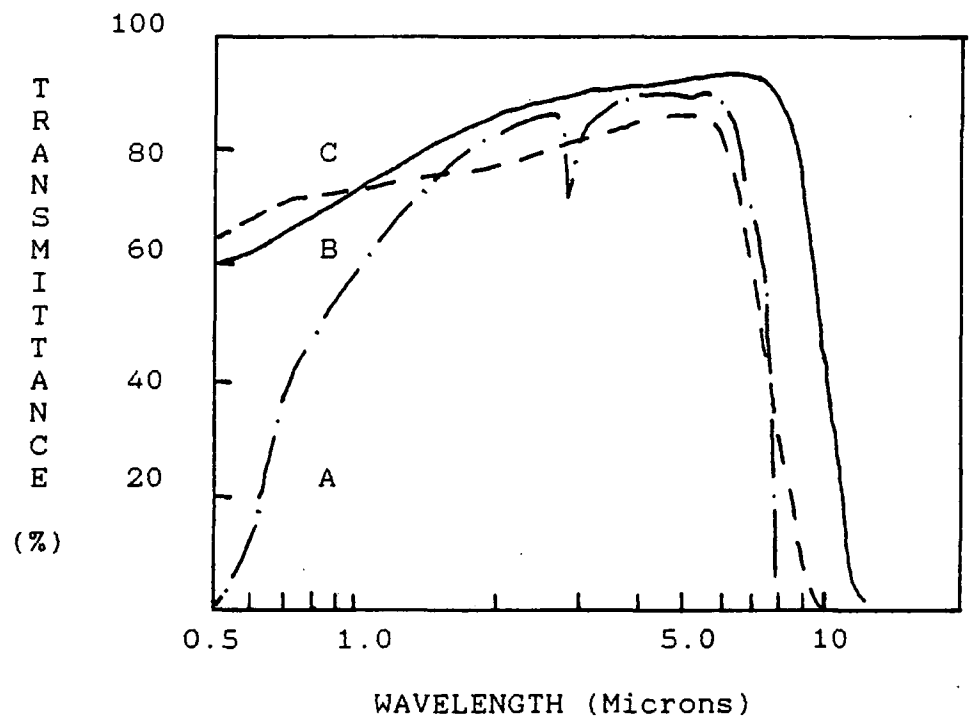

FIGURE 2.3.5

TRANSMITTANCE OF SAPPHIRE

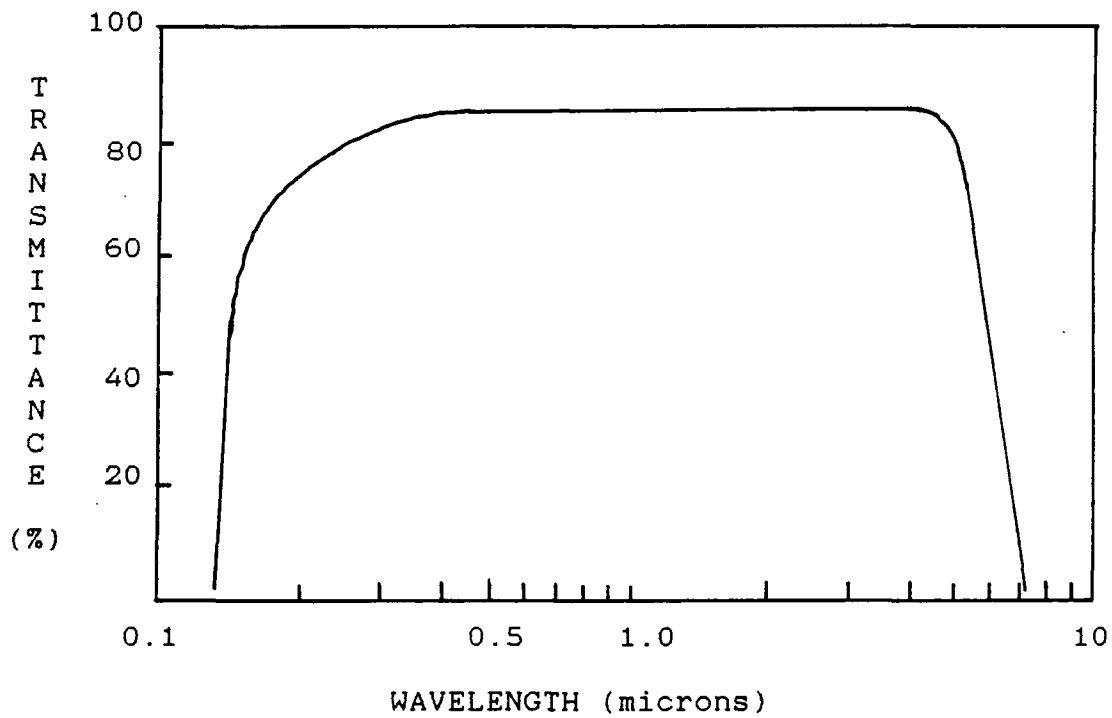

2.3.3.d Silicon

Over the last 30 years or so, silicon has been developed as the world's major semiconductor material. It is thus readily available in high quality and quantity for use in infra - red optical applications. Transmission is shown in figure 2.3.6. In table 2.3.2 the major optical properties of silicon are outlined, along with the mid infra - red materials discussed above. Optical homogeneity is likely to be good because high quality monocrystalline material for substrate manufacture is routinely grown. Equipment has been developed to pull monocrystals up to 150mm diameter, a size most suitable for infra - red optical applications.

2.3.4 Far Infra - Red

2.3.4.a Germanium

Germanium is the most useful semiconductor for use as a far infra - red window or lens material. A major asset of germanium is its low dispersion in the far infra - red range, since this means that for all but very stringent applications, the small amount of chromatic aberration in germanium lens systems need not be corrected. Hence extra cost and complexity are avoided as a second optical element material is not necessary. In addition, the high refractive index of germanium allows high optical power to be generated in thin optical components, and the degree of hardness and mechanical strength of the material make it an ideal candidate for applications where ruggedness is a prime factor. Until silicon solid state devices became established, germanium was used extensively as a

FIGURE 2.3.6

TRANSMITTANCE OF SILICON

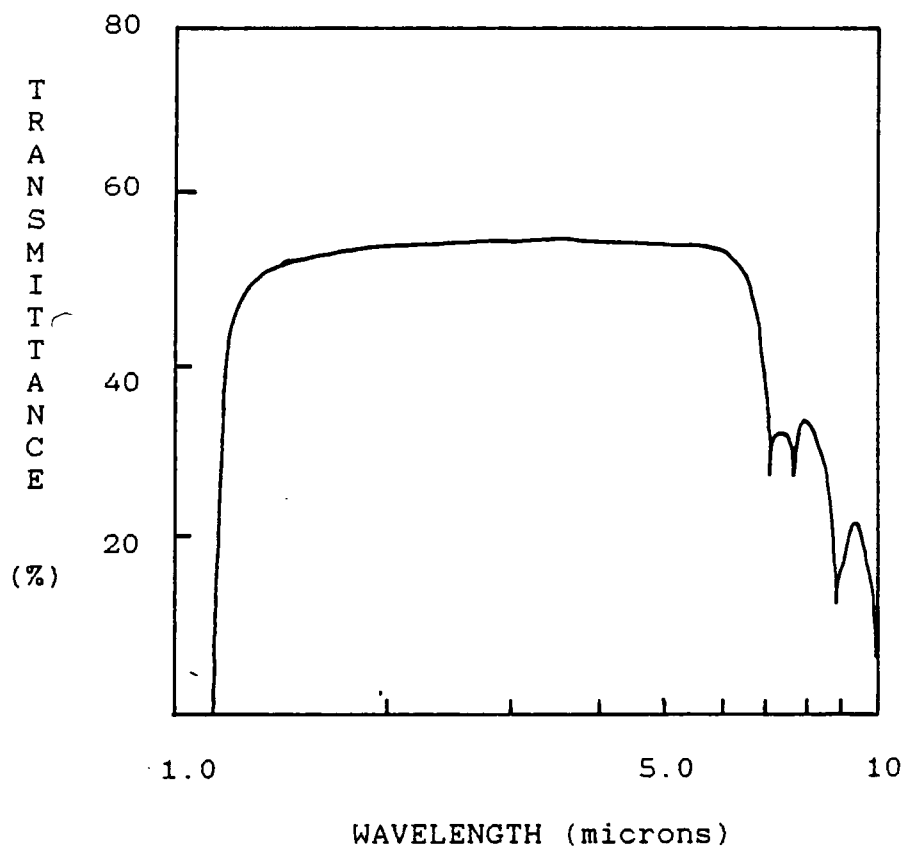

TABLE 2.3.2

OPTICAL PROPERTIES OF MID INFRA RED MATERIALS

MATERIAL	REFRACTIVE INDEX AT x MICRONS 1.0	3.0	5.0	V_{3-5}	THERMAL EXPANSION COEFFICIENT ($x10^{-6}/^{o}C$)
BS37A CALCIUM ALUMINATE GLASS	1.6538	1.6266	-	-	9.15
CORNING 9754 GLASS	1.650	1.625	1.582	14	6.2
IRTRAN 1	1.3778	1.3640	1.3374	13	11.9
IRTRAN 3	1.4289	1.4179	1.3990	22	21.7
IRTRAN 5	1.7227	1.6920	1.6368	12	12.7
SAPPHIRE	1.7555	1.7122	1.6240	8	7.7
SILICON	-	3.4316	3.4217	238	2.3

semiconductor. It was therefore already well characterised in terms of its electrical properties, whilst its basic optical and mechanical properties were moderately well known by the time interest developed in it as a major optical component material. The transmittance of germanium is shown in figure 2.3.7.

There are two methods of producing germanium. The Stockbarger process results in a polycrystalline material; the Czochralski method produces a monocrystal. Considerable development on both of these processes has resulted in their homogeneity immediately after production being an acceptable 2 x 10^{-4}, avoiding the need for annealing. However the grain boundaries in polycrystalline germanium are lossy, leading to transmittance non - uniformity, and a typical loss of 1% in a 10mm blank. More significantly these boundaries produce localised refractive index variations, affecting the imaging performance of lens systems. Generally monocrystalline germanium is found to offer superior performance over that of polycrystalline material for requirements where diffraction limited performance needs to be achieved.

2.3.4.b II-VI Compounds

The work carried out in the 1960's (mentioned above) in the development of a range of hot pressed polycrystalline solids, by Eastman Kodak, included three II-VI compounds:

ZnS (Irtran 2) ZnSe (Irtran 4) and CdTe (Irtran 6)

These were intended to be used in the far infra - red window. In fact they turned out to be multispectral, transmitting

FIGURE 2.3.7

TRANSMITTANCE OF GERMANIUM

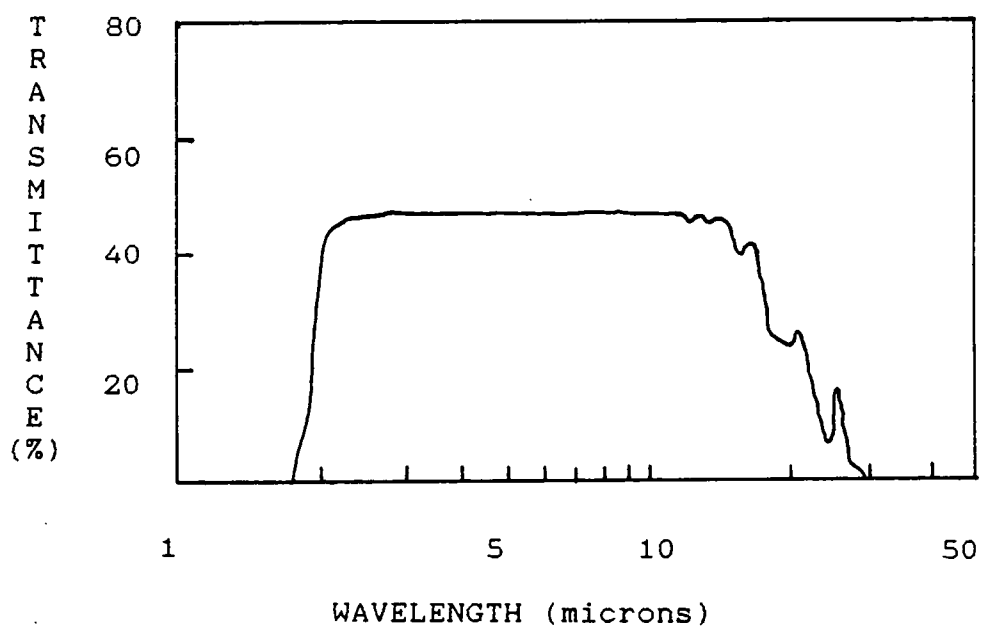

in all three of the windows in this discussion. However the transmittance was relatively low (see figure 2.3.8) and they suffered from problems of contamination, non - uniformity and scatter.

Two of these compounds, ZnS and ZnSe are used in infra - red optics today, but they are produced by vapour deposition. This produces an improved transmission (figure 2.3.9) and reduces non - uniformity and scatter. ZnS itself offers good far infra - red transmittance, but poor visible and near infra - red transparency, because of scatter and a yellow orange colouration attributed to hydride impurity. However, by subjecting a piece of normal grade CVD ZnS to a post deposition treatment at high temperature and pressure the overall optical transmittance of the material can be significantly enhanced, in particular at short wavelengths as shown in figure 2.3.9. This product is sold under the name of Cleartran.

Finally a summary of some of the properties of these far infra - red transmitting materials is given in table 2.3.3.

FIGURE 2.3.8

TRANSMITTANCE OF CERAMICS

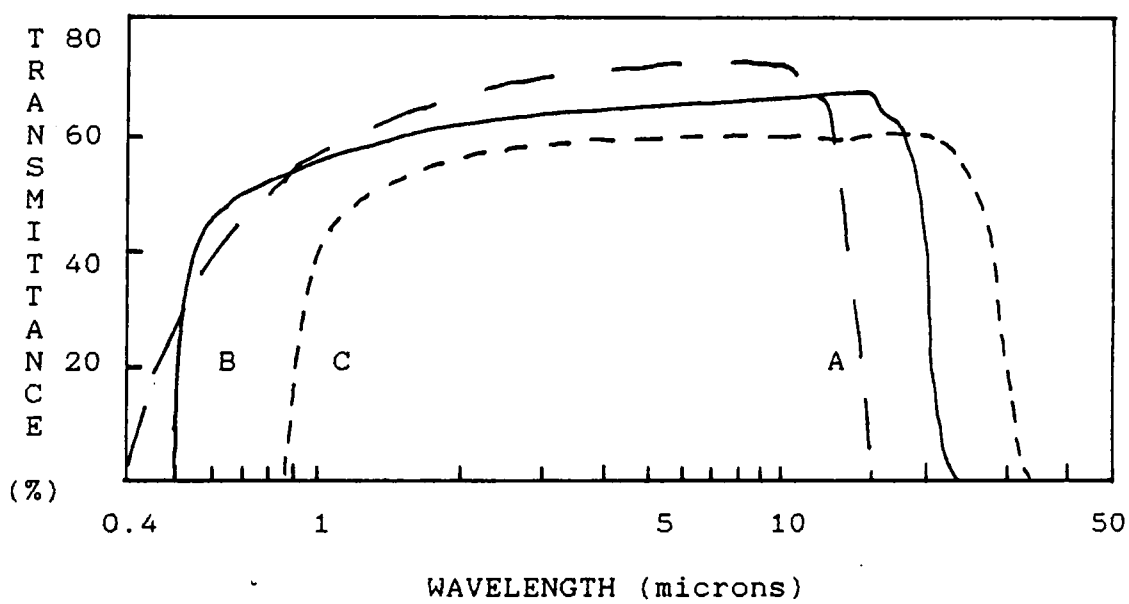

A: IRTRAN 2 ZnS

B: IRTRAN 4 ZnSe

C: IRTRAN 6 CdTe

FIGURE 2.3.9

TRANSMITTANCE OF MULTI - SPECTRAL MATERIALS

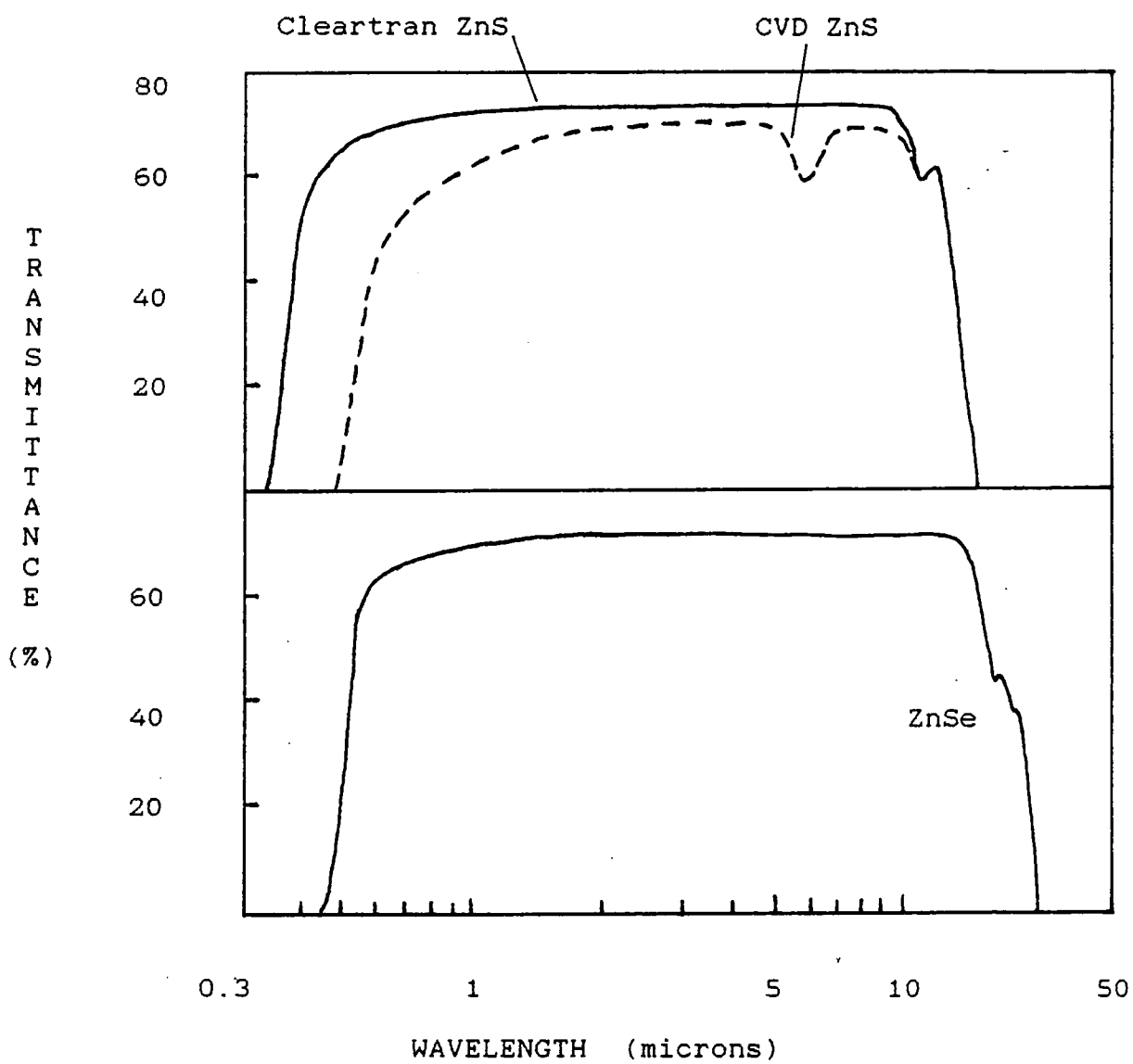

TABLE 2.3.3

OPTICAL PROPERTIES OF FAR INFRA RED AND MULTISPECTRAL MATERIALS

MATERIAL	REFRACTIVE INDEX AT x MICRONS 0.7	4	8	10	12	V_{8-12}	dn/dt x 10^{-4}/°C	THERMAL EXPANSION COEFFICIENT x 10^{-6}/°C
GERMANIUM	-	-	4.0054	4.0032	4.0019	858	3.9	6.1
IRTRAN 2 ZnS	-	-	2.2213	2.1986	2.1688	23	-	6.9
IRTRAN 4 ZnSe	-	-	2.418	2.407	2.394	59	0.48	7.7
IRTRAN 6 CdTe	-	-	2.677	2.672	2.666	152	0.93	5.9
CVD ZnS	-	-	2.2228	2.2002	2.170	23	0.5	7.85
CVD ZnSe	2.5568	2.4332	2.4173	2.4065	2.3930	58	1.5	7.57
CLEARTRAN	2.5452	2.2523	2.2233	2.2008	2.1710	23	-	7.85

2.4 Detectors

2.4.1. Introduction

Optical and infra - red detectors have developed in two ways; the discovery of new phenomena, and the preparation of new materials. Most of the important photodetection phenomena have been established for decades (although photon drag, Josephson junctions and negative electron affinity photocathodes are more recent discoveries). In the past two decades the emphasis has been on exploiting the established phenomena in new materials.

2.4.2. Detectors for Visible Wavelengths

2.4.2.a Photon Effects

Photon effects have received the greatest emphasis in the development of optical and infra - red detectors. Nearly all such detectors employ a semiconducting material of one form or another. Figure 2.4.1 summarises the known types of photon effect. It can be seen that there are two types of classification; internal and external effects. The internal ones are those in which the photoexcited electron or hole remains within the sample. In the external photoeffect the incident photon causes the emission of an electron from the surface of the absorbing material. The internal photoeffect is subdivided further. Firstly an incident photon can interact with a bound electron to produce either a free electron-hole pair (intrinsic photoeffect), or a free electron and bound hole (or free hole and bound electron) - the extrinsic effect. Secondly an incident photon can interact with electrons or holes that are already

FIGURE 2.4.1

PHOTON EFFECTS

INTERNAL

1. **EXCITATION OF ADDITIONAL CARRIERS**
   - PHOTOCONDUCTIVITY
     - Electrically biased
       - (Intrinsic; Extrinsic)
     - Microwave Biased
   - PHOTOVOLTAIC EFFECT
     - p - n Junction
     - Avalanche
     - p - i - n
     - Schottky Barrier
     - Heterojunction
     - Bulk
   - PHOTOELECTROMAGNETIC EFFECT
   - DEMBER EFFECT
   - PHOTOTRANSISTOR

2. **FREE CARRIER INTERACTIONS**
   - PHOTON DRAG
   - HOT ELECTRON BOLOMETER
   - PUTLEY DETECTOR

3. **LOCALISED INTERACTIONS**
   - INFRARED QUANTUM COUNTER
   - PHOSPHOR
   - PHOTOGRAPHIC FILM

EXTERNAL

1. **PHOTOCATHODES**
   - CONVENTIONAL
   - NEGATIVE ELECTRON AFFINITY

2. **GAIN MECHANISMS**
   - GAS AVALANCHE
   - DYNODE MULTIPLICATION (PHOTOMULTIPLIERS)
   - CHANNEL ELECTRON MULTIPLICATION

free. Thirdly, the photon can excite the electron into a higher energy state of the atom, without the electron ever leaving the atom.

Although figure 2.4.1 shows a large number of photon effects. Only the photoconductive, photovoltaic and photoemissive ones have been widely exploited.

2.4.2.b Photoconductivity

This is the most widely employed effect. Here the electrical conductivity of a material is changed by incident radiation. Table 2.4.1 lists the energy gaps of some semiconductors which have been employed as intrinsic photodetectors. Also listed are their operating temperatures and long wavelength limits. Table 2.4.2 lists the ionisation energies and long wavelength limits for some controlled impurities in extrinsic Ge and Si photoconductors.

2.4.2.c Photovoltaic Effect

The photovoltaic effect requires an internal potential barrier with a built in electric field to separate a photoexcited electron pair. This condition exists within a p - n junction.

Figure 2.4.2 illustrates the two ways in which the photovoltaic detector is used. In the first case a direct measurement is made of the voltage across the photodiode, since the open circuit voltage is proportional to the incident radiation. In the second case, a reverse bias is applied to the detector. The photocurrent produced by radiation is now measured across a load resistor. This latter case is described as photoconductive operation, even though the configuration is not

TABLE 2.4.1

CHARACTERISTICS OF VARIOUS INTRINSIC PHOTODETECTORS

SEMICONDUCTOR	T(K)	Eg(eV)	λ_o (μm)
CdS	295	2.4	0.52
CdSe	295	1.8	0.69
CdTe	295	1.5	0.83
GaP	295	2.24	0.56
GaAs	295	1.35	0.92
Si	295	1.12	1.1
Ge	295	0.67	1.8
PbS	295	0.42	2.9
PbSe	195	0.23	5.4
InAs	195	0.39	3.2
InSb	77	0.23	5.4
$Pb_{0.2}Sn_{0.8}Te$	77	0.1	12
$Hg_{0.8}Cd_{0.2}Te$	77	0.1	12

TABLE 2.4.2

CHARACTERISTICS OF VARIOUS EXTRINSIC PHOTODETECTORS

SEMICONDUCTOR:IMPURITY	E_i(eV)	λ_o(μm)
Ge : Au	0.15	8
Ge : Hg	0.09	14
Ge : Cd	0.06	21
Ge : Cu	0.041	30
Ge : Zn	0.033	38
Ge : B	0.0104	120
Si : In	0.155	8
Si : Ga	0.0723	17
Si : Bi	0.0706	18
Si : Al	0.0685	18
Si : As	0.0537	23
Si : P	0.045	28
Si : B	0.0439	28
Si : Sb	0.043	29

FIGURE 2.4.2

PHOTODIODE CIRCUITS

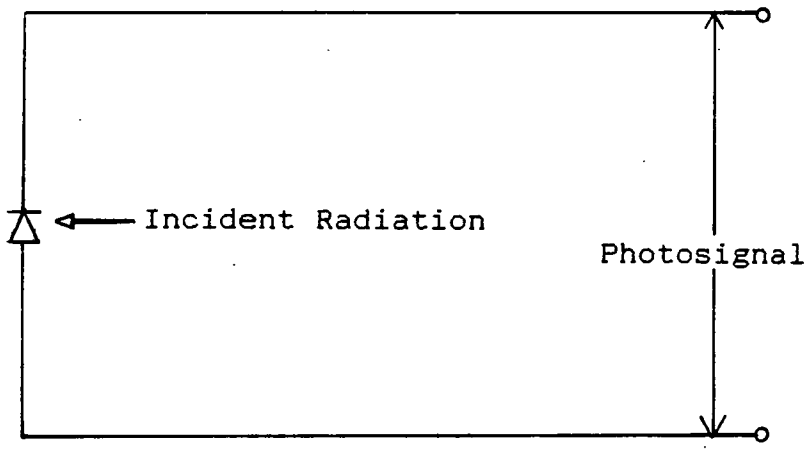

Open Circuit Photovoltage

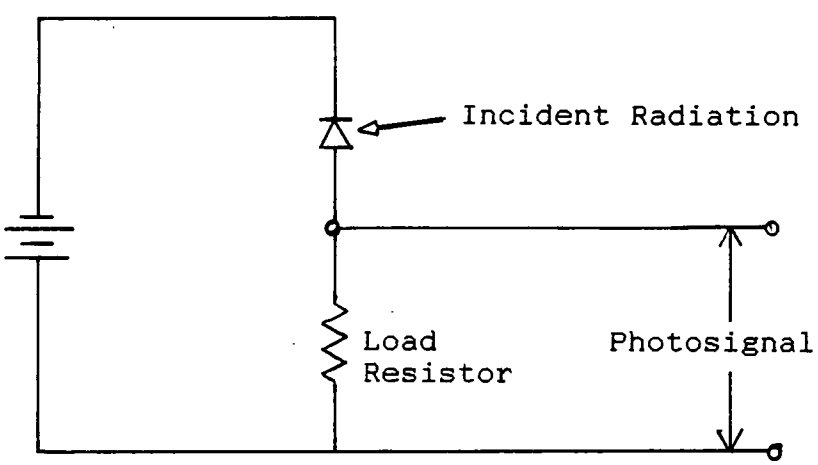

Reverse Bias Photoconductivity

that of the photoconductor already discussed.

The typical geometry employed in a p - n photodiode is shown in figure 2.4.3.

2.4.2.d Avalanche Photodiode

This is a basic p - n junction photodiode which incorporates its own internal gain mechanism. Thus the photosignal of an avalanche photodiode is larger than that of a normal p - n junction photodiode made from the same material and of the same area in response to the same incident radiation power. Although the internal gain cannot increase the signal to noise ratio, and may even reduce it, internal gain is useful in that it reduces the requirements for a high gain low noise amplifier. The gain can also be achieved without much effect on the response time of the photodiode.

In an avalanche photodiode, the bias applied to the structure, and the arrangement of the junction is such that the electric field levels in the depletion region are large. Any electron-hole pairs created by incident photons are accelerated within the high field region of the junction to velocities so high that their collision with lattice atoms transfer energy sufficient to free additional electrons. These are then accelerated, undergo additional collisions, and free more electrons. Thus an avalanche of electrons occurs within the high field region of the junction. In a limited sense, an avalanche photodiode can be considered to be the solid state analogue of a photomultiplier.

The bias levels across the structure are chosen such that the gain is typically between 10 and 100. There are problems

FIGURE 2.4.3

PHOTODIODE GEOMETRY

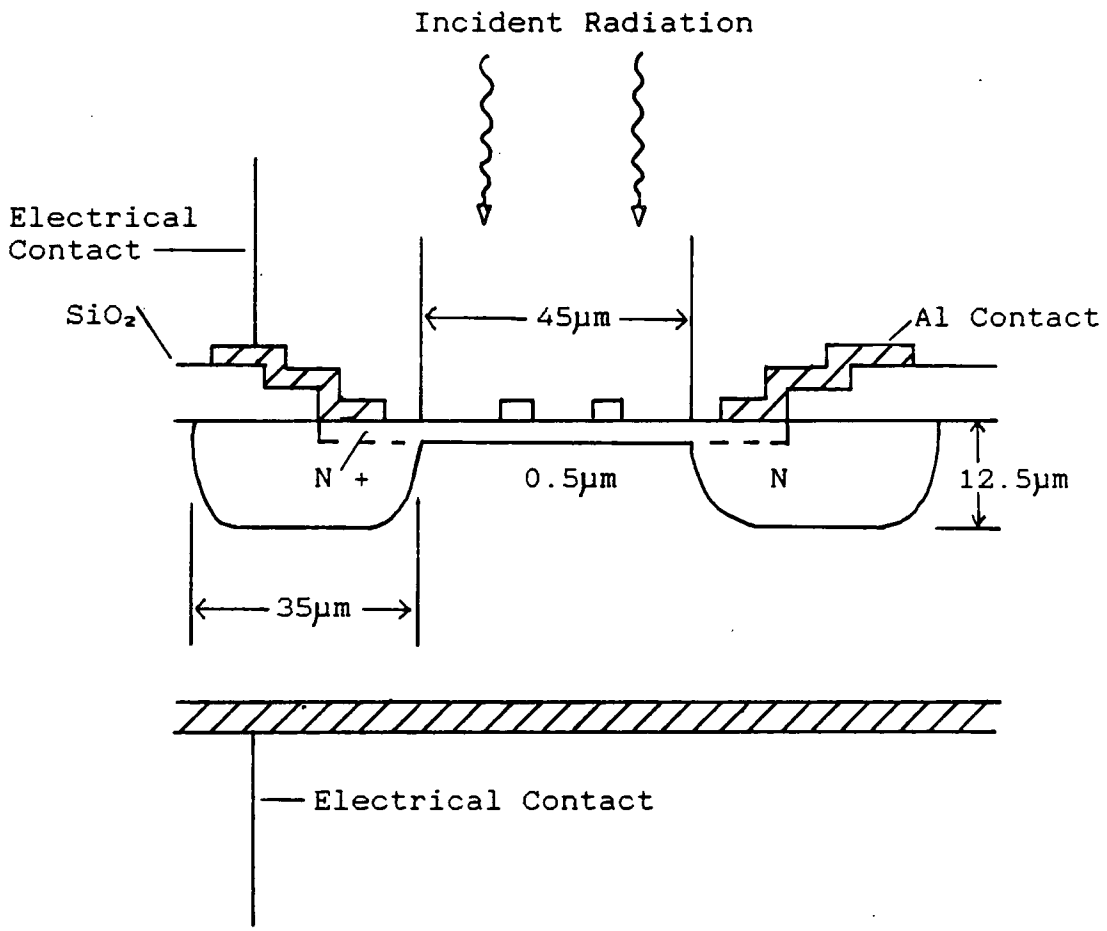

involved in exploiting this gain. The ionisation coefficients, which determine the gain characteristics, are a strong function of temperature. Thus the bias circuit requires compensation for thermal drifts. The ionisation coefficients are also exponentially dependent on the electric field, so that even at constant temperature the bias applied to the device needs to be kept constant to within close limits. The gain process is also statistical in nature. One electron hole pair will create perhaps fifty electrons, all with their own collision histories. This results in an associated noise factor.

Since it is difficult to cause uniform avalanching over a broad area, avalanche photodiodes usually have small sensitive areas. Finally, the bias normally required for these units is around 200V.

2.4.2.e PIN Photodiode

In this detector, a layer of intrinsic semiconductor material is placed between the positively doped and negatively doped regions. The arrangement of a typical device is shown in figure 2.4.4. The surface region (p type in this case) is thin compared to the optical absorption depth. The intrinsic region is thick enough to absorb most of the incident light at the wavelength of interest. Electron - hole pairs are created within the intrinsic region by the incident light, which has passed through the p type region. With the natural potential barrier across the intrinsic material from the p type and n type regions, and an additional reverse bias, the electron - hole pairs are swept rapidly to the electrical contacts by the electric field in the material. Whereas the two regions of charge distribution in a

FIGURE 2.4.4

SECTION THROUGH A PIN DIODE

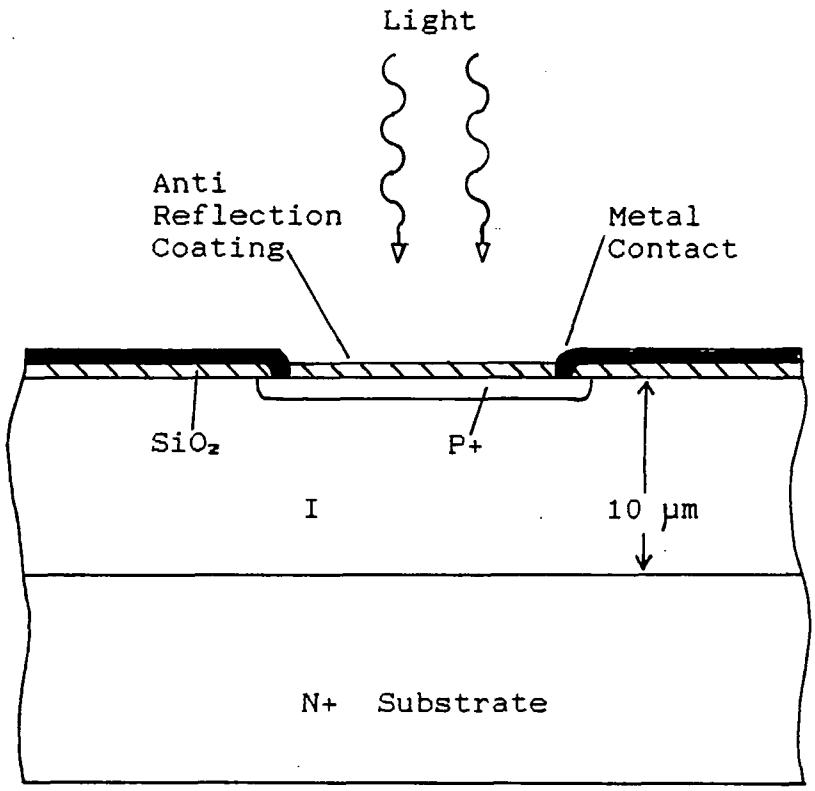

normal p - n junction create a capacitive effect that limits the frequency of light modulation that can be detected to about 100 kHz, p-i-n junction diodes have cut off frequencies as high as GHz.

2.4.2.f Schottky Barrier Photodiode

Not all semiconductors can be prepared in both p and n types. With these materials, a Schottky barrier, one formed at a metal - semiconductor interface, can be produced. As with a p - n junction, a metal - semiconductor interface, when properly made provides a potential barrier which causes separation of photoexcited holes and electrons, thereby giving rise to a short circuit photocurrent, and an open circuit photovoltage. In most cases the metal is in the form of a very thin film which is semi - transparent to the incident radiation. Photoexcitation can occur within the semiconductor or over the potential barrier at the metal - semiconductor interface.

Schottky barrier photodiodes have much faster response times than normal p - n junction photodiodes (GHz). This makes them useful as laser receivers, as does their operation at visible and uv wavelengths.

2.4.2.g PIN - FET Modules

The PIN - FET Module is a combination of small area, low capacitance photodiode and a high output impedance FET preamplifier. The device is used as a hybrid assembly in which all lead lengths and stray capacitances are kept to the minimum. Since the capacitance is low and the output impedance is high the effects of thermal noise can be kept to a minimum. The system

compares favourably with an avalanche photodiode in that a low power supply voltage can be used and it is stable over a range of temperature and electrical bias conditions. Signal to noise ratios of both devices are similar. The PIN - FET advantages are very relevant to instrumentation, where units may be required to operate in environments which are hostile in many respects, including temperature and electrical interference.

2.4.2.h Photoemissive Effect

The third widely used photon detection effect (along with the photoconductive and photovoltaic effects) is the photoemissive effect. As the name implies, the action of incident radiation is to cause the emission of an electron from the surface of the photocathode into the surrounding space, there to be collected by an anode.

There are many applications of the photoemissive effect. Vacuum phototubes, consisting only of a photocathode and an anode, are used for very fast response. Gas filled phototubes, which rely on an avalanche effect arising from impact ionisation of the gas are used for high gain without external amplification. Two of the most well known uses for photocathodes are in image intensifiers, and photomultipliers.

2.4.2.i Image Intensifiers

A basic diagram of an image intensifier is given in figure 2.4.5. Radiation from the object is collected and imaged onto the photocathode by the objective lens. Provided the radiation is of an appropriate wavelength, the emission of electrons will result. These electrons are attracted by an

FIGURE 2.4.5

LAYOUT OF AN IMAGE INTENSIFIER

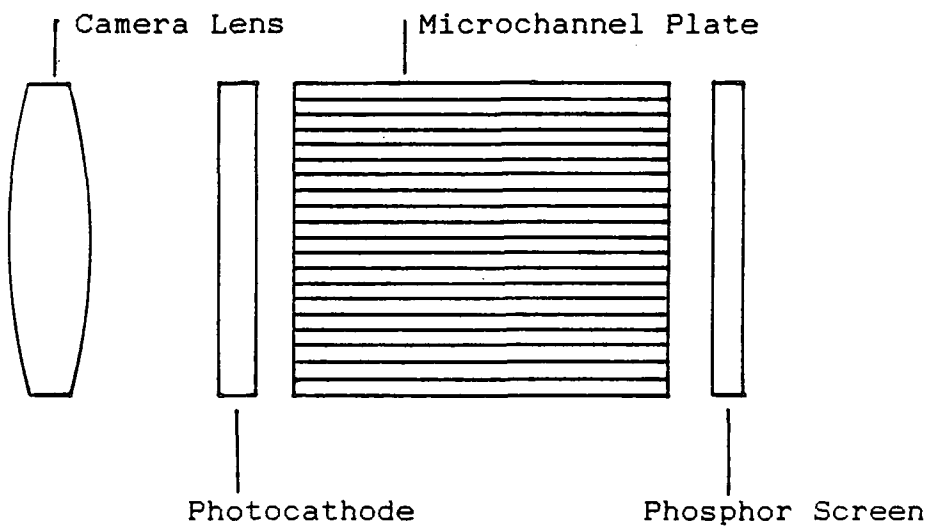

applied field onto a microchannel plate, which is placed as close to the photocathode as possible, to prevent lateral wander of the electrons. At the output end of the microchannel plate is a phosphor screen. Figure 2.4.6 illustrates the conventional image intensifier phosphor screen; and the recently developed intagliated screen.

Today, image intensifiers are being used from the X - Ray through the visible to the near infra - red regions. Although most of the development has been provided by the military, which is still the largest user, image intensifiers have found applications in many other areas. In astronomy they extend the capability of telescopes when images of weak radiation or short duration are to be observed. Law enforcement and the study of nocturnal animals are aided by image intensifiers. They allow faster recording in spectrometers. In medicine, X-ray intensifiers are widely used to reduce dosage rate and to observe dynamic processes.

2.4.2.j Photomultipliers

Photomultipliers produce a current output which is proportional to the light intensity incident upon them. The characteristics of photomultipliers are considerably affected by different methods of construction, and specifications must be studied carefully to match any unit with the requirements of an instrument.

Standard windows in photomultipliers are made from borosilicate glass. This material works well for detection of wavelengths of light longer than 350nm. However, below this wavelength, the transmission of these windows drops

FIGURE 2.4.6

IMAGE INTENSIFIER SCREENS

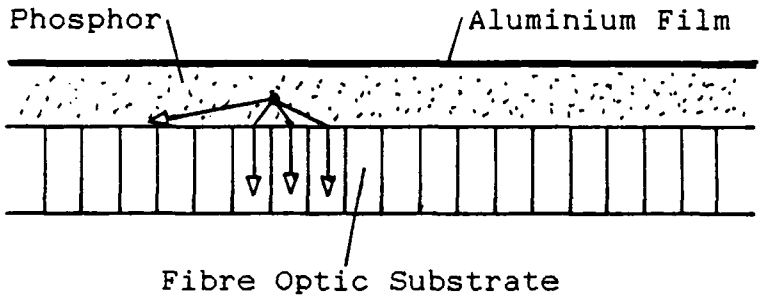

CONVENTIONAL PHOSPHOR SCREEN

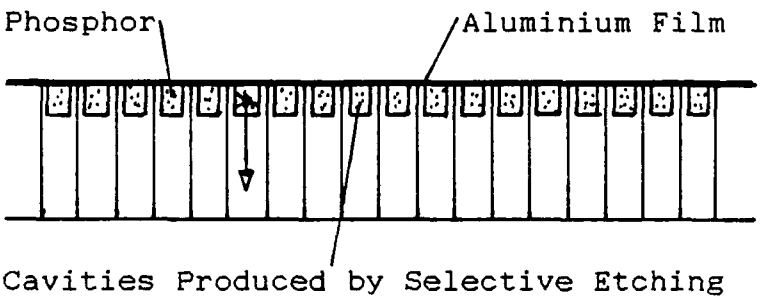

INTAGLIATED PHOSPHOR SCREEN

dramatically. For a unit which is sensitive down to 175nm, a quartz window is required; and a MgF_2 window will allow ultra - violet light extending to around 110nm to be detected. See figure 2.4.7.

The photosensitive material which forms the semi transparent coating on the photomultiplier window can be manufactured from a variety of compounds. This has a considerable effect on the sensitivity of the instrument as a function of wavelength, and care must be taken to match this to the required performance. In general it is easier to produce sensitivity at shorter visible wavelengths than longer wavelengths.

The design of the electron multiplier also affects the perfomance of the unit. It is important to match the number of dynodes to the gain required. If too many stages are used, the inter electrode voltages will be too low, resulting in poor linearity. With an insufficient number of stages, it will not be possible to lift the gain to the required level. At the extremes of perfomance, the materials used on the surfaces of the dynodes become important. Beryllium copper dynodes exhibit good long term stability and pulsed current linearity, while caesiated antimony dynodes achieve rapid settling times between different light levels. Finally, electron multipliers can be made in a number of different geometric structures. Table 2.4.3 gives a comparison of the relative characteristics of each type.

Recent research into improving the characteristics of photomulipliers has concentrated on extending the wavelength sensitivity of the photocathode material. The responsivity in the red and infra - red parts of the spectrum has been steadily improved over the last few years.

FIGURE 2.4.7

TRANSMISSION CURVES FOR PHOTOMULTIPLIER WINDOWS

1: Magnesium Fluoride

2: Spectrosil

3: Sapphire

4: Corning 9741

5: Borosilicate

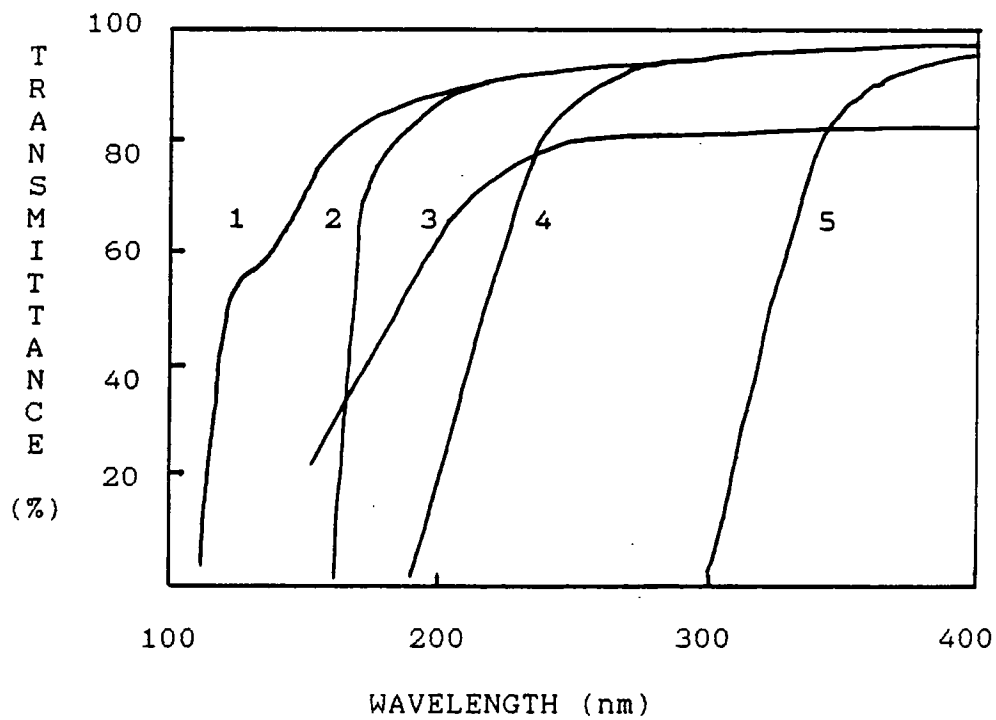

TABLE 2.4.3

ELECTRON MULTIPLIER CHARACTERISTICS

TYPE OF STRUCTURE	SIZE Smallest Volume	GAIN Maximum Overall	TIMING Fastest	LINEARITY Highest Pulsed Current	MAGNETIC IMMUNITY Best
VENETIAN BLIND	3	2	3	3	3
COMPACT FOCUSSED	1	4	2	2	1
BOX AND GRID	2	3	4	4	2
LINEAR FOCUSSED	4	1	1	1	1

Photomultipliers have a wide dynamic range, and gain factors as high as 10^8. However, the responsivity is greatly affected by incident wavelength; they consist of an evacuated glass tube, and as such are delicate instruments, and they require a high applied voltage, which in certain circumstances can be considered undesirable.

In comparison with other visible light detectors they are expensive, with the basic complete unit starting at around £300, and an average price being around £600.

2.4.3 Infra - Red Radiation Detectors

Most infra - red detectors fall into one of two general classes: thermal detectors, and photon detectors. In photon detectors, as already discussed, the incident radiation excites electronic transitions which change the electronic state of the detector. In thermal detectors, the energy of the absorbed radiation raises the temperature of the detecting element. This increase in temperature will cause changes in temperature dependent properties of the detector. Monitoring one of these changes enables the radiation to detected.

2.4.3.a Thermal Infra - Red Detectors

Alhough most types of thermal detector have been in use for many years, they are all still employed in modern instrumentation. They have not been rendered obsolete by the more recent development of photon detectors because for many types of application, use of the appropriate thermal detector is more suitable than a photon detector.

2.4.3.b Thermopile

Thermopiles have been used for over 150 years, and modern thin film versions are still of importance in space instrumentation. The basic element in a thermopile is a junction between two dissimilar conductors having a large Seebeck coefficient θ. Efficient detectors have a large electrical conductivity, a small thermal conductivity (preventing heat losses) a high absorption coefficient, and a small thermal mass (for fast response time).

Early thermopiles were made using fine metallic wires for the elements and attaching the hot junction to a receiver made of blackened gold foil. The use of semiconductor elements produces a much improved sensitivity, however, these thermopiles are difficult to make and are delicate. An improved metal version is used today, where the gold foil receiver is also used as a contacting link between the two active elements. Although metal thermopiles are not very sensitive, their robust nature and reliability make them widely used. The development of thin film techniques has allowed thermopiles to be designed with antimony and bismuth elements, which are cheap, reliable, and can be fabricated as complex arrays. Thermopiles are still widely used in infra - red spectrometers.

2.4.3.c Bolometers

A bolometer makes use of a material in which the resistivity is a function of temperature. In a sense it is the thermal analogue of a photoconductor, where incident radiation causes the heating effect. The signal is detected in the same way as for a photoconductor. The thermistor, and cryogenic semiconductor bolometers are of most importance; metal bolometers

are not very sensitive, and superconducting and superinducting bolometers are highly complex.

A thermistor bolometer is a thermally sensitive resistor. It is made of an oxide of manganese, cobalt, or nickel. An electrical bias is applied across the material. Self heating effects due to internal power dissipation from the bias current must be considered. With increasing bias the temperature rises rapidly and the slope of the current-voltage characteristic decreases and eventually becomes negative. Unless a ballast resistor is employed, thermal runaway will occur at this point, and the thermistor will burn up. They are usually operated below this critical bias. They are also operated uncooled and so are relatively inexpensive. Since ambient temperature affects the resistance, a bridge circuit is employed in which one of the two identical elements is shielded from the incident radiation. Thus radiation energy will imbalance the bridge but changes in the ambient temperature will not. Figure 2.4.8 shows a typical thermistor bolometer.

A cryogenic bolometer employs Ga doped single crystal Ge as the sensitive element operated at 4K. These semiconductor bolometers exhibit high sensitivity and reproducibility, and low noise. While their low operating temperature is a disadvantage for instrumentation as a whole, they are especially useful for astronomical applications.

2.4.3.d The Golay Cell

In the Golay cell, radiation absorbed by a receiver inside a closed capsule of gas (usually xenon for its low thermal conductivity) heats the gas causing its pressure to rise which

FIGURE 2.4.8

THERMISTOR BOLOMETER

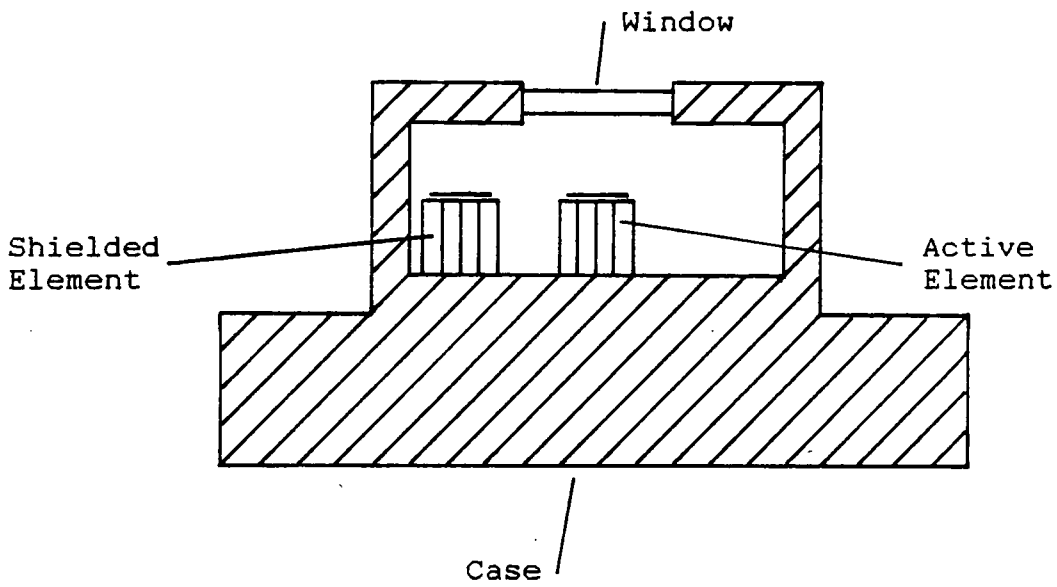

distorts a flexible membrane on which a mirror is mounted. The movement of the mirror is used to deflect a beam of light shining on a photocell and so producing a change in the photocell current as the output. In modern Golay cells the beam of light is provided by a light emitting diode and a solid state photodiode is used to detect it. Figure 2.4.9 shows the outline of a Golay cell.

Another method of obtaining an electrical output from the gas cell is to place a fixed conductor near the distorting membrane forming a variable condenser which can be measured with a suitable circuit. This arrangement is used in the ONERA detector, and it is also used in gas analysers (Luft cells) in which the gas to be analysed is placed in one cell and the output compared with that from another cell containing a reference sample of gas.

Although these various types of pneumatic detector seem awkward compared with modern solid state devices, their importance should not be underestimated. Although they are bulky, comparatively fragile, sensitive to vibration and have a slow response time, their high room temperature sensitivity means that they are still the basic detector used in a large amount of laboratory instrumentation, and gas analysis employing the Luft cell is widely used.

Performance relative to other uncooled detectors is illustrated in figure 2.4.10, which shows the detectivity (commonly expressed as D^*) versus wavelength for a number of detectors.

FIGURE 2.4.9

GOLAY CELL

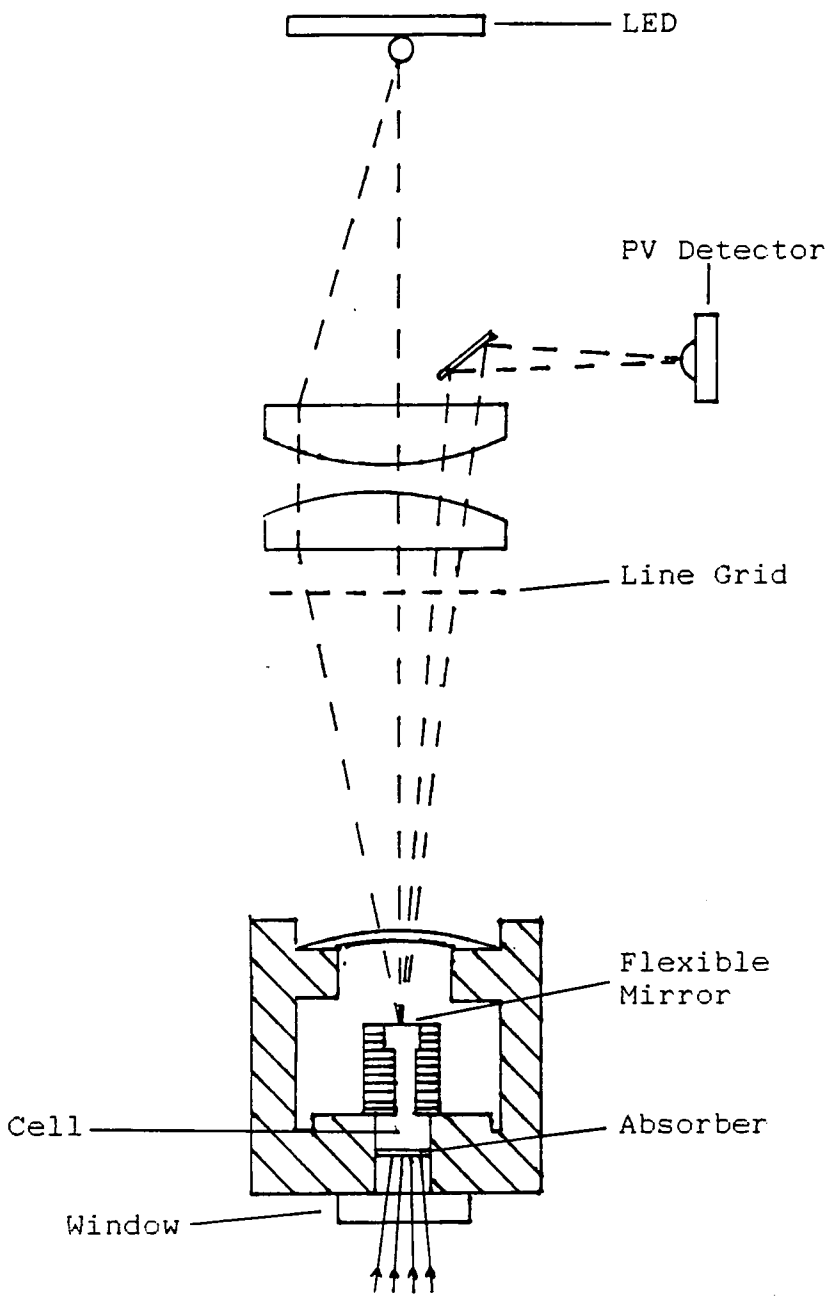

FIGURE 2.4.10

PERFORMANCE OF UNCOOLED THERMAL DETECTORS

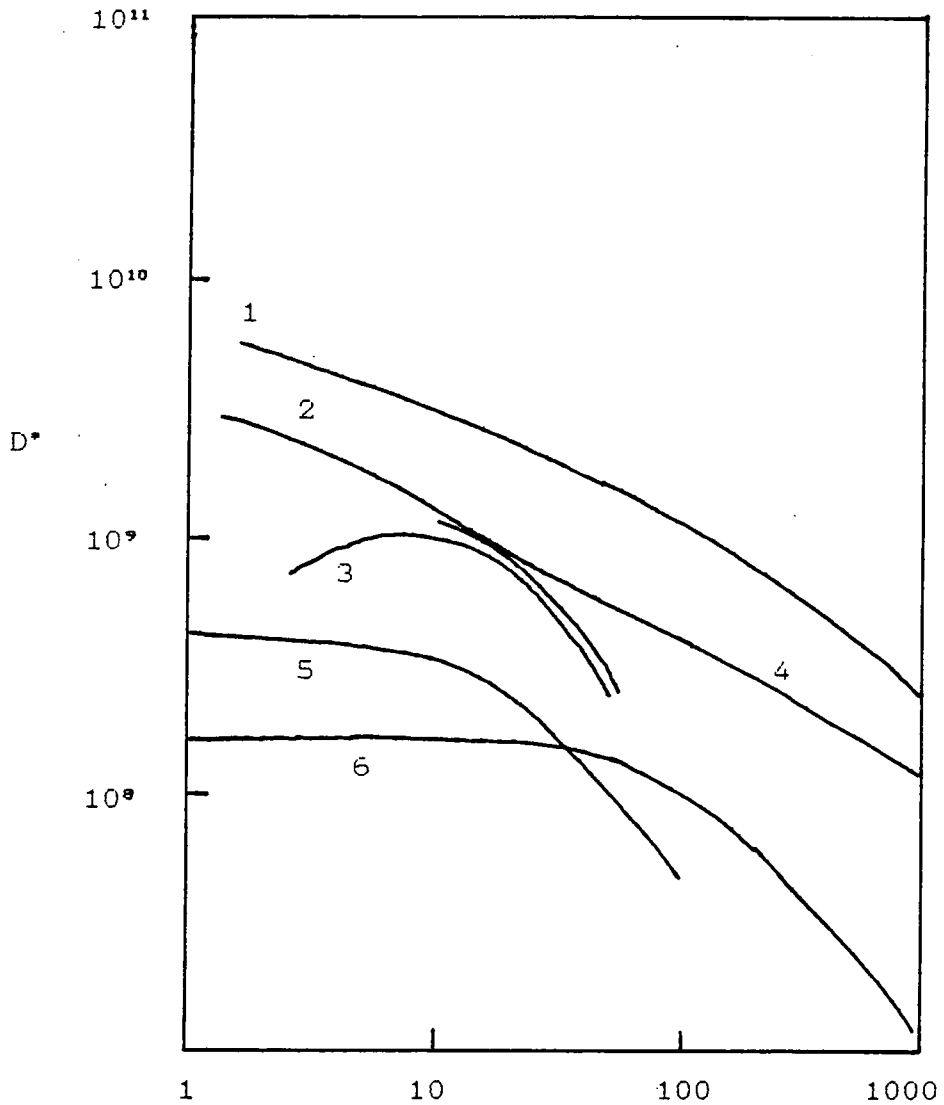

1: TGS: alanine
2: Spectroscopic Thermopile
3: Golay Cell
4: TGS: ruggedised
5: Evaporated Film Thermopile
6: Immersed Thermistor

2.4.3.e Pyroelectric Detector

Pyroelectric detectors are capacitors, having metallic electrodes applied to opposite surfaces of a temperature sensitive ferroelectric crystal. A ferroelectric crystal is one which possesses an internal electric dipole moment; that is it exhibits spontaneous electric polarization. At a constant temperature the internal charge distribution will be neutralised by free electrons and surface charges, so there will be no voltage across the electrodes. However, if the temperature is rapidly changed, the internal dipole moment will change, producing a transient voltage until the internal charge distribution is neutralised once again. This pyroelectric effect can be exploited as a sensitive detector of modulated radiation, operating at ambient temperature. Large signals are obtained from pyroelectric materials which have a large ratio of pyroelectric coefficient to dielectric constant.

The principal materials used for pyroelectric detectors are members of the triglycine sulphate (TGS) group, lithium tantalate, strontium barium niobate, ceramics, members of the lead zirconate titanate (PZT) group, and more recently, films of the polymers polyvinyl fluoride (PVF) and polyvinylidene fluoride (PVF_2). The TGS materials are used for the most sensitive detectors and also in the pyroelectric vidicon.

A growing application for the simple ceramic detectors is in burglar alarms and other security devices. The higher performance devices are becoming more widely used in infra - red instrumentation, including satellite radiometers and horizon sensors.

2.4.3.f Infra - Red Photon Detectors

Infra - red photon detectors, in general, work in the same way as the visible light photon detectors just described. The principles of intrinsic and extrinsic photoconduction, and the photovoltaic effect, are all the same. Although the same materials, such as silicon and germanium are still used, a range of different materials appear, to cope with the long wavelengths. Table 2.4.4 shows the various characteristics of the most well known solid state infra - red photon detectors.

The most noticeable difference between visible and infra - red photon detectors is the operating temperature. While some operate at room temperature, most have to be cooled: some to 195K, others to 77K, others to even lower temperatures.

Room temperature detectors can simply be housed in a modified transistor package fitted with an infra - red transmitting window.

For detectors that must be operated at low temperatures, a simple packaging technique is to use a liquid cryogen such as liquid nitrogen in a simple glass Dewar, once again with an infra - red window. More robust metal Dewars have been developed within which detector elements, filters and windows can be changed if necessary. However, these packages are usually larger, and must be periodically evacuated.

An alternative method is the thermoelectric cooler (using the Peltier effect). Present thermoelectric coolers can be made to operate at around 195K in room temperature ambient conditions, using about 5W of electrical power.

Finally, two other infra - red photon detectors are worthy of note.

TABLE 2.4.4

PERFORMANCE OF INFRA RED PHOTON DETECTORS

DETECTOR TYPE	MODE	SPECTRAL RANGE (um)	TEMPERATURE (°K)	λ_m (μm)	D^* RANGE (cm $Hz^{1/2}W^{-1}$)
PbS	PC	1 - 3.0	295	2.4	$0.8 - 1.5 \times 10^{11}$
PbS	PC	1 - 3.5	195	2.8	$4 - 8 \times 10^{11}$
PbS	PC	1 - 4.0	77	3.2	$1.5 - 2.5 \times 10^{11}$
InAs	PV	1 - 3.8	295	3.4	$3 - 5 \times 10^{8}$
InAs	PV	1 - 3.5	195	3.2	$5 - 8 \times 10^{11}$
InAs	PV	1 - 3.2	77	3.0	$0.5 - 1 \times 10^{12}$
$Hg_{0.8}Cd_{0.2}Te$	PC	1 - 5.0	192	4.6	$1 - 2 \times 10^{11}$
InSb	PV	1 - 5.4	77	5.3	$1.5 - 2 \times 10^{11}$
PbSe	PC	1 - 4.4	295	3.8	$0.3 - 1.5 \times 10^{10}$
PbSe	PC	1 - 5.1	195	4.8	$1 - 5 \times 10^{10}$
PbSe	PC	1 - 7.0	77	5.0	$1 - 2.5 \times 10^{10}$
GeAu	PC	2 - 10.6	77	5.5	$3 - 7 \times 10^{9}$
$Pb_{0.2}Sn_{0.8}Te$	PC	1 - 12	77	11.0	$2 - 6 \times 10^{10}$
$Hg_{0.8}Cd_{0.2}Te$	PC	1 - 13	77	12.0	$2 - 6 \times 10^{10}$
GeHg	PC	2 - 14	30	11.0	$1 - 2 \times 10^{10}$
SiGa	PC	2 - 17	23	16.0	$1 - 2 \times 10^{10}$
GeCd	PC	2 - 22	20	21.0	$2 - 3 \times 10^{10}$
SiAs	PC	2 - 23	18	22.0	$2.5 - 4 \times 10^{10}$
SiP	PC	2 - 28	15	23.0	$1.5 - 3 \times 10^{10}$
GeCu	PC	2 - 30	14	24.0	$1.5 - 3 \times 10^{10}$
GeZn	PC	2 - 40	8	38.0	$1 - 2 \times 10^{10}$

2.4.3.g Rollin Detector

In this device, a long wavelength photon is absorbed by an electron near the bottom of the conduction band, so promoting it to a higher energy state within the conduction band. This increases the mobility of the electron; when this happens for many electrons an increase in electrical conductivity results. This device is different from all the other photon devices described above, because in those cases the carrier concentration is changed. The probability of absorption of a photon by a free carrier electron is proportional to the square of the wavelength: the device is therefore most effective at long wavelengths (above 50um).

2.4.3.h Putley Detector

This is an improved Rollin detector. A magnetic field is applied to the semiconductor. This moves the energy levels of the impurities away from the conduction band, thereby increasing the responsivity over that of the Rollin detector. The magnetic field also produces a Landau sub band from the conduction band. Electrons from the impurities can be excited into this sub band with very small photon energies - less than 1 meV - so that response beyond 1000μm is possible.

However the Putley detector has limited applicability since it must be cooled with helium, and requires a superconducting electromagnet to produce the magnetic field.

CHAPTER 3 DETECTING UNWANTED MATERIALS AMONGST CULLET

3.1. Introduction

This chapter describes an instrument designed to detect unwanted material amongst cullet on a conveyor (see plate 3.1). The original problem is discussed, and then the development of the instrument is followed through from the principle of the design to completion of the trials.

Cullet consists simply of pieces of broken glass. Its use is important in glass production. It obviously reduces glass wastage, but it also forms part of the melting process, since cullet is easier to melt than raw materials. It has two major origins in the glass industry: internal, which is largely from broken up sheet, plate, or ribbon glass containing faults; and external, from building sites where glazing is carried out, or from broken bottles salvage. Whatever the source, the cullet is normally transferred by conveyor belt to large tanks at the head of the melting furnace to be released when necessary.

Clearly it is desirable to prevent any substances other than cullet or raw materials for glass from entering the furnace, thereby maintaining a consistent product. However unwanted items do appear from time to time, especially amongst the cullet. These range from metallic objects such as cans or wire, to wood, paper, packing material and even clothing.

A powerful electromagnet positioned above the conveyor will remove ferrous materials. A metal detector will pick out any other metallic objects, and it can be used in conjunction with a method of removing material from the conveyor. However, non - metallic objects present a more difficult problem. Many years ago

PLATE 3.1

REFRACTORY DETECTION EQUIPMENT

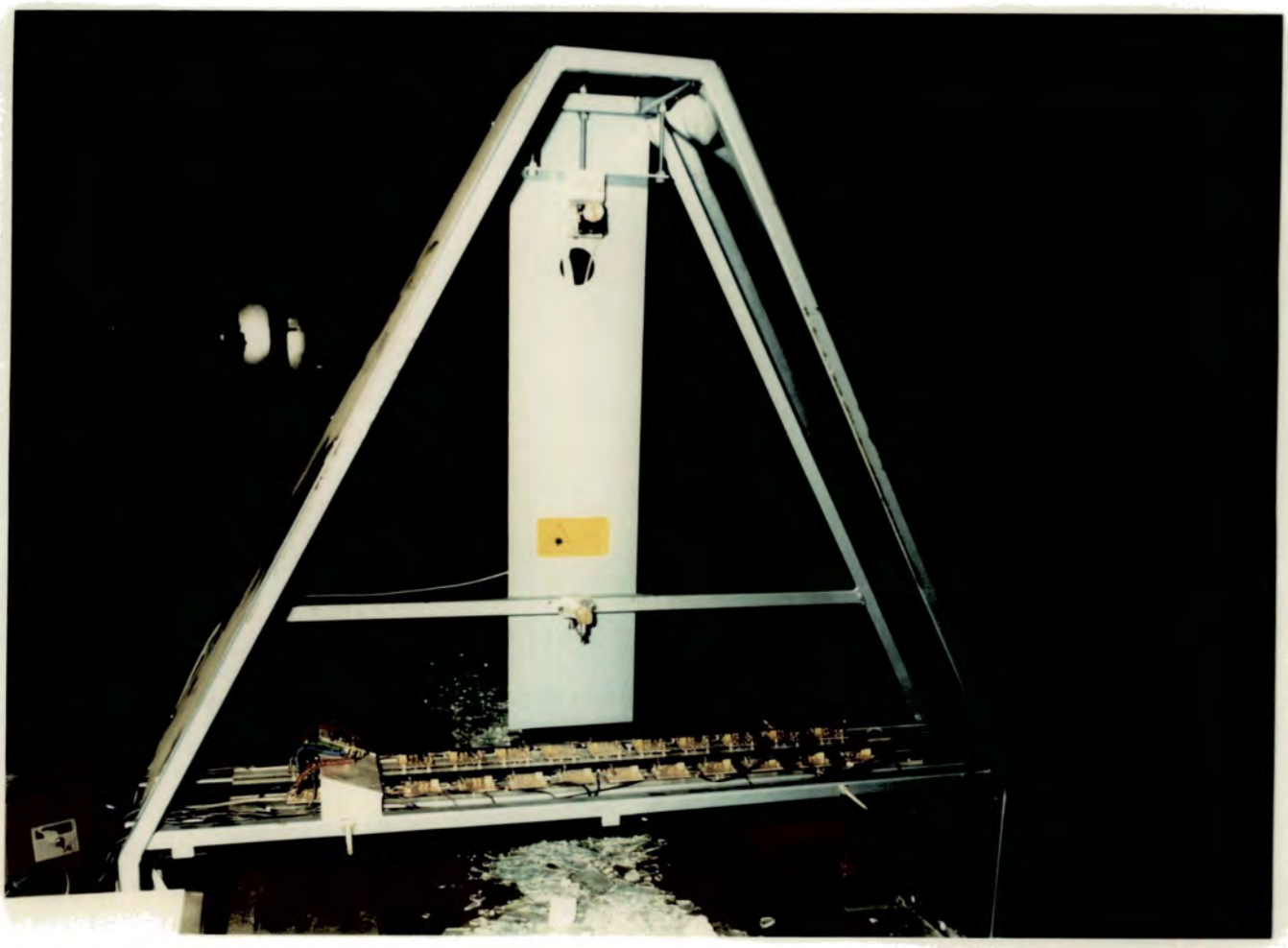

people were employed to inspect the cullet conveyors and remove anything other than glass. This was labour intensive, prone to mistakes, and considered to be dangerous to the operator in any case. There therefore remained the difficulty of distinguishing between broken glass, and other non - metallic substances amongst it. Any instrument capable of doing this automatically would have to do so across a belt 800mm wide, piled several centimetres high with glass, travelling at 1 metre per second.

3.2. Principle of Detection of Non - Metallic Contaminants and Prototype Instrument

3.2.1 Experimental Basis

After removing the ferrous and non - ferrous metals, some method was needed to distinguish between broken glass and the remaining unwanted materials amongst it. As already stated, these materials included wood, paper, polystyrene blocks used as glass packing material, house bricks, and refractory bricks, which are used to construct furnaces.

The most obvious distinguishing feature from an optical point of view is that the surface of glass reflects light shone upon it, whereas the surfaces of most of the other materials scatter it. This is true provided that the glass has a surface which is continuous over the width of the light shone on it: If the glass has been broken into pieces smaller than the incident light beam, the large number of randomly oriented surfaces would produce an effect similar to scattering. Pieces of glass in cullet are typically of the order of a few centimetres in size. It is therefore necessary to devise an optical system which can determine whether an area of one centimetre or less contains a

reflective material or a scattering one.

The fine, directional beam produced by a laser is ideal for this application. An experiment was therefore devised to study the effects of illuminating different materials with a helium neon laser beam (helium neon lasers are discussed in section 2.2.2.a). The layout is illustrated in figure 3.1. The laser beam was directed at the material to be examined. Around the material was a turntable in the form of an annulus, which could be rotated without affecting the sample. Attached to the turntable was an arm with a photocell on it. The photocell was a 100mm² active area UDT version, which gave a calibrated readout in watts. The arm was 90cm long, to provide sufficient angular resolution. Measurements were taken at angular intervals of 5 degrees from the axis of the input laser beam.

The results of these experiments can be seen in figures 3.2 and 3.3. These show that in the case of the unwanted materials, the level of scattered light was uniform to within a factor of two from a viewing angle on axis to one at 45 degrees. That level was approximately 15 to 30 uW / cm² . However the material that was wanted, the glass, behaved entirely differently, even when very dusty. On axis, clean glass returned approximately 500 uW / cm² of the laser light (corresponding to 8% of the output of the 5mW laser, as expected: 4% from each surface). Dusty glass produced half this amount; 250 uW / cm². Off axis, no signal could be picked up from either of the two samples. Consequently any light signals detected at angles larger than 5 degrees from the incident beam indicated scattering from a non - glass surface.

It is this clear distinction which is used in the basic

FIGURE 3.1

MEASUREMENT OF SCATTER

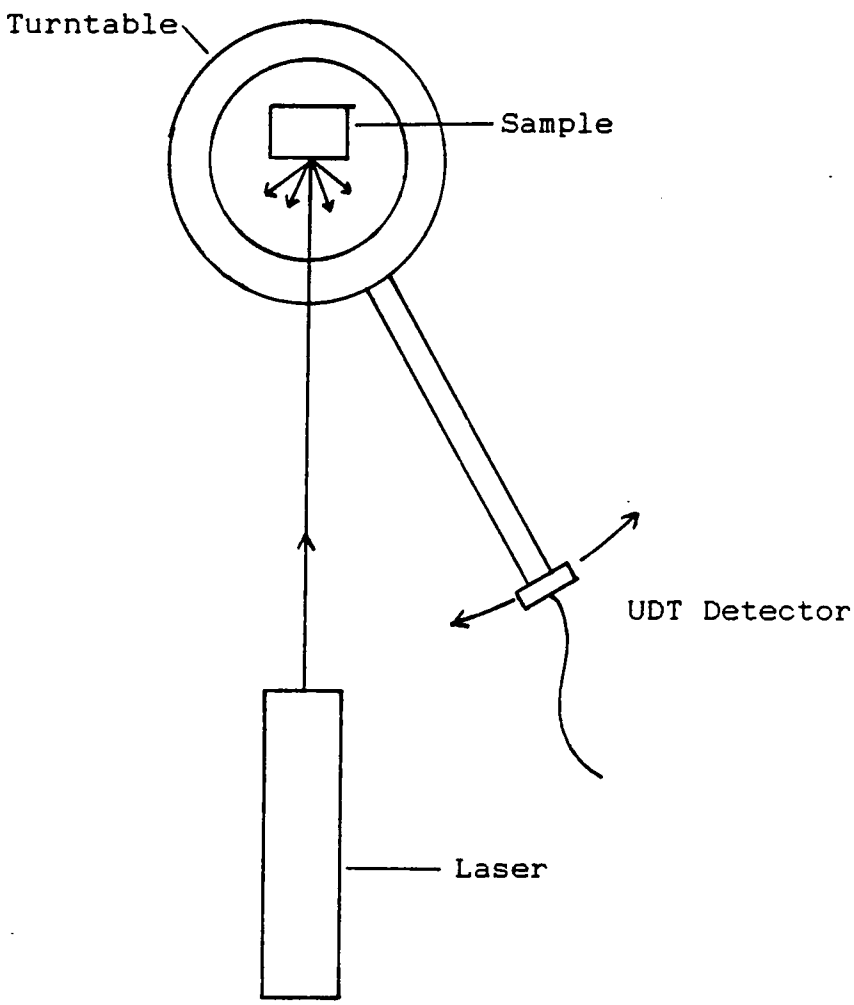

FIGURE 3.2

SCATTER FROM CONTAMINANTS

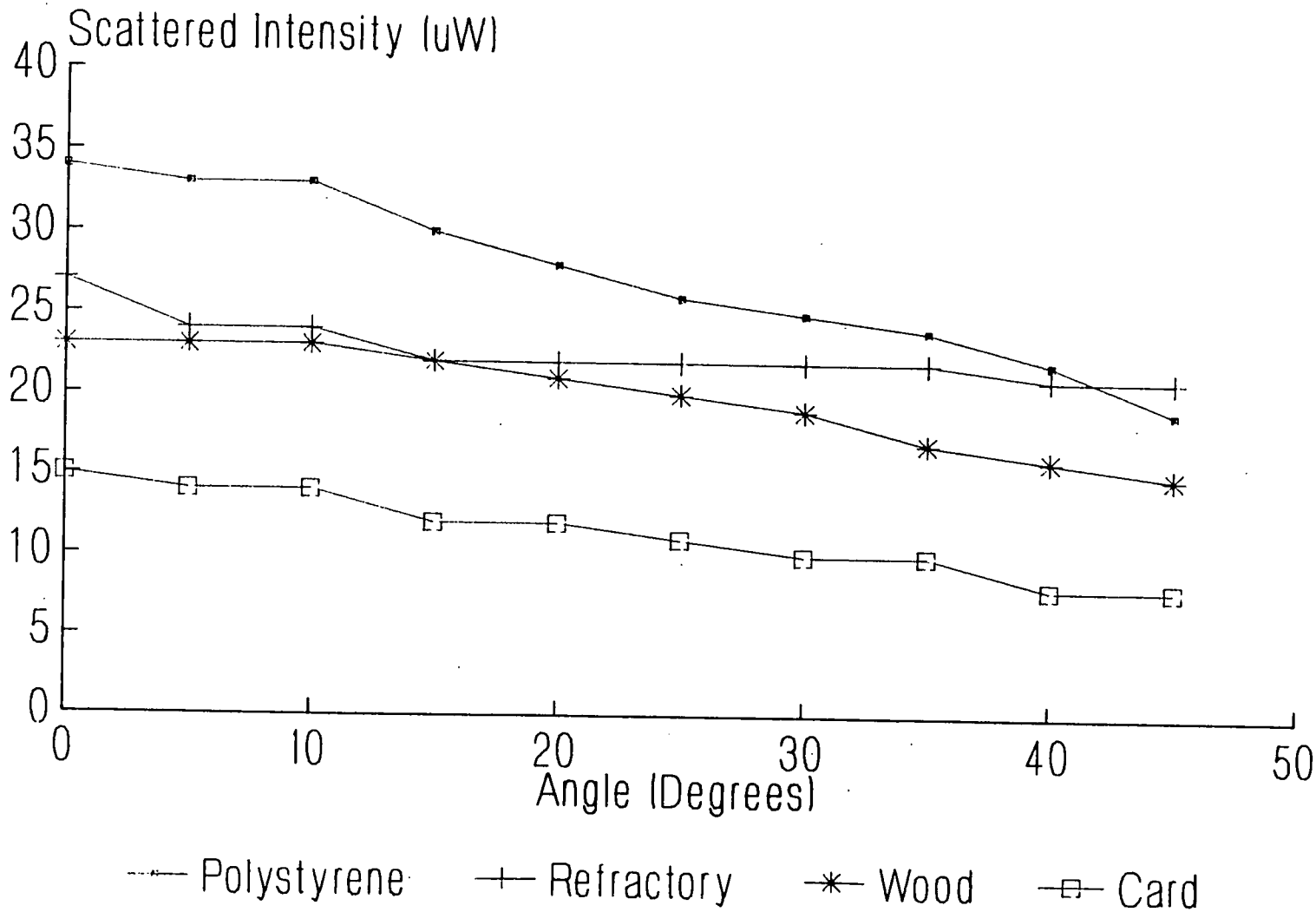

FIGURE 3.3

SCATTER FROM GLASS

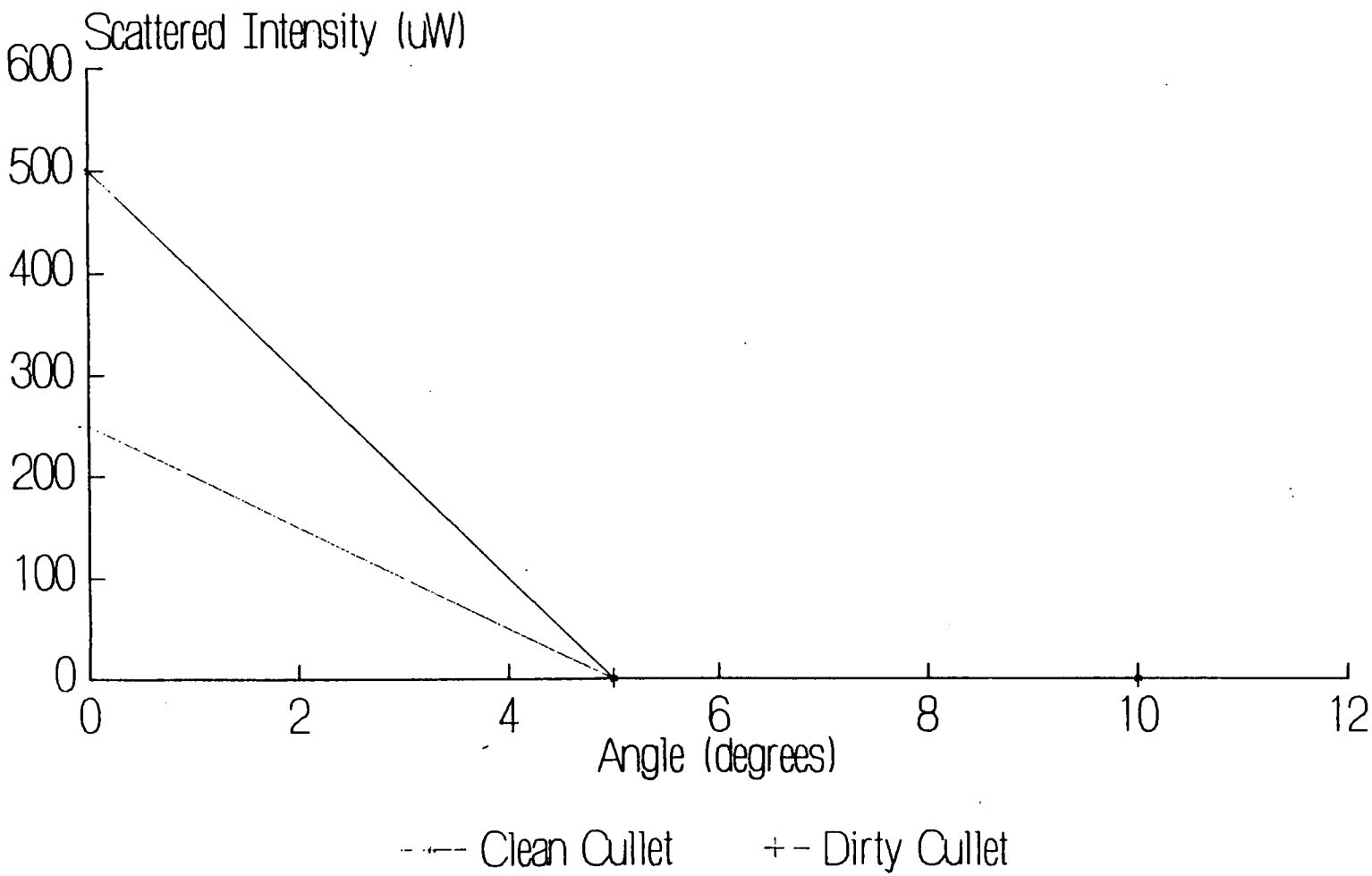

design for the instrument.

3.2.2 Basic Design

In the laboratory, a long thin pile of cullet was made, and small pieces of refractory were placed amongst the glass to simulate the contaminated conveyor belt. A low power helium neon laser was directed onto a small mirror, and then vertically down onto the cullet. Above the mirror was a piece of ground glass acting as a screen. The laser, mirror and screen were placed on a slide, and moved along the pile of cullet.

As the laser beam was moved across the cullet, the patterns on the screen above the mirror showed the light distribution produced by the cullet and the refractory. A difference could clearly be seen; the cullet produced one or two bright spots, or an occasional cusp from an edge, whereas the whole screen was illuminated when the laser was incident on the refractory. This confirmed the results of the different reflection properties of glass and cullet. The monitoring of the cullet depended on detecting this difference reliably.

Several schemes involving imaging the plane of the screen onto a one or two dimensional array were considered. However as the information lay at the position of the screen itself, it was decided to remove the screen, and place four discrete photodiodes around the mirror, with the mirror (and therefore the vertical laser beam) being at the centre of the square. Adjacent detectors were approximately 75mm apart. The outputs of all four detectors were displayed simultaneously on a monitor, using a small microcomputer. As this assembly was moved along the slide, it could be seen that the cullet produced an occasional large signal

in one, or at most two detectors, whereas the pieces of refractory produced a consistent signal, albeit lower, from all four detectors. It was a simple matter to program in a threshold level, also displayed on a screen, and an audible alarm to be activated when all four detectors exceeded this level.

This crude instrument was used to carry out several initial experiments. It was found that no amount of rearrangement of the pile of cullet would produce a signal from glass on all four detectors, although two would often register, and very occasionally a third showed a small signal well below the threshold. Dusty glass produced a higher level of background light, but reflections were still predominant. Wet glass (the cullet is often washed to cut down on dirt and dust) behaved in a similar way, with a higher background level, but signals still appearing in only one or two detectors.

The response from the other materials was more varied. The colour of the material was important: obviously, the darker the material the more light was absorbed by it, and less light was scattered towards the detectors. From this point of view it was fortuitous that the cullet conveyor belt was black, since this would absorb most of the beam and not produce spurious signals. It was also fortunate that most of the unwanted materials were brightly coloured, and so produced a large amount of scattered light. It was found however that most of the materials produced a certain specular component within the scattered beam, so that scattering surfaces at a large angle to the horizontal produced an uneven signal from the detectors. Usually though, as the instrument was moved over the material there would be some point on it at which a large scattered signal

was received in all four detectors simultaneously.

The geometry of the instrument was considered, though the configuration which had originally been set up was close to the optimum for this application. Reducing the separation between the detectors made the signals from the cullet more likely to cover all four of them, whereas increasing the separation moved the detectors away from the point of incidence of the light beam on the glass or refractory, reducing the level of scattered light incident on them.

The laboratory test rig demonstrated that unwanted non - metallic objects could readily be detected amongst the cullet. However the test rig was essentially a static device. That it would work on cullet moving on a conveyor belt, 800mm wide, at 1 metre per second, had to be demonstrated.

3.3. Operation

In order to use the above principle to analyse a large amount of cullet, it was obvious that the laser beam should be moved across the conveyor belt at regular intervals, whilst the conveyor belt moved the glass in the orthogonal direction. It also became clear that the design of the instrument described above was no longer suitable for carrying this out: moving four detectors and a mirror (or the laser itself) back and forth across the conveyor belt would be slow, cumbersome and expensive. It was therefore decided to scan the laser beam across the cullet belt, and keep the detectors stationary.

The level of light reaching the detectors would be low for two reasons. Firstly, laser safety was a prime consideration in an industrial environment, and so a low powered (Class 1, 0.5

mW) laser would have to be used if possible. Secondly, scattered light, by definition, would be produced over a wide solid angle, and so to a first approximation, the flux through any given area (such as that of a detector) would reduce as the square of the distance from the point of incidence of the laser beam on the surface. It was therefore decided to place a number of groups of four detectors across the belt, to maintain signal from each detector.

The type of detectors used were chosen carefully. Versions were chosen with a large sensitive area; 100mm square, to catch the scattered light. These were also the hybrid type, which have an amplifier inside the same container as the detector itself. This reduces the length of the leads to a minimum, thereby reducing stray capacitance; and it also results in a relatively high output voltage as a proportion of signal, reducing electrical interference. These type of detectors are discussed in section 2.4.2.g.

The level of scattered laser light which required detection was so low that some means had to be found to distinguish between it and ambient light. One way of doing this is to filter out wavelengths of light other than that produced by the laser. Interference filters could not be used, because of the expense of fitting one to each of the many detectors (twenty four are used in the production line instrument), and also because the transmission wavelengths of these filters change with the angle of incident light. Since the scattered light would approach the detectors from a large range of angles as the laser was scanned, a correspondingly large range of transmission wavelengths would be required. This would have allowed much of the ambient light to

reach the detectors. Another possibility may have been to use absorption filters. However, the changes in transmission with wavelength of absorbing materials are not so abrupt as can be achieved with interference techniques, and so these filters would also transmit a large amount of ambient light. With these problems in mind, the use of phase sensitive detection was considered as the best method of blocking out ambient light.

Phase sensitive detection is commonly used in instrumentation. Its operation is summarised in figure 3.4, and a full analysis can be found in Horowitz & Hill (3.1). In short, phase sensitive detection is based on modulation. The intensity of the light source is modulated at a fixed frequency, and the electronics associated with the detector(s) are configured to amplify only signals of that same freqency. This is normally done by averaging the detector signal about zero, amplifying the positive half of each cycle positively, and amplifying the negative half of each cycle negatively. This produces in effect a rectified output, which is usually subsequently smoothed. Light signals of other a.m. frequency, therefore have no effect on the signal, provided they do not saturate the detector. It was required that the instrument should be able to resolve materials of approximately 25mm square in size. This meant that at a conveyor belt speed of one metre per second, 50 laser scans a second were needed to be within this target. As is explained later, the scan time across the belt was a little less than the dead time between scans. Therefore each scan lasted 1/100 of a second. It was necessary to resolve an item approximately 1/40 the width of the belt, which would be scanned in 1/100 x 1/40 = 1/4000 of a second. Now in phase sensitive detection, the light

FIGURE 3.4

PHASE SENSITIVE DETECTION

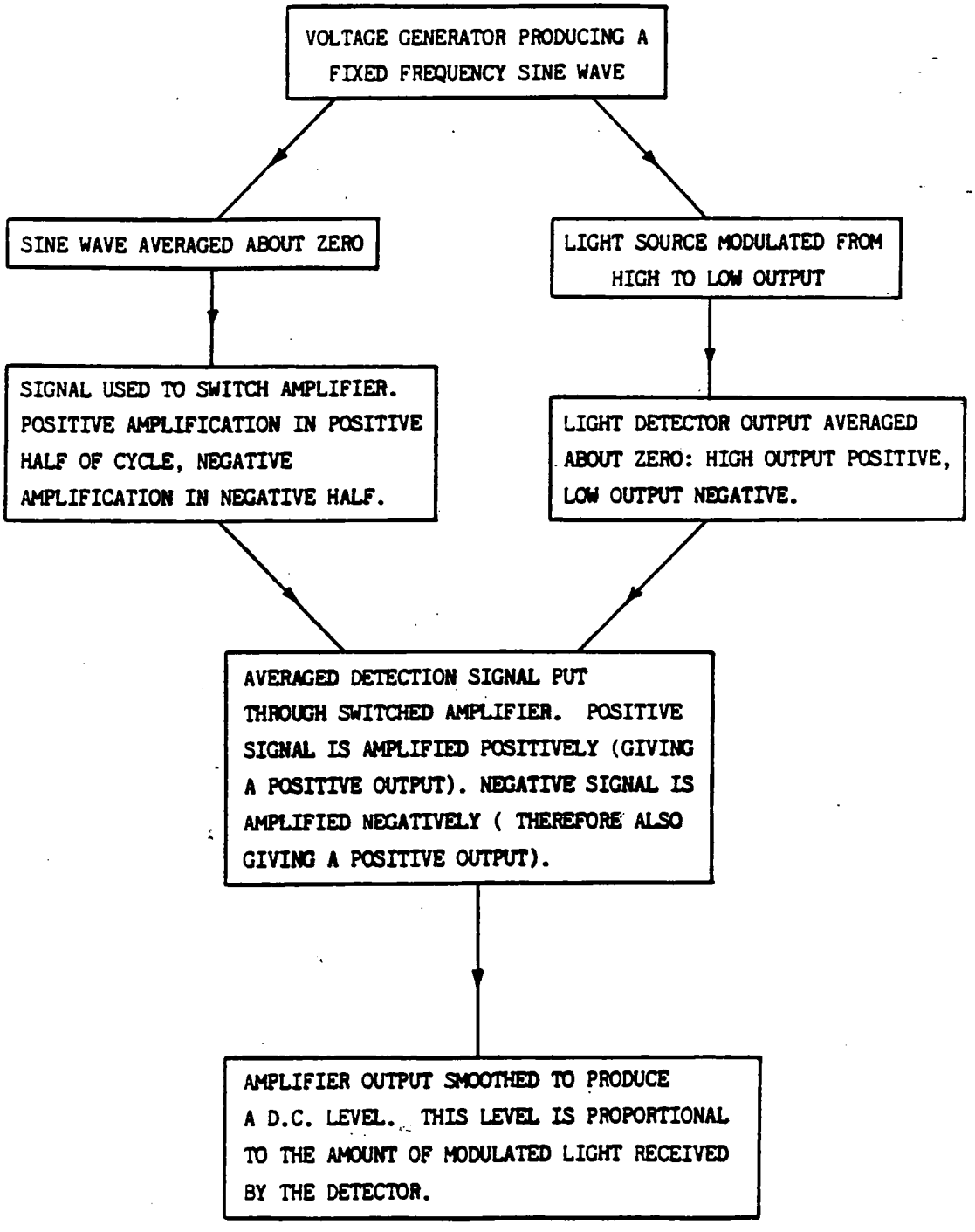

source must be modulated several times during any one detection period. This means that the modulation frequency required for the instrument is of the order of 50kHz. A simple way to modulate the output of a light source is to use a rotating chopper which alternately blocks and transmits the beam, but no chopper could be found which was capable of rotating fast enough to produce this frequency. However a form of chopping is possible using acousto optic modulation. These components would have modulated the beam quickly enough, but they are relatively expensive. The output of a helium neon laser can be modulated, but once again, not at the necessary speed. However, laser diodes have a very quick response of light output to input voltage. A frequency generator was therefore connected to the input voltage of a laser diode package with integral collimating optics, and modulation of its output was achieved well above 50kHz. This is a simple, cheap and appropriate light source for the instrument. The properties of semiconductor lasers are discussed in section 2.2.2.f.

In fact the final system uses both phase sensitive detection and absorption filters. Laser light at 820nm was used, and filters absorbing radiation below 750nm were fitted to the detectors. This was necessary to prevent the high gain on the photodiodes, necessary to detect the scattered light, from driving them into saturation.

3.4. Apparatus

The instrument used on the production line is shown in figure 3.5. The cullet conveyor belt transports a stream of cullet in the direction arrowed. Spanning the conveyor belt is a gantry. Running along the centre of the gantry is a slot through

FIGURE 3.5

CUTAWAY DRAWING OF THE DETECTION SYSTEM ABOVE THE MOVING CONVEYOR BELT

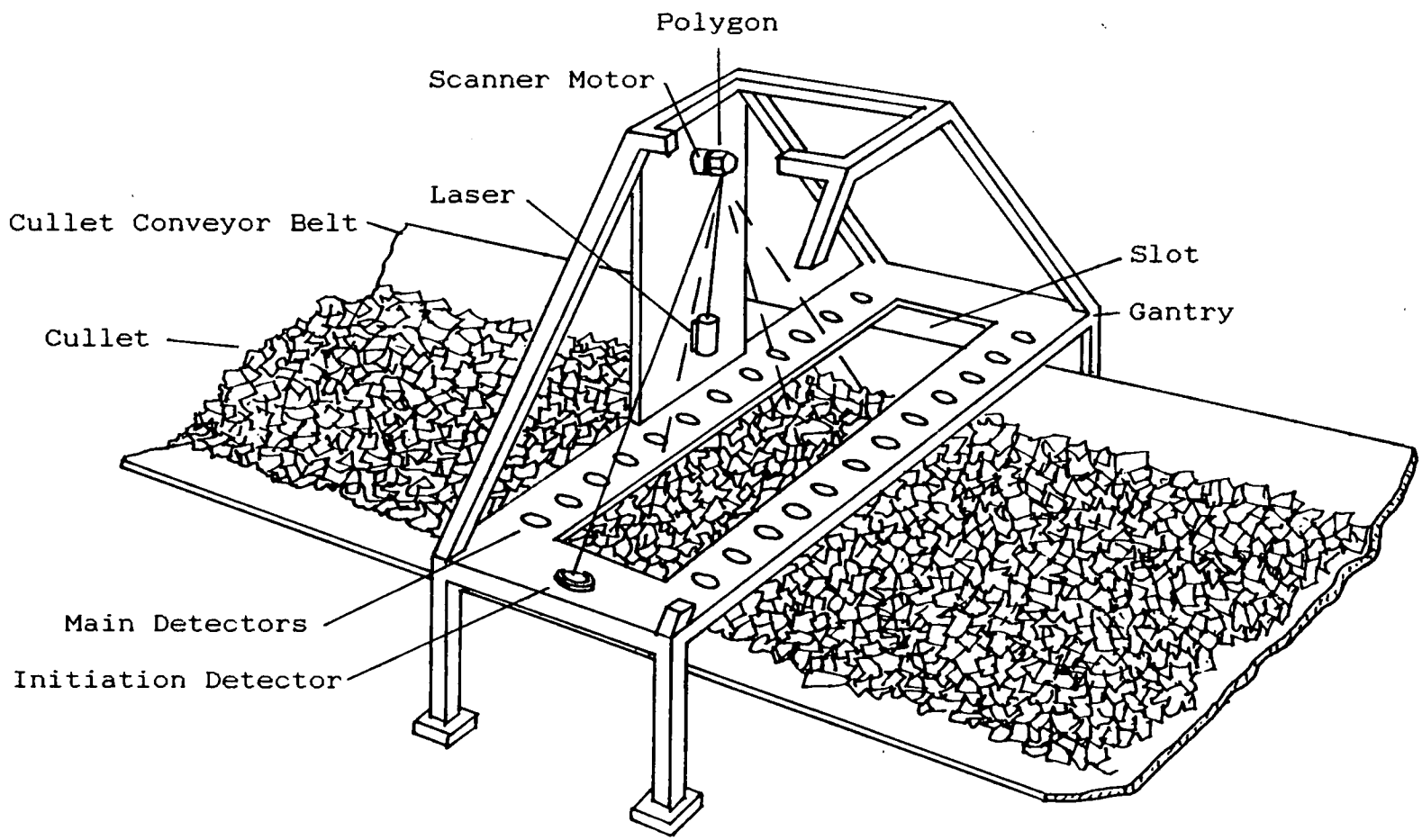

which the laser light is scanned. A single reference light detector is attached to one end of the gantry, and aligned centrally with the slot. When the laser light passes over this detector, the inspection process for each scan is initiated. Either side of the slot are twelve light detectors which project through to the underside of the gantry and face the cullet on the conveyor belt. Above the gantry is a frame (and normally a sheet metal cover, which is excluded in the figure to allow the components to be illustrated). At the centre of this frame is a backplate on which is a solid state laser and a multi faceted mirror scanner wheel driven by a scanner motor.

To protect all these components during operation the metal cover on the gantry has a dust tight seal on it. Also, underneath the gantry is a clear laminated windscreen, which transmits the laser light, and protects the detectors from any accidental impacts. This screen is also attached with a dust tight seal. Some of the beam is obviously reflected by this window, but the direct beam from the laser is merely directed onto the inside of the sheet cover, and the scattered light from the unwanted materials is reduced in intensity by approximately 10%, as would normally happen through glass. The window does not significantly affect the performance of the instrument.

In operation, the collimated beam (approximately 5mm diameter) from the laser diode is directed onto the underside of the scanner wheel, which is rotated by the scanner motor. There are eight reflective sides on the wheel, which successively scan the laser beam in the manner indicated in figure 3.5, that is, through the slot in the gantry and across the cullet on the conveyor belt. To record the beginning of each scan, the laser

beam passes over a reference photodiode. When a signal is received from this photodiode, the inspection photodiodes are activated. A rotary encoder is fixed to the back of the motor, which produces 500 pulses for every revolution of the shaft. The pulses from this encoder are used to activate sets of four detectors as the laser beam is scanned between them, leaving the other detectors de-activated. The scanning polygon is placed high enough above the conveyor belt to ensure that the whole part of the laser beam is reflected onto the cullet at all times. It was found that this would occur providing the scanner was at least one metre above the belt, scanning the beam through an angle of 42 degrees.

To maintain a separation of approximately 75mm between each detector, 12 are needed on each side of the scan. In order to make the most efficient use of the detectors, they are used as illustrated in figure 3.6. One set of four detectors is used at any one time, such that the set immediately above the laser beam is activated, whilst the sets to either side are deactivated. In figure 3.6, the area of the conveyor belt covered by the first set of four detectors is designated 'A'; the area covered by the second set is designated 'B' and so on. Thus when the beam of laser light is sweeping across that area of the cullet belt designated by 'A', the four light detectors immediately above the area are activated, whereas adjacent light detectors are deactivated. Similarly, when the beam of light is scanning across the area 'B' on the cullet belt, those detectors immediately above it are activated and light detectors on either side are deactivated.

Obviously it is desirable to produce an electronic pulse

FIGURE 3.6

COMBINATION OF DETECTORS

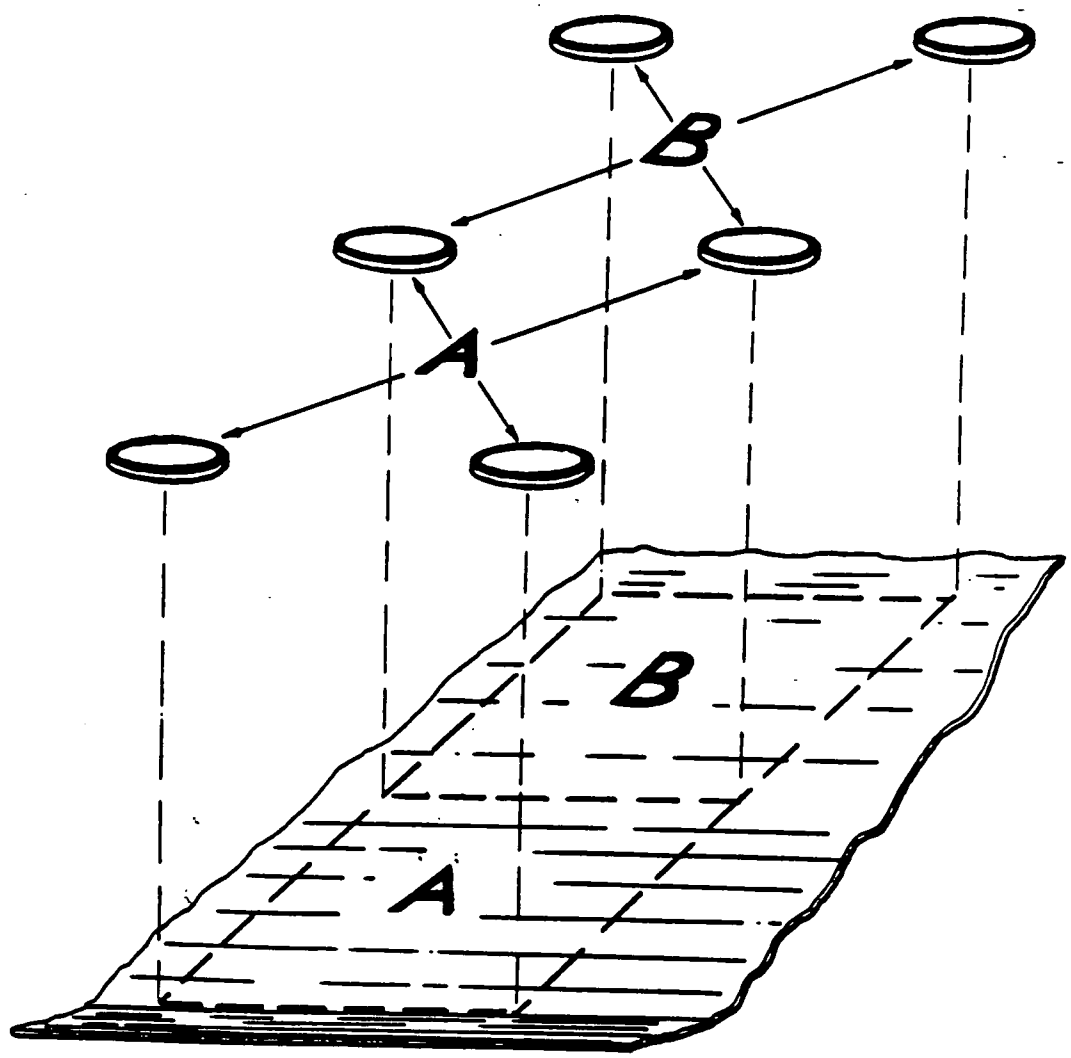

each time the laser scan moves from one area to the next, so that the appropriate detectors can be activated. Since the progress of the laser beam is monitored by the encoder on the scanner motor, opposite pairs of detectors are placed on the gantry such that the scanner wheel moves through an equal angle to move the beam from one pair to the next. This results in the central two pairs of detectors being 69.6mm apart, and the outermost pairs being 76.4mm apart. However the angle of scan between all twelve pairs is the same: 3.82 degrees. This corresponds to a 1.91 degrees movement of the scanner wheel. The photodiode used to produce the initiation pulse was then placed centrally on the gantry in a position which corresponded to 1.91 degrees of scan before the first set of four detectors. To translate the 0.72 degrees separation between the 500 pulses of the encoder to 1.91 degrees, a combination of a gearbox on the output shaft of the motor to reduce the separation between the pulses, and successive halving of the pulse rate using logic circuits to increase the separation between the pulses, was necessary. The combination which resulted most closely in the desired angular separation was a 6:1 gearbox (resulting in pulses every 0.12 degrees rotation) and halving the pulse rate four times, producing a pulse for every rotation of 1.92 degrees of the scanner.

The function of the electronics associated with the instrument is summarised in Figure 3.7. The 'raw' signals from all twenty four detectors are fed separately into the multiplexer board. This board receives the initiation pulse, and then after 1.92 degrees rotation of the scanner wheel, switches the first set of four detectors through to their phase sensitive detector boards. After a further 1.92 degrees rotation the second set of

FIGURE 3.7

SCHEMATIC DIAGRAM OF ELECTRONICS

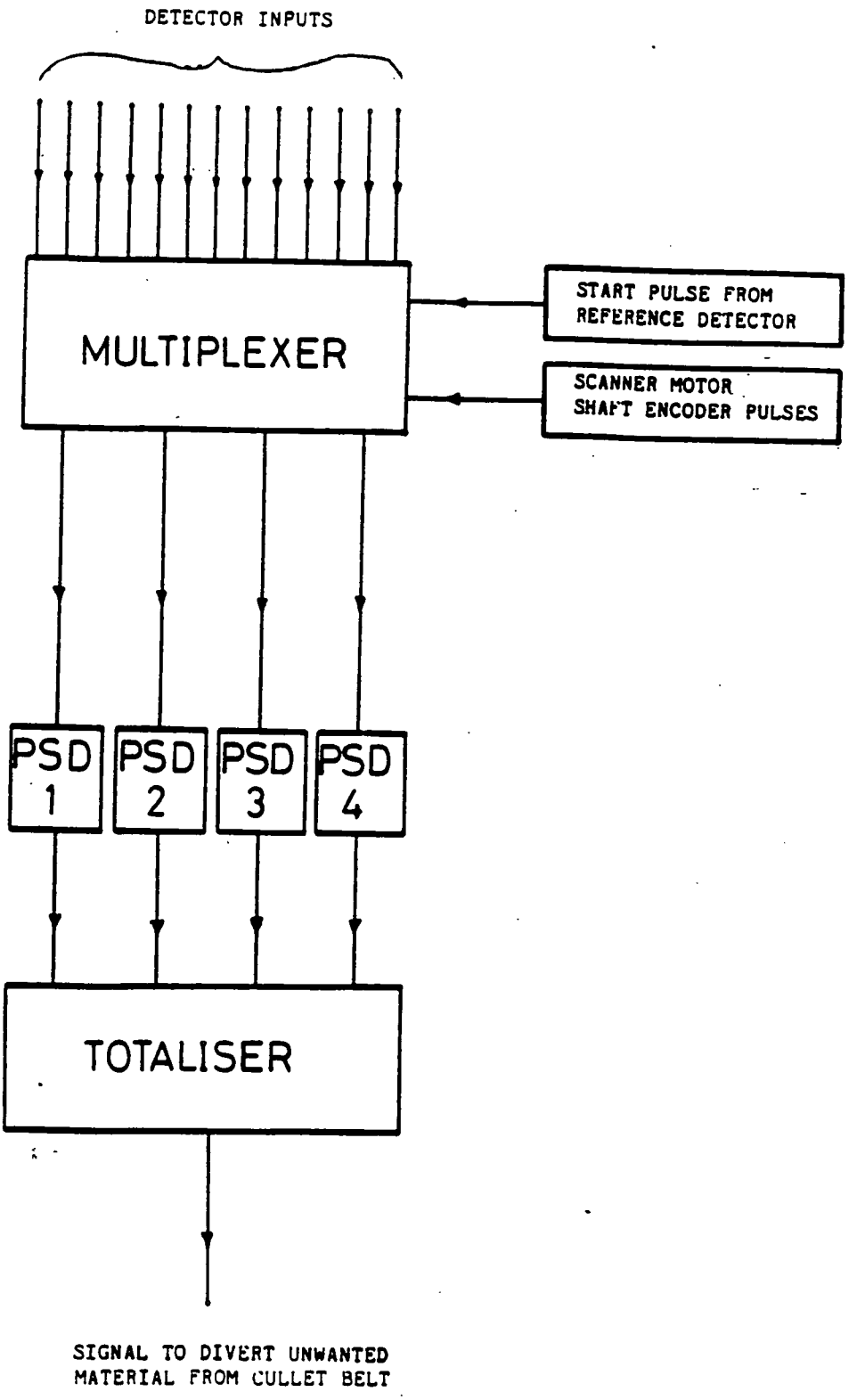

four detectors is switched through. After passing through the phase sensitive detection circuitry, the four detector outputs are fed into a totaliser. Should all four detectors simultaneously produce an output higher than the predetermined threshold level, this circuit will produce an output that can be acted upon. It is normal in instrumentation to convert low levels of signal, or high frequency signals, into a form less likely to suffer from electrical interference. From this point of view it could be argued that the phase sensitive detection circuitry should have come before the multiplexing. However PSD circuits are complex and expensive, so to have a complete circuit for each of the twenty four detectors was considered impractical. Instead, care was taken to prevent interference and crosstalk in the detector outputs.

In the instrument on the production line, the output from the totaliser circuit is processed further. The conveyor belt where the instrument sits carries 'internal' cullet. The most common type of unwanted material in this case is polystyrene blocks used as glass packing material. Small pieces of packing material simply pass into the furnace and vapourise. Large pieces, however, can block up the movement of the glass; this has major consequences in a totally automatic cullet conveyor system. It was therefore desirable that the instrument should ignore small pieces of polystyrene, but act on large ones. This is done in a very simple way; the instrument simply counts the number of consecutive scans of the laser beam in which the totaliser output goes high. If this number exceeds a preset value then the instrument produces an alarm. The preset value can be set by a thumbwheel on the front of the electronic control box.

3.5. Performance of the Detector

The performance of the instrument was determined in an engineering laboratory, using a small flat motorised conveyor to simulate a conveyor belt. The belt was only ten metres long, but could be run at a wide range of speeds, and had fixing places for experimental apparatus. Glass had to be fed manually.

Performance was examined under two working conditions. Firstly, the belt was run at 1 metre per second, with the gantry positioned 280mm above it. This was to simulate operation in a float glass factory. Secondly, the belt was run at 0.25 metres per second, with the gantry 150mm above it, to simulate operation in a plate glass factory.

An occasional drawback of this full sized production prototype was that, when placed on the conveyor belt, it did produce an alarm signal occasionally from cullet. This was in the form of a very short spike from the totaliser during some scans. Various explanations were developed as to why this occurred. The two most likely were firstly that there was a degree of crosstalk between the twenty four detector inputs (despite the efforts to keep this to a minimum), so that if one detector received a very large signal the other three picked it up and were driven over the threshold; and secondly that the signals received by the four detectors were in fact temporally separated, but that the smoothing of the signal by the phase sensitive detection circuits held them high long enough to be simultaneously over the threshold. Unfortunately, time and money did not permit a thorough investigation into the the cause of these "false alarms". On the other hand, they occurred so infrequently, and for such a small number of consecutive scans,

that the instrument could still be used provided a lower limit was placed on the size of object to be detected.

Two performance parameters were quantified. Firstly, resolution was studied by passing successively smaller cubes of polystyrene packing material under the instrument, until the reliability of detection became significantly reduced. This was done with no glass on the belt, to distinguish between the detection of packing material, and any signals produced by the glass itself. Secondly, the false alarm rate was quantified for different conditions and glass loads, in terms of the number of consecutive scans any spurious signal lasted for. The results were as follows:

a) Float Plant Operation

Resolution: The instrument could reliably detect 100mm lengths of polystyrene packing material, either alone on the belt, or amongst cullet. Using successively smaller samples, it was estimated that 35mm cubes were detected 85% of the time, and 25mm cubes were detected 50% of the time.

False Alarm Rate: False alarms produced by passing cullet under the instrument did not exceed 3 consecutive laser scans.

Recommended Limit of Operation: It was recommended that the instrument be used to detect spacers no smaller than 120mm in length. At a one metre per second belt speed this corresponded to 6 consecutive laser scans. It was thought that this was sufficient to prevent confusion between false alarms from cullet and readings

from unwanted materials.

b) Plate Factory Operation

Resolution: 25mm cubes of polystyrene packing material could reliably be detected. It was estimated that 12mm cubes were picked up 80% of the time.

False Alarm Rate: At this setting the false alarm rate was found to be heavily dependent on glass load. A monolayer of glass was required to achieve acceptable results. False alarms produced by passing a monolayer of glass under the instrument did not exceed 4 consecutive scans. With heavy glass loads it was found that this could exceed 10 consecutive scans.

Recommended Limit of Operation: It was recommended that the instrument in its present form be used to detect material no smaller than 40mm square amongst a monolayer of glass. With a belt speed of 0.25 metres per second this corresponded to 8 consecutive laser scans, which was once again thought to be sufficient to prevent confusion between false alarms and proper readings.

Other Materials: Since the plate factory operation involved external cullet, a range of likely unwanted materials were passed under the instrument. Various pieces of refractory could be detected, ranging in colours from white to light brown. Black, and very dark brown refractory was not detected. Light coloured paper, card and wood were all detected. Painted aluminium cans were also detected.

From the many cullet conveyor sites available, the most suitable site for early trials was considered to be in a float plant, where large pieces of packing material constituted the unwanted material, and the cullet was generally clean. This gave the best chance of success. The instrument performed perfectly well for this purpose, as is explained below.

3.6. Works Trials

Once the performance of the instrument had been quantified as above, it was placed on a cullet conveyor within a float glass factory. It behaved as predicted from the outset, but a considerable time trial was undertaken in which the only action taken in an alarm condition was the illumination of an LED. After three months of continuous operation with no faults, and no apparent degradation of the signal levels, the connection was made to a cullet diverter. This is a device which is capable of shifting the flow of cullet from one direction to another. In our case the cullet diverter was constructed by allowing cullet to fall off the end of the conveyor down a vertical chute to a second conveyor. In the event of an alarm signal, a flap entered the chute and diverted the cullet down to a skip ready for disposal.

A controlled set of tests were carried out, to determine:

a) The ability of the instrument to detect spacers

and b) The ability of the diverter to remove them.

Polystyrene spacers were cut into a range of lengths:

150mm; 200mm; 300mm; 400mm; 500mm; and 600mm.

Five pieces of each length of spacer were thrown onto the cullet belt, in random orientations. As each spacer passed

the detector and diverter, two pieces of information were recorded:

a) The detection of the spacer

and b) The successful removal of the spacer

As above, the instrument would only send a signal to the diverter if a preset number of consecutive scans showed scattering material present. The laser scan frequency was 50Hz, and the conveyor belt speed was one metre per second. Thus each laser scan corresponded to 20mm of belt travel. The trials were carried out for four different settings on the control box:

1) 10 - 200mm of spacer material

2) 15 - 300mm of spacer material

3) 20 - 400mm of spacer material

4) 25 - 500mm of spacer material

The results are shown in Table 3.1 and graphically in Figure 3.8. It can be seen that the instrument worked as intended, acting on spacers of a preset size. The step between acting on the spacer and not doing is not abrupt; this was caused by the random orientations of the spacers on the conveyor. However spacers found within the conveyor system generally lay lengthways on the conveyor belt, so restricting resolution to the direction of belt travel was acceptable in this case. The cases where a spacer was detected but not successfully removed was simply caused by the spacer being delayed by the machinery around the diverter, and not reaching the flap until the diverter action had finished.

TABLE 3.1

CULLET LINE DETECTOR TRIALS

THUMBWHEEL SETTING	150		200		300		400		500		600	
	A	B	A	B	A	B	A	B	A	B	A	B
10	0	0	1	1	5	5	5	5	5	5	5	4
15	0	0	0	0	4	4	4	3	5	5	5	5
20	0	0	0	0	0	0	4	3	4	4	5	5
25	0	0	0	0	0	0	0	0	3	3	5	5

A : Diverter Operations B : Successful Divertions

FIGURE 3.8

SUCCESS RATES OF REFRACTORY DETECTION AND DIVERSION

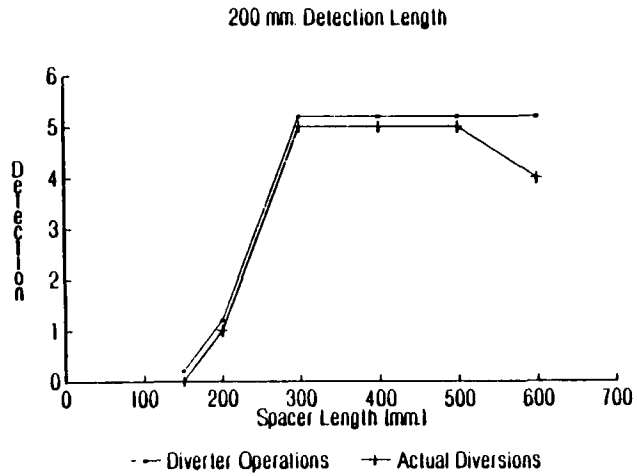

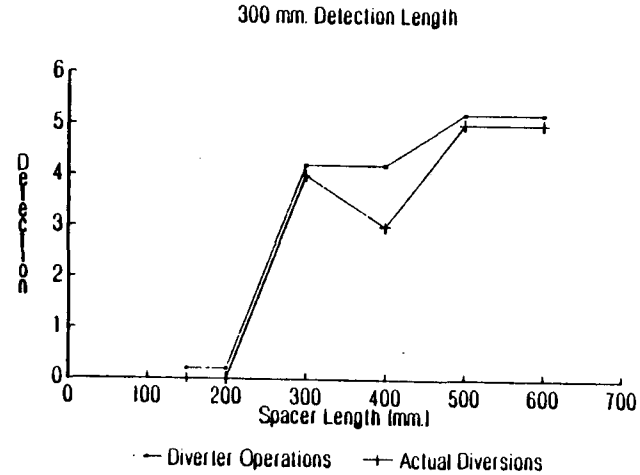

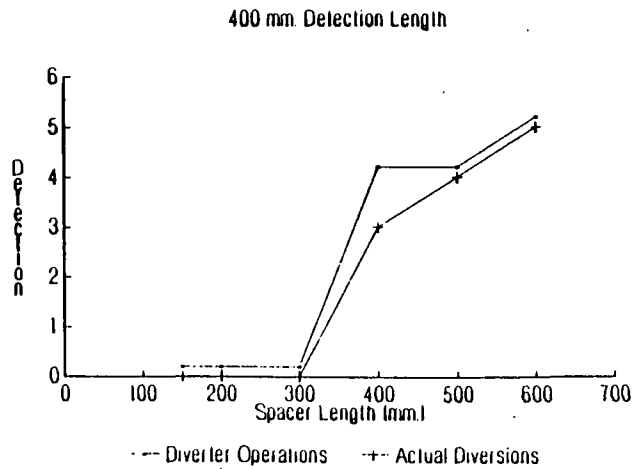

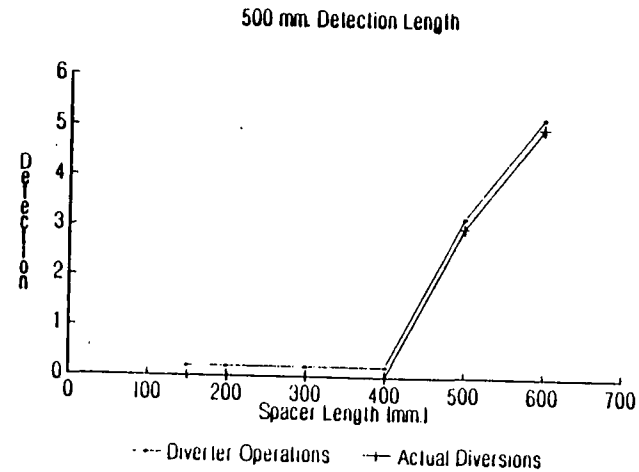

3.7. Summary

The instrument described uses a range of technologies within electro - optical instrumentation. Although the principle of operation was original enough to patent, it was only made practical by recent advances in semi conductor diode laser technology, and silicon detector technology. The advances in the electro - optics industries have made possible the application of a simple idea to solve a difficult problem.

CHAPTER 4 MONITORING THE FLATNESS OF GLASS

4.1 Introduction

Glass produced by the float process is generally considered to be "flat" - and certainly by construction industry standards it is flat enough for the majority of requirements. However some uses do demand a high degree of flatness. One example is in car windscreens, which are mounted at large angles of incidence to the driver's line of sight, and surface irregularities are more easily seen.

As car manufacturers improve the designs of their cars, the specifications required of the suppliers become more stringent. One such request is the supply of larger, stronger windscreens which weigh less than previous ones.

The response within Pilkington to this demand was to produce laminated and toughened windscreens with the same strength as before, but made with thinner glass. In general it was known that the flatness of float glass was inversely proportional to its thickness. Since the requirement was to produce thin, flat sheets, it was considered that the quick, routine measurement of the profile of the glass sheets was required.

4.2 Proposal

Although the requirement in this work was straight forward - to measure the shape of the glass - the practicalities of the problem were not so simple. A typical glass sheet submitted for measurement was 300mm by 600mm in size, but only 2mm thick. Any technique which relied on mechanical contact

inevitably involved forces, which would affect the shape of the thin glass. Further it was believed that most of the shape was matched on the top and bottom surfaces; in other words the predominant overall glass forms were ripple and bow. Features like this would reduce in magnitude if the glass was supported on a horizontally flat table, and could not be assumed to remain unaffected if the glass was subjected to forces while held vertically.

It was therefore considered that an optical technique was the best approach to the problem, and it was decided to build an instrument based on the Schlieren method to analyse the surface profile of the glass.

4.3 Optical System

A Schlieren system was set up as shown in figure 4.1. A quartz halogen lamp with a small (2mm x 1mm) filament was used to illuminate the system (see section 2.2.3.a). An image of this was formed on a slit by a quality condenser, and the transmitted beam allowed to fall onto an off axis paraboloid. This collimated the beam and directed it towards the glass to be analysed. Normally the collimating mirrors in Schlieren systems are spherical, and the systems are used qualitatively. However in this critical situation, where quantitative measurements were being taken, the spherical aberration and coma produced by spheres was not acceptable. The surface which produces an exact collimation from a point source is a paraboloid with its focus on the source; the use of an off axis paraboloid prevents the source from obscuring the beam. The glass was placed in a frame in which it sat near vertical; leaning back just enough for it to remain stable. In

FIGURE 4.1

SCHLIEREN SYSTEM

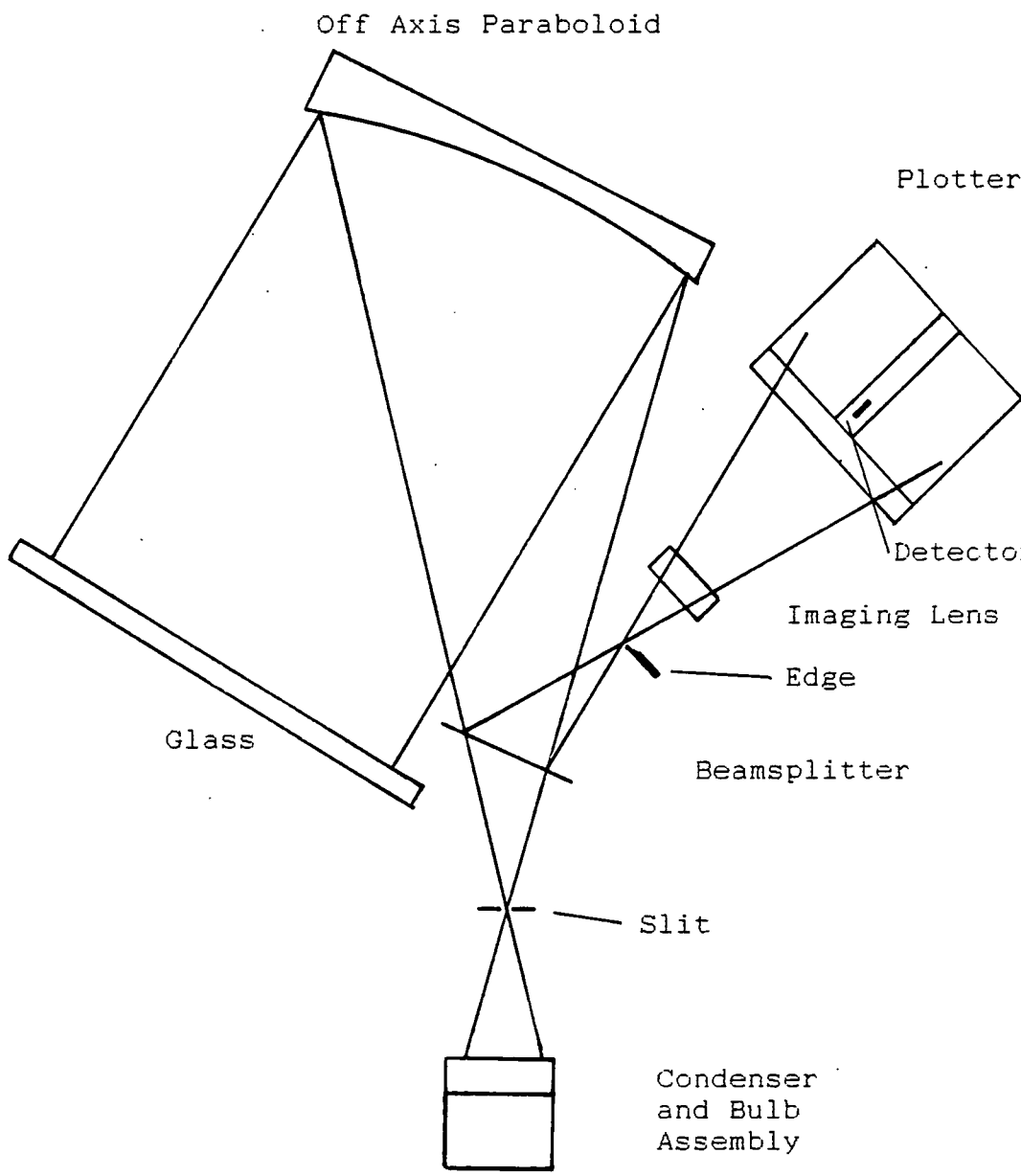

this way it was considered that the forces likely to affect the shape of the glass would be minimised. The glass was positioned in such a way that the light reflected from its surface returned along the same optical axis as the outward beam. A beamsplitter reflected the returning light onto a knife edge, which was positioned parallel to the long side of the image of the slit, and such that it obscured half of the image of the source. In the knife edge system, reflection from every part of the glass surface contributes to the final image. For a perfect surface all parts of the surface contribute equally. However, if part of the light source is distorted it will lead to its contribution to the image being partially inside (or outside) the knife edge. Consequently in the light beam transmitted beyond the knife edge the apparent intensity of this part of the surface is reduced (or increased). The light was then passed through a lens which produced an image of the glass. A small area (1mm) photodiode was placed at the image plane. The photodiode was mounted on the traversing arm of an X Y t plotter, the same plotter being used to record the intensity of the beam incident on the diode as it was traversed across the image of the glass.

It was decided to coat the top surface of the glass with aluminium, to ensure that the top and bottom surfaces would not be confused, and to improve the level of signal.

Using this system variations in illumination at the image could quite clearly be detected, which from their nature (long dark and bright broad lines) indicated ripples, which is what had been suspected for the surface defects.

In a Schlieren system the variations in illumination of an image relate to a rate of change of refractive index, or in

this case of surface height. Thus the traces produced by the pen on the plotter could not be directly related to the surface profile, only to its derivative. It was therefore necessary to devise a way of integrating the output from the photodiode to yield the surface profile.

4.4 Integrating the Readouts

Two methods of integration were investigated, which were essentially independent from each other. The two methods would be compared in order to verify their validity.

4.4.a Electronic Integration

As was indicated above, the Schlieren technique highlights the rate of change of (in our case) height, not the height itself. To obtain a trace of the actual surface profile, it was necessary to integrate the traces produced on the plotter.

A small electronic integrator was connected to the output of the photocell on the X Y t plotter. This is illustrated in figure 4.2. The basic integrating circuit, with an operational amplifier (resistor in series with the inverting input, and capacitor across the feedback loop) can be seen in the centre of the picture. Also in series with the input was a capacitor to prevent D. C. drift. A switch was connected across the feedback capacitor to 'zero' the output for each scan. A variable resistor was connected across two pins on the amplifier to vary the input bias. This acted as an electronic grey level.

An electronic grey level was necessary because the position of the detector at the start of the scan had an influence on the trace which followed. This was because the light

FIGURE 4.2

INTEGRATION CIRCUIT

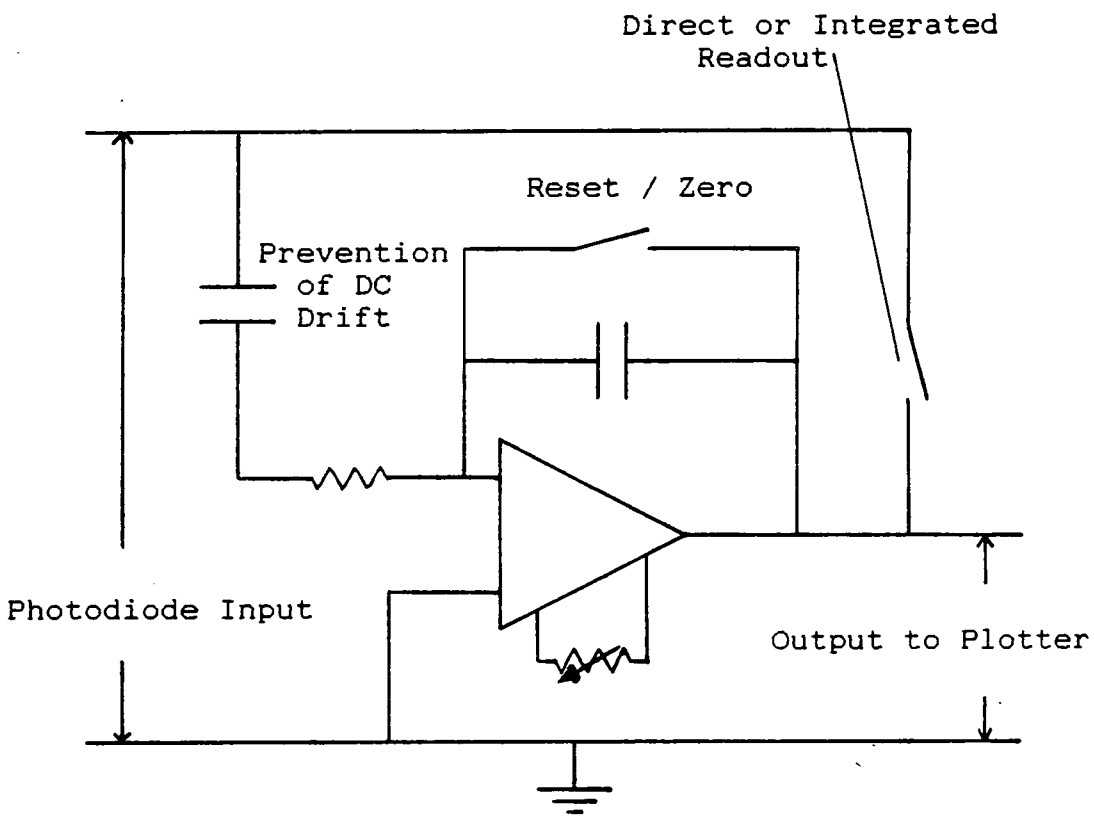

intensity at that point represented the 'zero mark' for the integrator. If the starting point was on a dark region, the rest of the picture would be lighter, and the integrator would continually add. If the starting point was a bright region the integrator would continually subtract over the darker parts of the picture. It could be seen from this that the initial input bias to the amplifier would have to be the average value over the whole picture. In this way the overall level would be flat.

This system could be made to function properly on its own, but fine tuning of the grey level was best achieved optically. This was done by simply scanning the photocell quickly across the image several times before taking a reading. This ensured that the correct grey level was achieved every time, and could be done in a few seconds.

Figure 4.3 shows an output trace from the Schlieren system. The integrated readout is shown below.

In these traces the Y axis (height) is only approximate: Schlieren systems do not generally lend themselves to quantitative analysis. The scale was derived as shown in figure 4.4. The glass mount was placed on two accurately made translation stages, with micrometer movements marked in 0.01mm intervals. A flat mirror was placed in the mount, and another mirror was placed to one side of it. Integrated readouts were taken across the two mirrors. Between each readout the mirror in the glass mount was moved through a small angle, by turning the micrometer through 0.01mm on one stage. This corresponded to a change in angle of 0.0006 degrees of the glass in the mount. It produced a change in angle of the trace of 15 degrees. From this it can be shown that a change in the height of the trace of 10mm

FIGURE 4.3

DIRECT AND ELECTRONICALLY INTEGRATED OUTPUTS

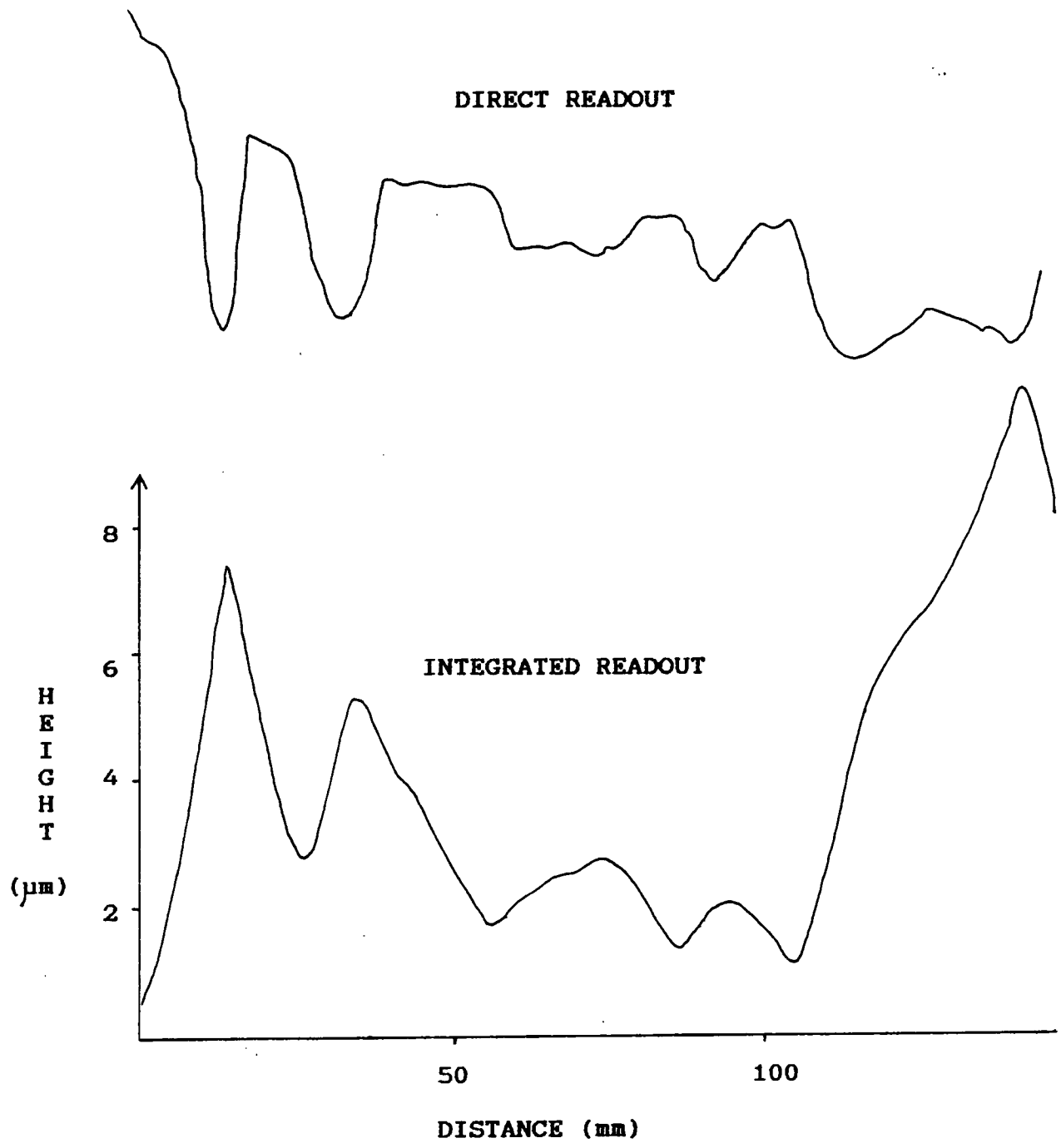

FIGURE 4.4

ESTIMATION OF SYSTEM SENSITIVITY

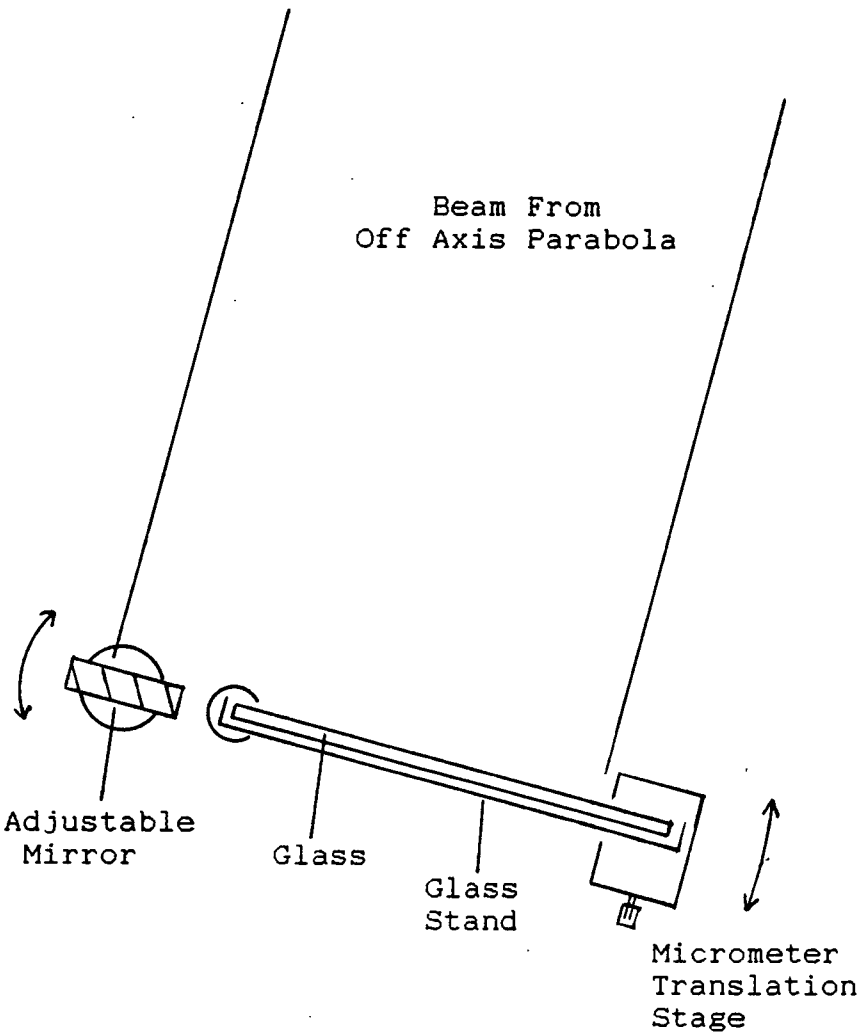

corresponds approximately to a change in the height of the sample of 0.5μm. Considerably more work would be required to verify this; tracing surfaces of known profile would be one method.

4.4.b Integration by Computer

In order to verify the results of the traces shown in figure 4.3, an alternative method of integration was developed. This was done by feeding the data into a computer and writing a program to integrate it.

The X Y t plotter output from the Schlieren system was placed on an Apple Drawing Tablet. This is an A3 sized pad with an electronic pen; the pad senses pressure from the pen and computes its coordinate. This can easily be done through paper. The plotter output was therefore traced on the Drawing Tablet.

The program written to produce the integrated output is shown in the appendix. The integration was done by calculating the average y value, subtracting that from the individual y values, and carrying out numerical integration on the remaining function. Thus bright areas, with a higher than average intensity, would produce a rising trace; dark areas with a lower than average intensity (and therefore with negative values in the new coordinates) would produce a falling trace.

Figure 4.5 shows an output trace from the Schlieren system, with the computed integration shown below. It was felt that the correlation with the trace from the electronic integration was encouraging, and confidence in the system was high.

FIGURE 4.5

DIRECT AND COMPUTER INTEGRATED OUTPUTS

DIRECT OUTPUT

COMPUTER INTEGRATED OUTPUT

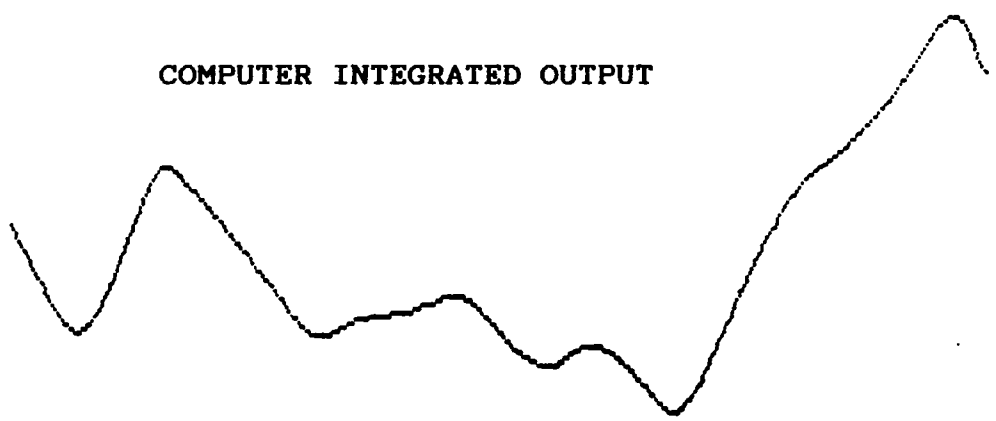

4.5 Summary

A system was developed, based on the Schlieren method, to measure the profile of glass without contacting it.

Since Schlieren methods display rates of change, the direct output from the system was the derivative of the height of the glass.

Two independent methods of obtaining glass profiles by integrating the readout from the optical system were developed. These methods were shown to be consistent: the system was shown to be capable of producing traces that were true to the shape of the glass.

Future work would have involved verification of the system still further by creating surfaces with known profiles. The system would then have been calibrated and made ready for use.

While a working system had been produced, it proved to be time consuming in its use, in the context of using it as a factory standard. The offer of developing the instrument further was therefore not taken up by the quality assurance staff at the factory.

CHAPTER 5 INFRA - RED SMARTT INTERFEROMETRY

5.1. Introduction

Optical interferometry has been used as a measurement and inspection tool in the production of lenses, prisms and other optical components for many years. The most common form of this equipment is two beam interferometry. A large number of such instruments have been described in the literature, and indeed made use of, but most are variants of only a few fundamentally different types. In almost all cases, the light from a 'point' source is first divided into two beams, to produce a test and a reference beam. These two beams follow separate paths, or at least have different geometries, such that the test beam has impressed on it any phase variations caused by the system under test, while the reference beam is unmodified. The interference pattern shows the variation of phase difference across the aperture of the system under test as variations of fringe position, in terms of the wavelength of light used. The dividing process which generates a reference and a test beam is usually accomplished by means of a partially reflecting plate, where one beam is reflected and the other transmitted.

The interferometers described above are well understood, and versatile. However they suffer from several disadvantages. Their design means that most of the samples under test have to be smaller in aperture than the interferometer itself. The instruments are therefore often large, and since their optics have to produce a negligible phase variation across the entire aperture, they are expensive to produce. Also, since the beams follow separate paths, they are prone to vibration causing

independent movement in the two arms. Bulky anti - vibration mounts are required to prevent this.

Within the Pilkington Group, experience of optical design and construction is considerable, both in the visible and the infra - red wavelength regions. Interferometry is used for test and measurement both in the design and production stages of systems. In order to maintain a competitive place in the market for infra - red systems, operating in the 7 to 14 μm wavelength region, Pilkington was amongst the first to produce a two beam infra - red interferometer that would automatically evaluate the interferograms produced by the units under test, providing data to the requirements of the customers, and producing information for the production engineers regarding any faults in the systems. Lenses could be provided in the knowledge that they were to specification before being installed in thermal imaging systems, which in fact gave Pilkington a distinct advantage over its competitors. However this automatic interferometer suffered from the same problems as described for the two beam systems mentioned above, namely size, cost and portability.

There was a need to find an alternative form of interferometer to that used in the first instrument, which was smaller, cheaper and more portable. Several of these could then be produced and used throughout the Pilkington Group.

5.2 Proposal

One instrument which solves some of these problems is the Point Diffraction Interferometer (Smartt & Steel - ref. 5.1). The principle of operation of the PDI is illustrated in figure 5.1. Its operation is closely related to a fundamental principle of

FIGURE 5.1

POINT DIFFRACTION INTERFEROMETER

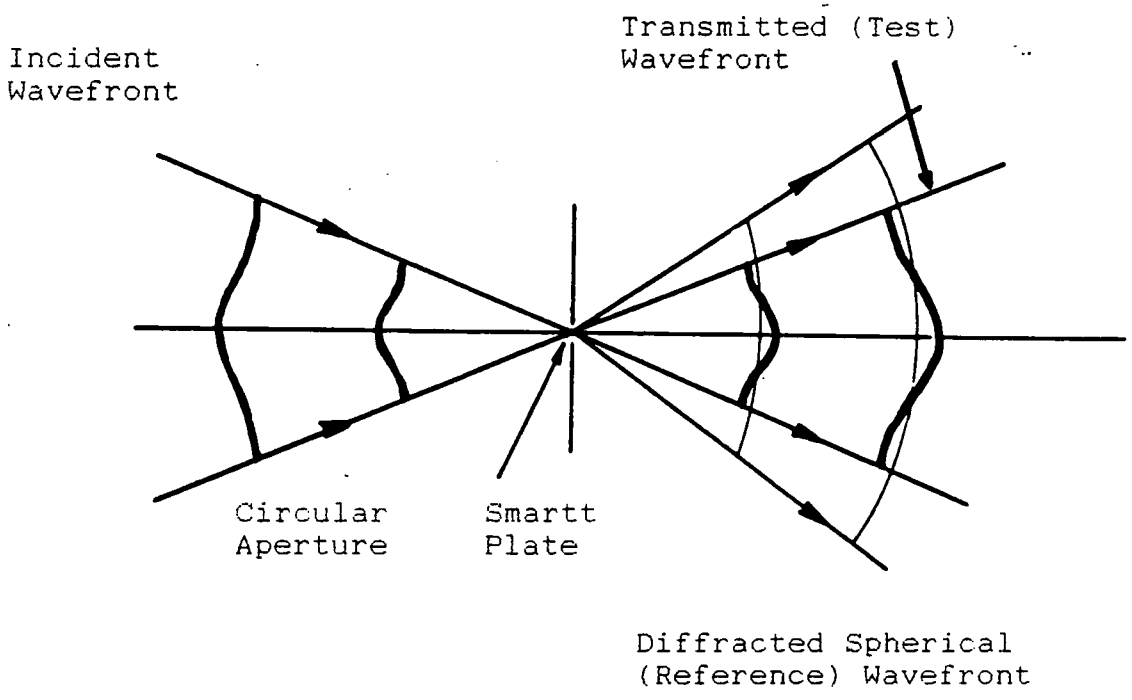

physical optics: when a beam of light is interrupted by any object in its path, part of the light is diffracted. If the object approximates to a point, the diffracted light forms a spherical wave. In the PDI, there is an extremely small, precisely circular aperture in an evaporated thin film on a rigorously non - scattering substrate. The thin film is partly transparent. The aperture is positioned close to the image formed by the system under test. The direct wavefront is transmitted by the thin film with reduced amplitude, but is otherwise unchanged. Some of the light is diffracted by the aperture to form the spherical reference wavefront, and interference between the two wavefronts occurs in the common region.

By its very nature the PDI solves many of the problems of conventional two beam interferometers. It is small. In the visible wavelength version, the circular diffracting aperture is approximately 5um; the substrate aperture is 0.8mm. One unit available on the market, which has three degrees of translational freedom (to position the aperture at the focus of the system under test, both laterally and longitudinally), stands little more than 200mm high and 150mm wide. It is inexpensive - provided the system to be tested has a focal plane, no extra high quality optics are required. As it is a common path instrument, both the reference and the test beam follow the same path in space, making the unit relatively insensitive to vibration and air turbulence in the interferometer itself.

It could be seen that an infra - red PDI could potentially solve many of the problems associated with the original automatic infra - red two beam interferometer made at Pilkington. It was considered a valuable exercise to build such

an instrument, analyse its properties, and examine its suitability, if any, for use in an automatic interferometer.

5.3 Initial Work

In a PDI, the plate with the aperture is called a Smartt Plate. The plate was made using a germanium disc. Pilkington have a considerable amount of experience in the production and use of crystalline germanium for optics in the far infra - red region of the spectrum (7 to 14μm). The properties of the material are favourable compared to others which transmit in this region; it is easily worked, is relatively non - toxic, and has good weathering characteristics (see section 2.3.4.a). This then was an obvious choice for the substrate. The disc was coated with a thin metallic film to reduce the light transmission to a similar amount to that used in the visible version. The circular 'hole' could be produced by placing glass beads on the discs before coating, leaving an uncoated shadow under each bead.

Various techniques were investigated for coating the substrates, and removing the beads after coating. The best approach tried is described below.

Beads were placed on a polished germanium disc, which was coated with aluminium in an evaporation coater. Since this method of coating is directional, with the vapourised metal travelling straight from the source to the substrate, any obstructions between the two will produce shadows. This is preferable to other coating techniques such as sputtering, in which the coating material interacts with the substrate over a wide solid angle. It was found that the best method of removing the beads was simply to brush them off with a camel hair brush; the aluminium coating

was tough enough to withstand this treatment. This was found to be better that non - contact techniques such as ultrasonic cleaning, which often left beads, or broken parts of them, on the surface. The surface of the germanium discs were examined by microscope, and it was found that the technique described above could reliably produce apertures in the aluminium coating.

It was considered that an infra - red Smartt Plate could be made provided the transmission coefficient of the coating, and the hole size, could be matched and optimised.

5.4 Optimising The Basic Technique

In the work which followed, the various factors affecting the performance of the plate were studied in order to determine the most appropriate technique for producing the Smartt plate.

5.4.a Aperture Size

It is possible to predict the optimum hole size for a Smartt Plate. For Fraunhofer diffraction the image of a point source produced by a lens is an Airy disc surrounded by (much fainter) rings. For a Smartt Plate to work properly, the circular aperture must be positioned within this Airy disc to ensure a uniform source for the diffracted reference wave. The radius of the Airy disc is given approximately by:

$$R = \lambda \, 1.22 \, (f/D)$$

where

f = focal length of lens

D = Diameter of lens

λ = Wavelength of radiation used

In the present case, the lens in use had an f/D ratio of 1.3, and the wavelength of light being used was 10.6μm. This meant that the diameter of the Airy disc would be

$$R = 30\ \mu m$$

Beads having a range of sizes centred on 30um would therefore be used. A measuring graticule, for use with an optical microscope, which had lines at intervals of 10um was used to select beads of appropriate size.

5.4.b Substrates

It was found that substrate preparation was as important an aspect as any. Firstly, the discs had to be anti - reflection coated on both sides. This not only improved the transmission characteristics of the plate, but since the light source used was a carbon dioxide laser, uncoated samples produced unwanted fringes from the front and back surfaces. The refractive index of germanium at 10.6um is 4.0. The reflection coefficient at a germanium / air interface, given by

$$(n-1)^2 / (n+1)^2$$

where n is the refractive index, is 36%. This shows why the intereference fringes between the faces of an uncoated disc would be unacceptable.

Secondly, in the literature describing visible wavelength versions of the Point Diffraction Interferometer (5.1), the

Smartt Plate was referred to as 'rigorously non - scattering'. This proved to be essential. In fact, in the absence of clean room facilities it became necessary to produce a marking system, in which the prepared plates were studied under a microscope. A map was drawn of the positions of the apertures and the unwanted items such as dirt or surface blemishes, likely to produce fringes, relative to a simple system of letraset markings on the surface. In this way it was possible to prevent confusion between various sets of fringes produced when the plates were under test.

5.4.c Transmission Coefficient

Initial work involved determining the optimum transmission coefficient empirically. In this way the first working plate that was made had a transmission coefficient of 0.02. This is close to the optimum range quoted by Smartt of 0.01 to 0.005, to produce the greatest amount of fringe contrast. Plates were therefore prepared with transmission coefficients of approximately these values.

5.4.d Input Power

It was found that there was a limit to the input power of the beam, above which irreversible damage to the coating occurred due to local heating. This discovery was made simultaneously with that of the first working plate. The aperture of the plate was placed approximately at the focus of the system under test. Longitudinal displacement of the aperture from the focus would result in the intereference of two (nominally) spherical waves of different radii of curvature. This would produce circular fringes. Lateral displacement of the aperture from the focus

would produce interference between two (nominally) spherical waves of the same radius of curvature but with their centres displaced. This would result in straight line fringes. The behaviour of the fringes can therefore be used to "home in" on the focus of the system under test, at which the intensity of the radiation is at its maximum. This intensity was estimated to be approximately 150W / mm^2 . As the focus of the system was located, the aperture was destroyed by the local heating. This came about because a carbon dioxide laser was used as the source of radiation, and it is difficult to produce laser action at powers of less than a few watts. Carbon dioxide lasers are discussed in section 2.2.2d.

A power density of approximately 15W / mm^2 was found to be safe for use on the aluminium coatings.

5.5 Using The Smartt Plate

It was found that Smartt plates could be successfully produced, provided that the restrictions described above were adhered to. Plate 5.1 is a photograph of one of the apertures which was found to work, taken using an optical microscope. Plate 5.2 illustrates the type of interferograms produced by the Smartt plates, using 10.6um radiation. The plate transmission was 0.02.

The reason for building the Smartt Plate was to produce a portable version of the Pilkington infra - red interferometer, as discussed in section 5.1. Consequently the detection equipment already in use in the interferometer was used to analyse the signal strength and contrast of the fringes being produced by the plates. This is shown in figure 5.2. The HgCdTe detector (see

PLATE 5.1

DIFFRACTING APERTURE

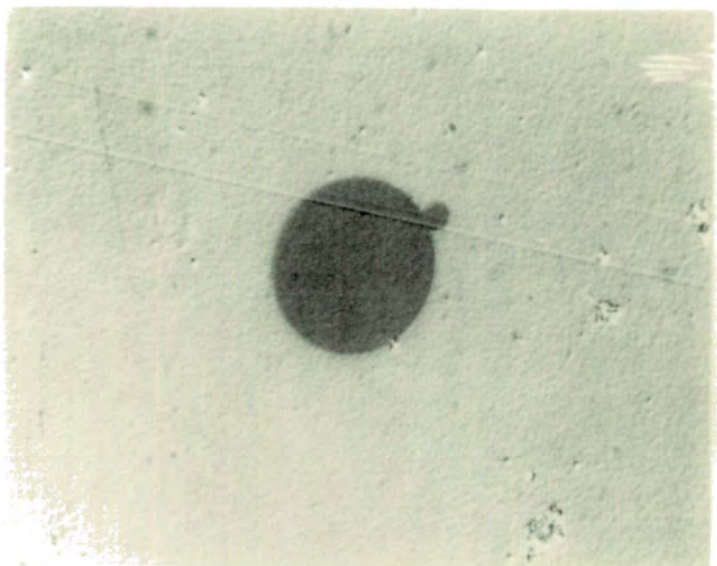

PLATE 5.2

INTERFEROGRAMS PRODUCED

FIGURE 5.2

THE SMARTT PLATE IN USE

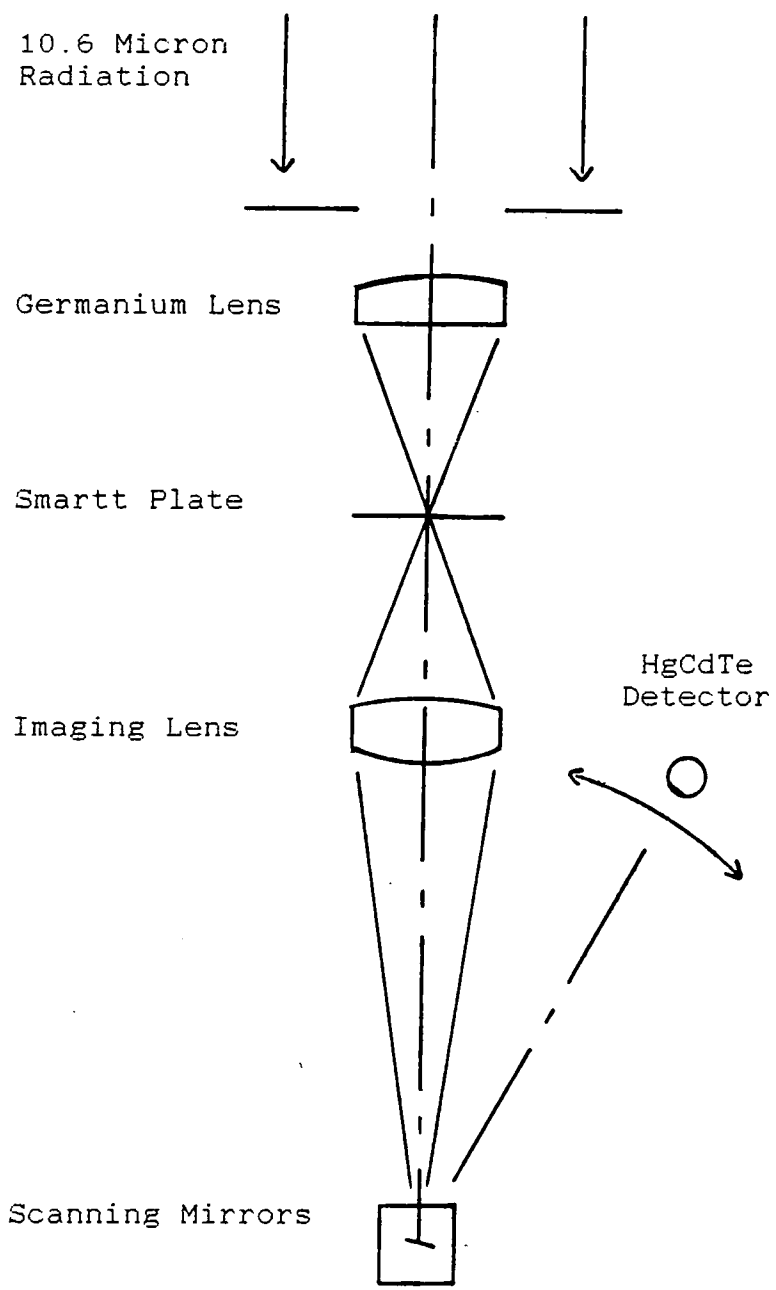

section 2.4.3.f) was cooled with liquid nitrogen. The beam was scanned by two orthogonally mounted scanning galvanometers.

While using these discs it became evident that the contrast of the fringes was a function of the lateral and longitudinal displacement of the diffracting aperture from the focus of the system under test. The reason for this is explained in section 5.6, page 5.10. However the variation in signal strength and contrast across the aperture caused severe difficulties in optimising viewing conditions for the whole interferogram. Displaying the scanned signal using a storage oscilloscope was known to be perfectly adequate for the two beam interferometer already in use. Unfortunately it was clear that the PDI was nowhere near as 'well behaved'. Only small regions of the interferogram could be viewed at any one time.

It can be seen from figure 5.2 that the apertures were not perfectly circular, and that the surrounding coating was not perfectly clean. From this point of view it could be argued that the interferograms could have been improved using more carefully prepared plates. However there was yet another problem which led finally to the work being abandoned.

The automatic interferometer at Pilkington analyses the intensity distribution of the fringes, and plots out a map of the phase variation across the aperture by determining the positions of the maxima and minima of each fringe. For this technique to produce sufficient data, fifteen to twenty fringes are required across the aperture.

It was found that in order to produce this large number of tilt fringes, the lateral displacement of the aperture from the focus reduced the intensity of the reference beam to such an

extent that the fringes could not be seen. Although the intensity of the reference beam could have been improved by increasing the transmission of the plate, this would have resulted in a reduction in fringe contrast, which was too low for our detection equipment even for the present level of transmission.

It was therefore decided that Smartt interferometry was not a suitable basis for making a compact version of the Pilkington infra - red interferometer, and work on this project was stopped.

5.6 Critique

In order to understand why the infra - red PDI was not suitable for the intended uses within Pilkington, it is necessary to look at the nature of its operation more closely.

By definition, interferometry involves interference between two beams, one usually a reference, the other the test or sample beam. It is desirable to produce interference fringes which are clear and of high contrast. Contrast, or fringe visibilty, is given by

$$\text{Imax - Imin} \;/\; \text{Imax + Imin}$$

and this is obviously at its maximum when Imin = 0. This occurs when the two interfering beams are of equal intensity and fully coherent.

In the production of a PDI then, it is clear that the design should take into account the relative intensities of the two beams. However this is not a simple matter (see figure 5.3).

The intensity of the transmitted beam containing the

FIGURE 5.3

INTENSITIES OF TEST BEAM AND DIFFRACTED BEAM

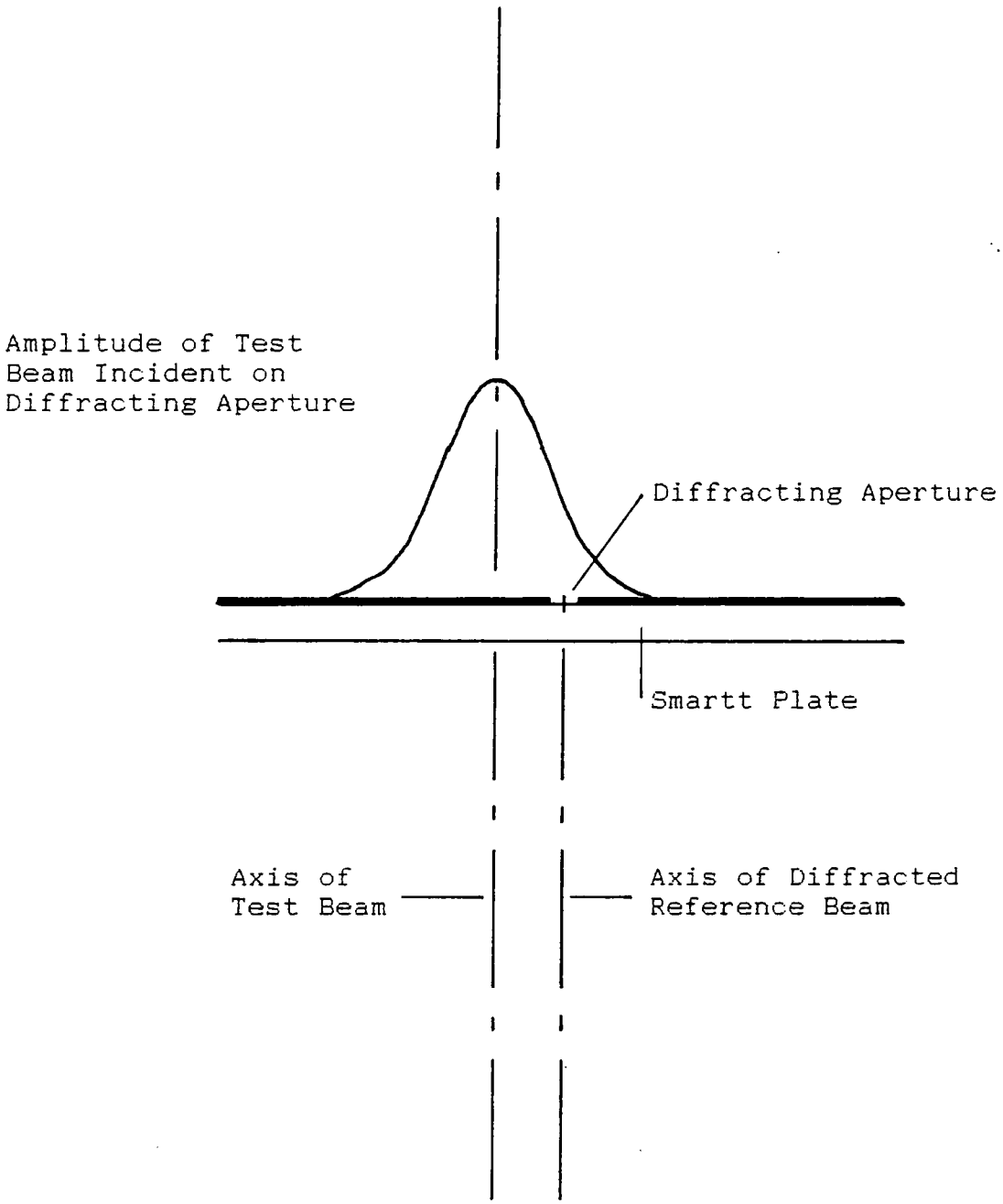

information about the system under test is given by its original intensity reduced by the transmission coefficient of the coating on the plate.

However the intensity of the reference beam is dependent on the intensity of the beam impinging on the diffracting aperture. This is a function of the position of the focus of the test system relative to the aperture. It is at its maximum when the best focus of the test system is incident on the aperture. If the focus is longitudinally displaced from the aperture, the beam incident on the aperture will blur out, reducing the intensity available for diffraction. If the focus is laterally displaced, the intensity incident on the aperture will be non - uniform as the (gaussian) profile moves across it, and will eventually disappear. Moreover, the actual intensity distribution across the aperture is dependent on the focus produced by the system under test, and as such is unpredictable. Only very well behaved systems will produce a predictable focus.

It was found that these restrictions were too great for the use that Pilkington had for an infra - red PDI. However, it is clear that it can be used to test systems that are known to be well behaved.

5.7 Summary

It was shown that a Point Diffraction Interferometer could be made for radiation of wavelength 10.6um.

This was done using anti - reflection coated germanium discs as substrates, placing glass beads of approximately 30um diameter on the surface, and coating the substrate by evaporation with aluminium, to produce a transmission coefficient of

approximately 0.02.

As described in the literature for the production of visible wavelength versions, the substrates of such discs needed to be rigorously non - scattering.

When plates prepared as described were placed with the diffracting apertures near the focus of a germanium lens of f/no. 1.3, interference fringes could be seen between the spherical diffracted beam produced by the aperture, and the incident beam from the lens.

However, the intensity and contrast of the interferograms varied considerably across the aperture. This was an intrinsic disadvantage of point diffraction interferometry, and its extent seen in the versions made in this work meant that the technique was considered unsuitable for automatic fringe analysis.

As such the technique has not yet found a use within Pilkington.

CHAPTER 6 OTHER APPLICATIONS OF OPTICS

6.1 Introduction

This chapter describes the way in which a number of problems typical of the glass industry have been tackled using geometrical and physical optics.

6.2 Measuring the Curvature of Lens Surfaces

One part of the Pilkington Group, SOLA, produces plastic spectacle lenses. These lenses are made by filling glass moulds with the plastic, and then curing them in an oven. Once cured, the plastic is removed from the mould, and placed in boxes according to their style, size and curvature. Only the curvature of the top surface is specified, and back surfaces are produced in a limited range of curvatures. This is because the back surface is worked in the prescription house to the exact requirement of the customer, in terms of lens power and any wedge or cylinder which may have to be incorporated. In the factory, a number of employees manually remove the newly cured lenses from their moulds, and put them in the appropriate boxes. This system is prone to errors however, and if the prescription house produces a lens with the understanding that the front surface has a curvature of say 2 diopters when it is in fact 3, an expensive mistake will have been made. (The term diopter (D) is related to the focal (f) length of a lens or surface by $D = (n - 1) / f$,

where n = the refractive index of the lens.)

As a result of this, we were asked to produce a system which could automatically measure the curvature of the lens surfaces. It was thought that the measurement could have been transferred onto a label for the box that the lens was (automatically) put into, thereby eliminating human error. The time scale for these measurements was to be around one second. The resolution of measurement necessary was better than one quarter of one diopter, since the lenses were produced in curvatures of quarter diopter steps.

The system that was used is illustrated in figure 6.1. Light from a bright source (such as a laser or a quartz halogen bulb) was expanded and collimated. The beam was then passed through a coarse grating. The resultant rectangular beams of light were deflected onto the lens surface at aproximately 45 degrees to the optical axis of the lens, as shown. The lens itself was presented to a rubber 'O' ring, making the orientation of the top surface repeatable. The series of light beams were reflected from the lens surfaces. Unwanted reflections from the back surface of the lens were blocked off by a small mask in the 'O' ring. The reflected beams from the front surface were then used to calculate its curvature. If the surfaces were convex, the beams were found to diverge. The more convex the surface was, the more the beams diverged. Therefore the separation of the beams at a known distance from the lens was an indication of its curvature. The light from the beams was collected from one plane in space. A small electronic camera was focussed onto that plane in space. The resultant measurement of the beam separation was then related to the lens curvature.

FIGURE 6.1

LAYOUT OF CURVATURE MEASURING INSTRUMENT

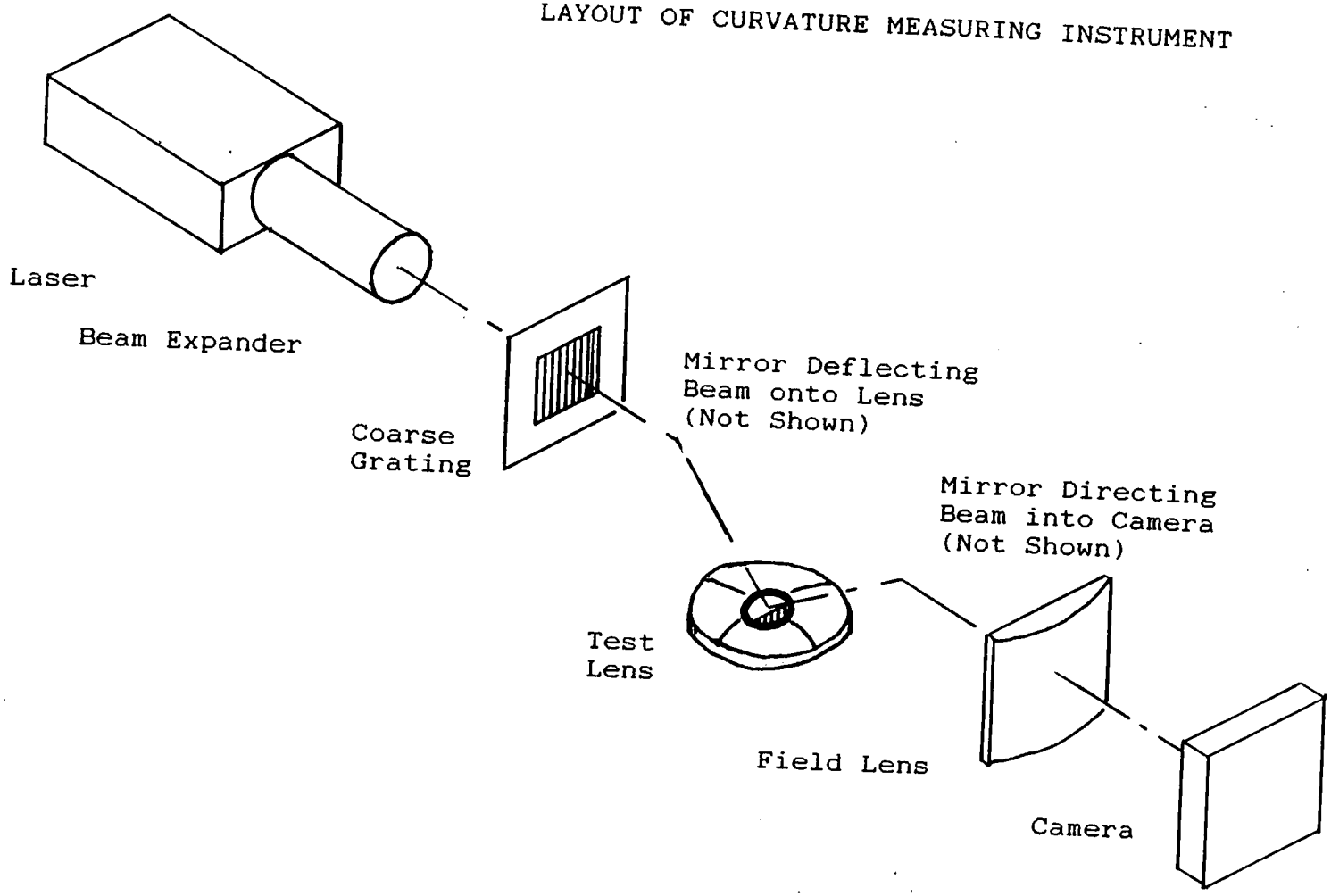

It can be seen from figure 6.1 that the beams, having been allowed to diverge from the lens surface, were then converged through the camera lens and onto the detector. This does not spoil the spatial information generated by the system. The result is the same as if the beams were deflected onto a screen, and the screen focussed on by the electronic camera. However this would be very much less efficient in terms of light collection. The collecting lens in this system is known as a field lens. Its effect on the spatial information in the object is the same as that produced by looking through a window. However all the available light is directed onto the detector. The measurement can therefore be made relatively quickly.

The image of the series of light beams was displayed on a VDU using a BBC microcomputer. An example of this can be seen in figure 6.2. The large black bars are the light beams detected by the camera. The two small horizontal lines at either side of the picture mark the line along which the image analysis was undertaken. The computer analysed the actual screen image. The beginning and end of each bar was found, and the middle calculated. Account had to be taken of noise in the image; a bar was only considered to begin when a minimum number of adjacent pixels registered the presence of light. Similarly, a bar was only considered to end when a minimum number of consecutive pixels registered the absence of light. Care had to be taken in setting the integration time of the camera, because higher curvature lenses diverged the beams to a greater extent, and so reduced their intensity. It was found that the range from 0.25 diopters to 13 diopters could be catered for with one integration setting. The small vertical lines above the bars indicate where

FIGURE 6.2

COMPUTER OUTPUT OF CURVATURE MEASURING INSTRUMENT

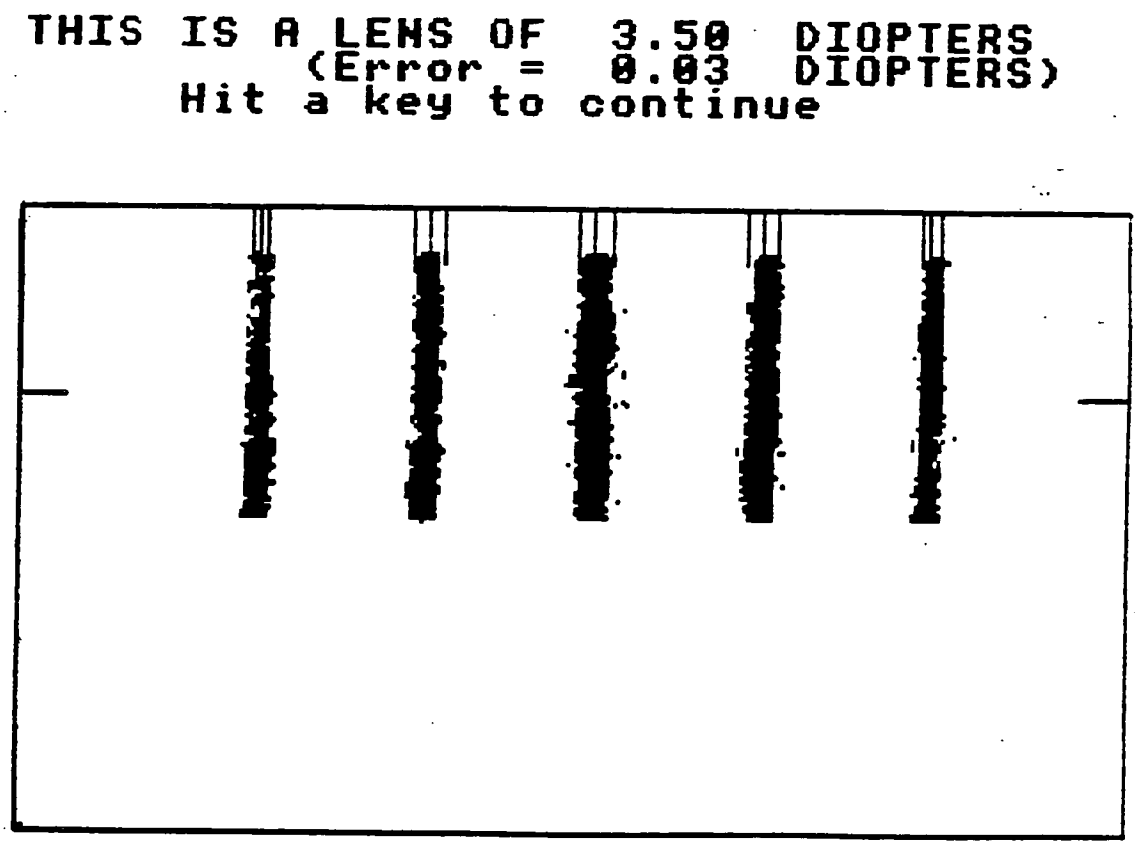

the computer had estimated the beginning, middle and end of each bar to be. The average spacing between the bars was calculated in terms of pixels, and converted into diopters. Since it was known that the surfaces were intended to fall into a category, to the nearest 0.25 diopters, this category was displayed on the screen, and the difference between the value of the category and the actual measurement was indicated as an error value. The program was written in basic, and each measurement could be made in about five seconds. This would have been very much faster if written in assembly language, and would have fallen within the one second timescale required.

The instrument was calibrated using a large number of measurements from marked lenses. This calibration is shown in figure 6.3.

This system solved the problem adequately. Quarter diopter steps could be resolved, and measurements made (potentially) within one second.

This particular version was not used to measure concave surfaces. This would have involved some modifications. The beams would have been projected onto the lenses in such a fashion that concave surfaces would converge the beams through a focus before reaching the measurement plane. Some form of assymmetry across the number of beams would then have been introduced in order to distinguish between convex and concave surfaces.

This instrument was demonstrated to the management of the SOLA group, who agreed that it did indeed meet the specifications required of it. However, having seen that this first request was successfully carried out, discussions began on an instrument that could do more than simply distinguish between curvature groups,

FIGURE 6.3

CALIBRATION OF CURVATURE INSTRUMENT

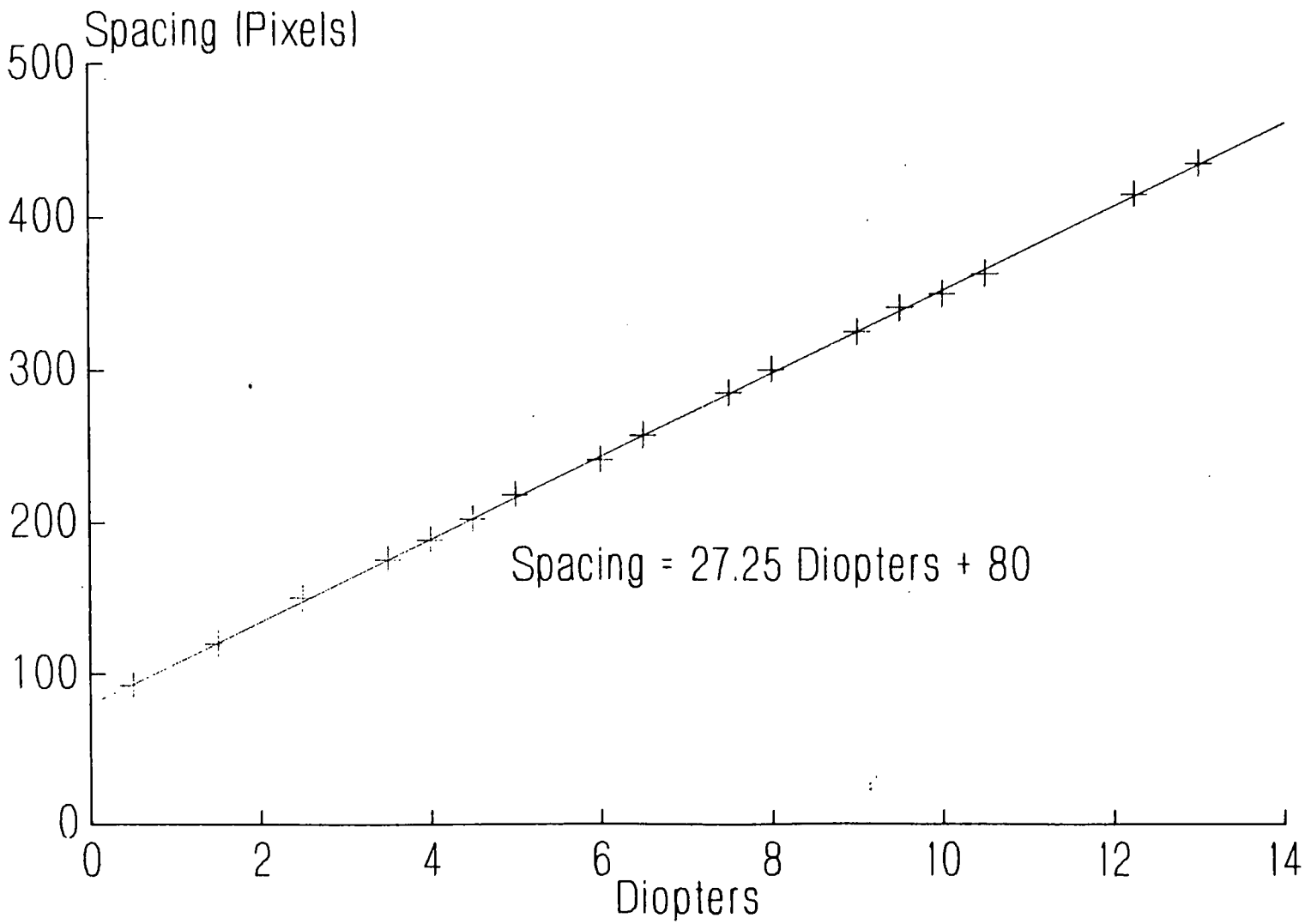

but could produce high accuracy measurements at speed. The accuracy required was +/- 0.01 diopters. This was for the new ranges of spectacles soon to be produced, with more than simple spherical shapes on them. It was also to check the accuracy of the mould manufacture.

The instrument just described used an electronic camera with a resolution of 256 pixels. This was just good enough to carry out the measurement task between +13 diopters to -13 diopters; a total of 104 different curvatures. however, to measure to 0.01 diopters over a 26 diopter range required a resolution greater than 2600 to 1. A new system was necessary to carry out this more demanding task. An instrument built to meet this specification has just been delivered.

6.3 Detecting Wire in Wired Glass

At Pilkington, wired glass, such as is used in fire doors or in schools where safety is a concern, is produced by the rolled plate method. Molten glass is drawn from two furnaces by rollers, and a wire mesh is sandwiched between the two ribbons. Tight control is required on the positioning of the wire mesh relative to the glass. It is desirable to keep the mesh as central as possible, since glass at the edges of a continuous ribbon is always of poorer quality than that at the centre. At the warehousing end of the factory the edges of the ribbon are cut off (the small region at either side containing no wire mesh is known as the selvedge). This is done by continuously scoring a line on the ribbon some distance from the edge of glass, cutting

across the width of the ribbon to leave it in predetermined lengths, and knocking the selvedge off with beams parallel to the edges of the ribbon. Although different types of mesh are used, the most common type has a pitch of 12.5mm and has wires running parallel and perpendicular to the ribbon edge. It is found that removal of the selvedge is more difficult if the original score on the glass is made directly above a wire running parallel with the ribbon edge. This tends to leave a jagged edge to the cut. Since the plate sizes are specified to millimetre accuracy, this has serious implications on the failure rate of the glass plates at the inspection stage.

It was therefore necessary to produce an instrument that would detect the wire in the glass; such a system should be able to recognise the fact that a continuous strand of wire was running under the scoring tool, and should produce some electrical signal to allow the score to be made elsewhere. The instrument should also be able to detect the passage of wires perendicular to the ribbon edge, and to distinguish this from the scoring tool being situated completely outside the wire mesh. This was to ensure that no selvedge was present in the cut plates. A limitation on the system was that it was to operate entirely above the glass; no part of the unit should have to be installed underneath the ribbon. It was also indicated that since the area of the factory where the unit was to go was heavily manned, the use of lasers would not be appreciated. The glass travelled at speeds of between 290m/hr and 380m/hr, which corresponded to 6 to 9 'cross wires' per second. The glass could be either 6.7mm or 7.7mm thick.

An instrument was built which relied on the principle

that most of the light incident on a sheet of clean glass would pass through it, whereas a strand of wire would scatter the light through a wide range of angles (unless it was particularly shiny, which was not the case in this instance). This meant that a beam of light incident on the wired glass would not be noticeable from above unless it impinged on a wire within the glass.

The optical layout of the instrument is shown in figure 6.4. A 6V 20W quartz halogen bulb was the light source. The light from this source was collimated as shown. In order to use as much light as possible, a lens of 50mm diameter but only 39mm focal length was used. The curved surface was an asphere to keep spherical aberration to a minimum. The glass was of a type resistant to heat, since it was to be placed close to the hot bulb.

A small proportion of the collimated light was split off by a beamsplitter, and directed onto a photodiode. The beamsplitter was anti - reflection coated on both sides, because as much light as possible was required for the detection of the wire. There was still sufficient intensity on the photodiode for it to work reliably. This part of the instrument had two functions. Firstly it continuously monitored the light level from the bulb so that the amount of light that could be expected to be scattered from the wire was known, even as the bulb faded during its working life. Secondly an immediate signal could be produced should the light from the bulb fail completely. This would prevent associated equipment from operating after such an event.

The collimated beam was then focussed down by a second lens, so that an image of the bulb was formed in the plane of the wire in the glass. The f/no. of this lens was a compromise: the

FIGURE 6.4

OPTICAL LAYOUT OF WIRE DETECTION EQUIPMENT

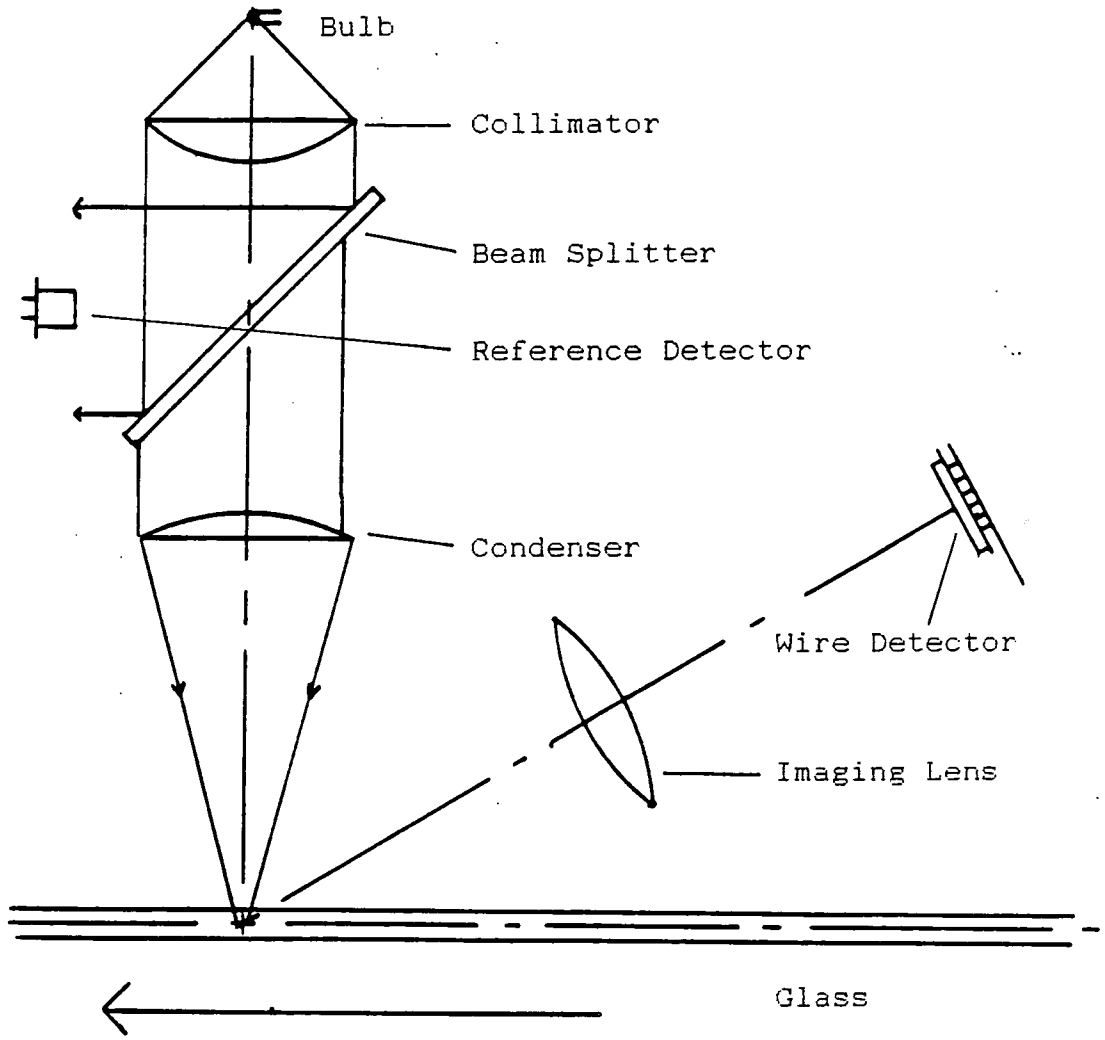

shorter its focal length the brighter the image of the filament would be; the longer the focal length the more movement of the wire in the vertical plane would be catered for. It was known that the depth of field (the range of heights of the wire) was approximately +/- 1mm. It was considered reasonable to limit the lateral spread of the image to 0.5mm over this depth of field. Since the aperture of the lens was 50mm, it was easy to calculate by similar triangles that the focal length of the lens should be of the order of 100mm. In fact an 80mm focal length lens was used, to keep the signal as bright as possible.

The scattered light was detected by means of a simple biconvex lens placed at 2f from the image of the filament, and a large area (100mm^2) photodiode. The large area allowed for shifts in the image with different positions of the wire as determined by the glass thickness. The angle of view of this detector was determined by the solid angle through which reflections occurred from the glass as a result of the incident light. Since the underside of the glass was mottled, reflections occurred over a solid angle of 50 degrees from the vertical axis of the incident beam. To avoid these reflections, the viewing axis was 60 degrees.

It was preferable to have a sloping side arm in line with the direction of travel of the glass, from an installation point of view. In addition to this, experiments with mock ups in the laboratory showed that more scattered light could be detected orthogonal to the wire axis than parallel with it. Since it was necessary for the instrument to detect both the cross wires and the orthogonal 'long' wires, this difference in signal level was compensated for to some extent by placing the filament of the

bulb parallel to the axis of the long wires, since they were to be viewed in the relatively insensitive parallel direction. This meant that more of the long thin filament was incident on the long wires than on the cross wires.

The output from the large area photodiode was used to determine the position of the beam. If the beam passed over cross wires, the output fluctuated at approximately 8 Hz. If the beam was positioned above a wire along the length of draw, the output still fluctuated, but maintained a higher level. If the beam passed along the selvedge, the output dropped to a low, d.c. level. In the electronic control box this output was compared with that of the bulb detector, producing a high logic level signal if it was higher, and a low logic level signal if it was lower. This logic signal was then processed by initiating a counting period of one second. During this period the number of times that the signal went high was counted. If this number exceeded a preset value then no alarm was generated (since the beam was passing over cross wires - a safe condition). If the count did not exceed the preset value then an alarm was generated within the circuit. The original logic level signal was then interrogated to decide which type of alarm was to be generated. If the original signal was high then the long wire alarm was activated, if it was low then the selvedge alarm was activated.

This unit was installed on line and found to work well from the outset. Several units are now being incorporated on line on either side of the ribbon, as part of an automatic system to control the position of the score lines.

Plate 6.1 is a photograph of the wire detection unit.

PLATE 6.1

WIRE DETECTION EQUIPMENT

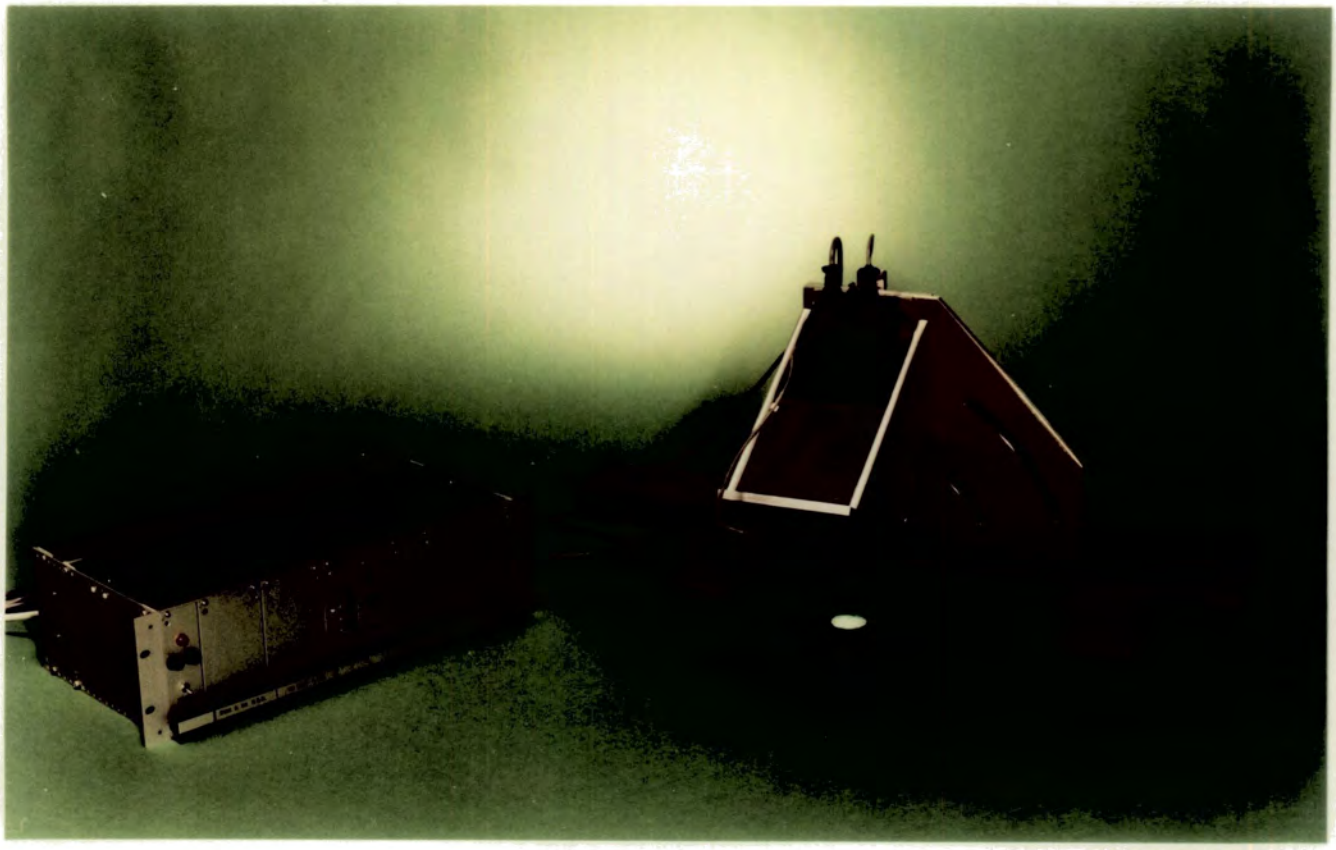

6.4 Measurement of Haze on Glass Surfaces

During the production of some of the glass products at Pilkington, the surface treatments required sometimes left a small degree of haze on the surfaces. The haze could be quite simply wiped off, but in order to find out its origins, and monitor attempts to prevent it from occurring, it was necessary to measure the amount of haze actually present. The problem was that there was no inexpensive haze meter on the market that could measure the amount of haze involved - less than two percent. Other instruments measured up to several tens of percent, and at low values gave unreliable results.

The solution to this problem therefore involved developing an optical system which would detect these small amounts of haze and quantify them.

The instrument which was built to carry this out worked by measuring the amount of light deviated from a collimated beam. It did this as shown in figure 6.5. The light source was a polarised helium neon laser. The amplitude of the beam was modulated for reasons that will be explained later. A microscope objective expanded the beam up to a practical diameter for making measurements. At the focus of the objective was a 25um pinhole, which acted as a spatial filter for any skew rays caused by dirt etc. The beam was collimated by a doublet lens (to minimise aberrations). A beamsplitter then removed a portion of the collimated beam to use as a reference of laser intensity; this was focused onto a large area detector. The sample was placed in the transmitted portion of the beam. Close behind the sample holder was a doublet lens which focused the collimated beam down

FIGURE 6.5

OPTICAL LAYOUT OF HAZE METER

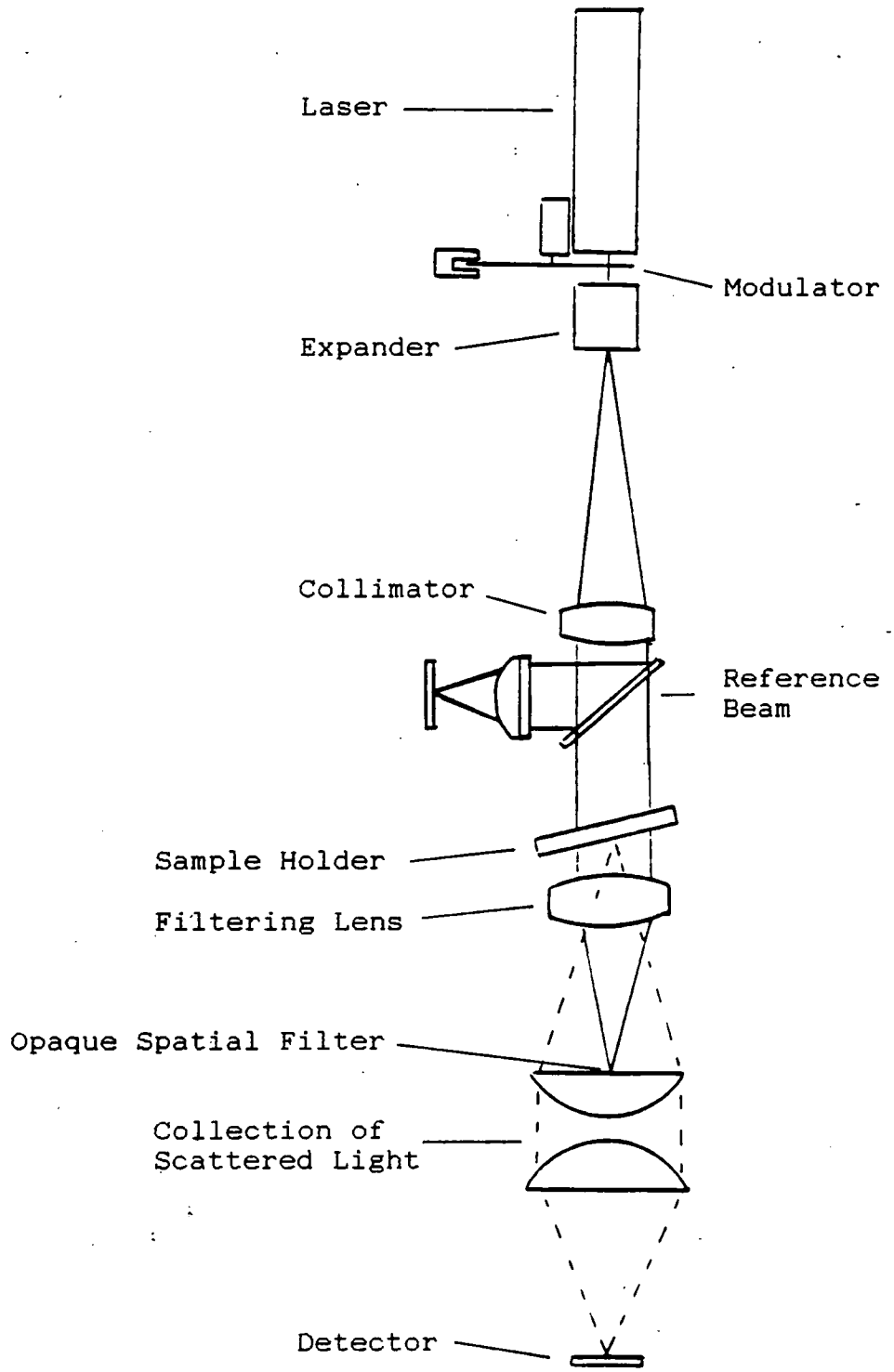

to a small spot. At this point the beam was blocked off by a small square of opaque material. The material was stuck to the first of two lenses which were used to collect any scattered light from the sample and focus it onto a second large area detector.

Therefore, providing that the beam was perfectly focused and that no scattering occurred from any of the optics, the sample detector should not have received a signal until a scattering sample was placed in the beam. In practice it was found that small amounts of scattering always occurred, which had to be corrected for.

The chopper, positioned after the laser, modulated the light beam so that the detectors were presented with signals of a square wave form. The level of signal was then derived using phase sensitive detection. This is discussed in chapter 3; a full analysis can be found in Horowitz and Hill (ref. 3.1). This allowed the unit to be used in room lighting conditions without the readings being affected.

In taking a reading of the amount of haze produced by a sample, the reference detector signal would be used in two ways. Not only was the magnitude of the reading taken as a proportion of the reference intensity (to allow for the gradual deterioration of the laser output), the offset (to compensate for the scatter present in the system itself) was also linked to it. Since the level of scattered light was very low compared to the intensity split off by the beamsplitter, a mask was placed in front of the reference detector which made the signal levels more even. This was done to cater for non - linearities in the detector sensitivities as a function of input level.

It can be seen from figure 6.5 that the sample holder is illustrated at some angle off axis. This was necessary because multiple reflections were produced within the sample by the coherent laser light, and if the sample holder was positioned normal to the beam then these reflections would become incident on the sample detector, and produce spurious readings. It was found that an angle of approximately 10 degrees was sufficient to ensure that this did not happen. Provided that the sample holder was not adjusted after calibration, the instrument performed perfectly well.

In terms of performance, the instrument was found to have a noise level equivalent to +/- 0.02% haze, and a repeatability of measurement of +/- 0.02% haze. The maximum reading level for the instrument was 2.6% haze.

The unit has been in use for a short time and has worked satisfactorily. A photograph of it has been included in plate 6.2. It can be seen that the components are all held in laboratory style clamps. This was because the customer wanted to be left with equipment of general use once the instrument had served its purpose.

PLATE 6.2

HAZE METER EQUIPMENT

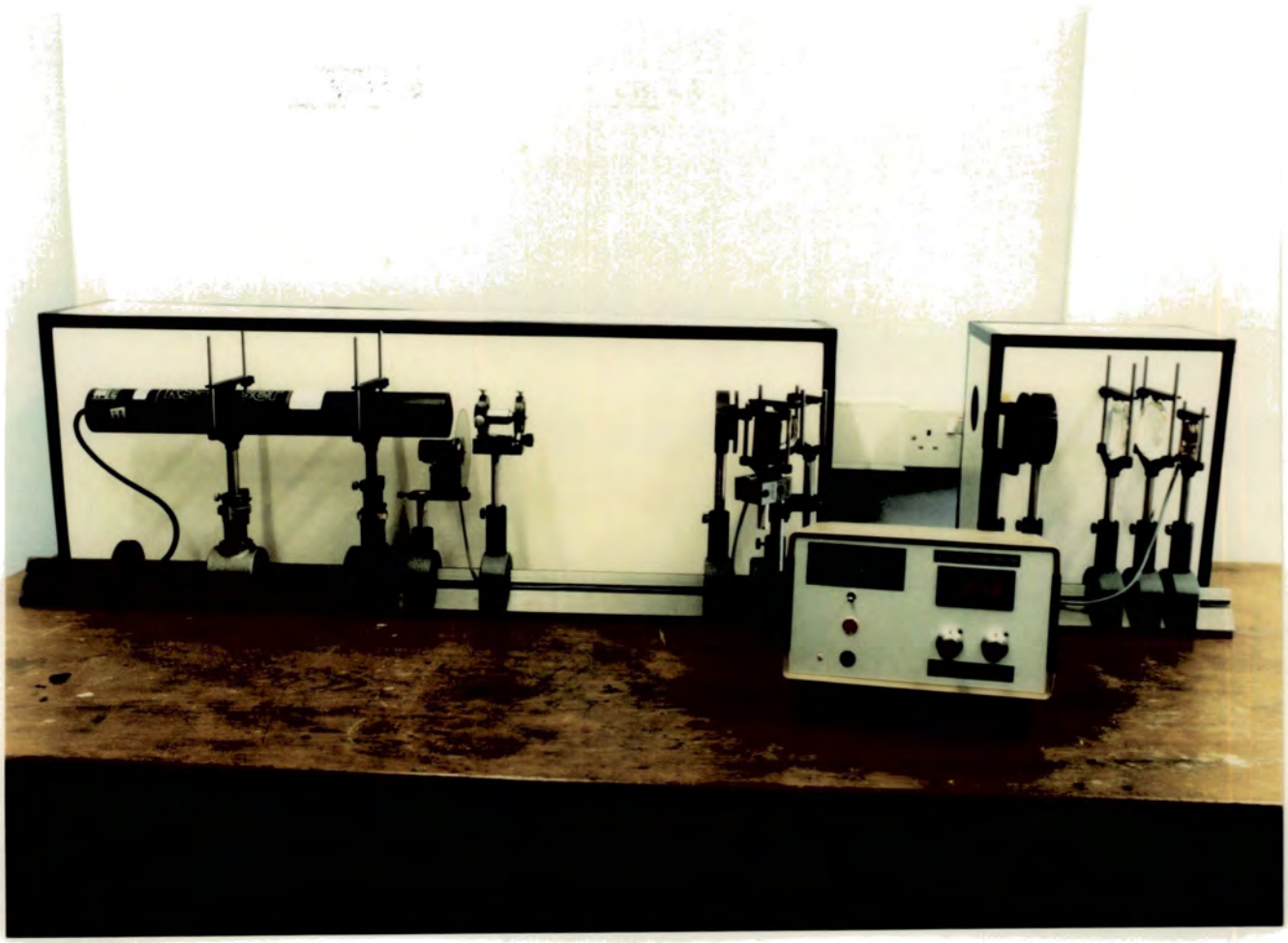

CHAPTER 7 SUMMARY

This thesis has described the use of electro - optical instrumentation to provide solutions to inspection and measurement problems within an international glass firm.

Types of light sources, media and detectors which are available to the industrial scientist have been reviewed. In describing the practical work carried out by the author these components have been discussed, with explanations given as to their choice where necessary.

The types of practical work carried out have included purely speculative projects, as in the study of infra - red Smartt interferometry; initial studies which have produced solutions, but which have, for one reason or another, not been taken any further forward; and more major undertakings which have been followed through to the final instrument.

Chapters 4, 5, and 6.2 have been entirely the work of the author under the guidance of Mr. Barry Hill. In chapters 3, 6.1 and 6.3 the optical principals, design and construction, plus the basis of the electronic function, have been the work of the author, with electronic design and construction carried out by electronics specialists within the laboratory.

An understanding of the science involved has been only one part of the knowledge required to carry out the work described in this thesis. The recognition of what can practically be achieved within time and monetary limitations has also been necessary, as has an appreciation of how the technology can be usefully applied within an industrial environment.

The author is continuing to work in this field, and is now carrying out more fundamental research to address the longer term interests of the company.

ACKNOWLEDGEMENTS

The author would like to extend his thanks to Pilkington plc for allowing the contents of the various projects undertaken whilst in their employ to be submitted for assessment as a higher degree thesis.

Thanks are also extended to colleagues within the Optoelectronics Department at Pilkington Technology Centre for their advice and helpful discussions, and in particular to Dr. Steven Collier and his fiancee Dr. Anne Bentley for proof reading the final draft.

APPENDIX

COMPUTER INTEGRATION OF SCHLIEREN SYSTEM OUTPUT

```
 10     MODE0                                  C  Graphics Mode
 20     DIM Y(150)                             C  Memory for Readings
 30     DIM Z(150)                             C  Memory for Output
 40     IMAX=0:IMIN=0                          C  Y Scale Tabs
 50     C=33:M=0.1                             C  Coefficients for
                                               C     average line
 60     FOR J=1 TO 140
 70     READ Y(J)                              C  Read Y Values
 80     AV = C - (M*J)                         C  Calculate Local Avge.
 90     Y(J) = Y(J)-AV                         C  Subtract Local Avge.
100     NEXT
110     FOR K=1 TO 140
120     Z(K)=Z(K-1)+0.5*(Y(K)+Y(K+1))          C  Numerical Integration
130     IF Z(K)>IMAX THEN IMAX=Z(K)            C     Setting up
140     IF Z(K)<IMIN THEN IMIN=Z(K)            C     Y Scale
150     NEXT
160     YSC = 400/(IMAX+ABS(IMIN))             C  Calculate Y Scale
170     CLS                                    C  Clear Screen
180     MOVE 0,500
190     FOR I%=1 TO 140
200     X=I%*6: Y=750+(Y(I%)+(C-(M*I%)))*5
210     MOVE X,Y : DRAW X,Y                    C      Draw Data
220     NEXT
230     MOVE 840,750+(C-M*I%)*5                C      Draw Data
240     DRAW 0,750+33*5                        C       Average
250     MOVE 0,250
260     FOR I%=1 TO 140
270     X=I%*6 : Y=250-YSC*Z(I%)               C      Draw Integrated
280     MOVE X,Y : DRAW X,Y                    C      Trace
290     NEXT
300     PRINT "Y = "; M "X - "; C              C  Print Calculated Avge.
310     *SDUMP                                 C  Print Picture from
                                               C       Screen
```

BIBLIOGRAPHY

1	Barr & Stroud	Single Frequency Helium Neon Laser LU12 Handbook	(1984)
2	Melles Griot	Optics Guide 3	(1985)
3	Speirs Robertson	Optical/Electronic Catalogue	(1986)
4	Lexel	Argon and Krypton Ion Laser Theory; Laser Handbook	(1977)
5	Coherent	Ion Laser Systems	(1981)
6	Coherent	Dye Lasers	(1982)
7	Butler	Applied Optics and Optical Engineering VI ed. Kingslake & Thomson (Academic Press)	(1980)
8	Eby & Levin	Applied Optics and Optical Engineering VII ed. Shannon & Wyant	(1979)
9	Culshaw	Optical Fibre Sensing and Signal Processing (Peter Peregrinus Ltd.)	(1984)
10	Savage	Infra Red Optical Materials & Their Anti-Reflection Coatings (Adam Hilger)	(1985)
11	Itoh	July 1985 Photonics Spectra p.55	(1985)
12	Gliemeroth	1983 SPIE Conference	(1983)
13	Photonics	Photonics Design and Applications Handbook	(1987)
14	Levi	Applied Optics I (Wiley)	(1968)
15	Levi	Applied Optics II (Wiley)	(1980)
16	Thorn EMI	Photomultuplier Catalogue	(1986)
17	Hamamatsu	Infra Red Detectors	(1985)

REFERENCES

3.1	Horowitz & Hill	The Art of Electronics p.628 (Cambridge University Press)	(1987)
5.1	Smartt & Steel	Japan. J. appl. Phys. 14 Suppl. 14-1 p.351	(1974)